ADDIS ABABA UNIVERSITY

ADDIS ABABA INSTITUTE OF TECHNOLOGY *(AAiT)*

SCHOOL OF GRADUATE STUDIES

SCHOOL OF MECHANICAL & INDUSTRIAL ENGINEERING

IMPROVING ENERGY EFFICIENCY OF AKAKI WELL-FIELD SUBMERSIBLE PUMPS BY IMPLEMENTING VARIABLE SPEED DRIVE CONTROLS

By

Sofiya Hussein

A thesis submitted to the School of Graduate Studies of Addis Ababa institute of Technology in partial fulfillment of the Masters of Science in Mechanical Engineering (Thermal Engineering Stream)

Advisor: ***Dr.-Ing. Edessa Dribsa***

Date: March, 2019

Addis Ababa University

Addis Ababa University Institute of Technology

School of Graduate Studies

School of Mechanical & Industrial Engineering

Improving Energy Efficiency of Akaki Well-field Submersible Pumps by Implementing Variable Speed Drive Controls

By: Sofiya Hussein

Approved by board of examiner

Dr. Yilma Tadesse	_____	_____
Chairman, Department	Signature	Date
Dr.-Ing. Edessa Dribsa	_____	_____
Advisor	Signature	Date
Dr. Yilma Tadesse	_____	_____
Internal examiner	Signature	Date
Dr.-Ing Wondwossen Bogale	_____	_____
External examiner	Signature	Date

Declaration

Addis Ababa University

Addis Ababa Institute of Technology

School of Graduate Studies

This is to certify that the thesis prepared by Sofiya Hussein, Titled: "Improving Energy Efficiency of Akaki Well-field Submersible Pumps by Implementing Variable Speed Drive Controls", and submitted in partial fulfillment of the Master of Science in Mechanical Engineering (Thermal Engineering Stream) complies with the regulation of the university and meet the accepted standards with respect to originality and quality.

Signed by Examining Committee:

Dr. Yilma Tadesse	_____	_____
Internal examiner	Signature	Date
Dr.-Ing Wondwossen Bogale	_____	_____
External examiner	Signature	Date
Dr.-Ing. Edessa Dribsa	_____	_____
Advisor	Signature	Date

_____

Chair of Department of Graduate Program Coordinator

ACKNOWLEDGMENT

I submit my highest appreciation to Dr. Ing. Edessa Dribsa for his advice that significantly helped me in this project, for his continuous support, scientific discussions and for reviewing my thesis. I am deeply indebted to his continuous supervision, original ideas and guidance.

My gratefulness is directed to Ato. Zelalem and Ato Wondwosen from Addis Ababa Ground Water Study, Design, Construction and Supervision Project Office and Addis Ababa Water Supply and Sewerage Authority and CT2 reservoir site crew for their various invaluable suggestions and support during data collection.

Table of Contents

LIST OF FIGURES

LIST OF TA BLES

NOMENCLATURES

H	Head
p_a	Pressure to the outlet section
p_e	Pressure to the inlet section
ρ	Density
g	Gravitational constant,
V_a	Outlet section velocity
V_e	Inlet section velocity
H_{geo}	Geodetic difference
H_r	Head loss conducted by friction
H_{st}	Static head
H_{dy}	Dynamic head
K	Constant describing the total system characteristics
Q	Flow rate
E	Energy
I	Current
NPSH	Net positive suction head
p_b	Air pressure
p_D	Vapour pressure
V_e	Flow speed
$H_{v,s}$	Sum of pressure drops
$H_{s,geo}$	Height difference
N	Speed
P	Power
P_{Hyd}	Hydraulic power
P_a	Absorbed power
T	Torque
T_n	Nominal torque
V	Voltage
η_{sys}	System efficiency
η_{pump}	Pump efficiency
η_{motor}	Motor efficiency
η_{vsd}	Efficiency of the VSD
E_s	Specific energy consumption
P_{in}	Input power
t	Time
V	Volume
Q_{tot}	Total flow rate
Cosφ	Power factor
Ns	Synchronous speed of the motor
f	Frequency of the supply voltage
p	Number of poles

P_{out},	Output power
T_{load},	Load torque
ω_r	Rotor speed,
V_{rms}	Percentage of rated voltage applied to the motor
m	Modulation index

Subscripts

VFD	Variable frequency drive
VSD	Variable speed drive
ASD	Adjustable speed drive
AFD	Adjustable Frequency drive
QH	Flow rate vs head
BHP	Best power
BEP	Best efficiency point
AC	Alternating current
DC	Direct current
PWM	Pulse width modulation
IGBT	Insulated gate bipolar transistors
KWh	Kilowatt hour
PV	Present Value
NPV	Net present value
IRR	Internal Rate of Return
Av	Average
max	Maximum
min	Minimum
sys	System
tot	Total
C	Cost
B	Benefit

ABSTRACT

In Ethiopia water pumping system is given less concern regarding to energy saving and in groundwater management. The amount of groundwater recharging is affected by many factors like seasonal rain variation, global warming, drought and also groundwater withdrawal. This changes significantly show in a water pumping system hydrodynamic head and flowrate changes. Since, the draw down in the system increases because of the ground water recharging is less in the system, the amount of water discharge decreases.

When the amount of the water availability in the ground decrease we need such control mechanisms to run the pumping system. The most commonly used controlling system in the country for water pumps are throttling.

This thesis is focused on ten deep-well pumps at Akaki well-field Phase-3A ground water pumping system. Studying and evaluate the efficiency the actual groundwater pumping system, make energy efficiency/saving analysis and economic analysis for the improved system.

The actual water pumps used to withdraw water from ground at this sites are fixes speed centrifugal submersible pumps, and throttled to the amount of water availability. This types of control techniques are characterized by low efficiency and high energy consumption. Therefore, this pumps draw nearly full horsepower and consume maximum energy full time regardless of water availability in the ground.

This research carried out the simulation and performance analysis of such pump motors by implementing a variable frequency drive control between the power supply and motor, using MATLAB/SIMULINK model and shows the motor perform in its maximum efficiency. Successfully achieved the control of the speed of the induction motor by varying the frequency of the applied voltage using pulse width modulation method. Affinity laws also used to predict the pump performance change to re-design the system in variable speed pump analysis. The economic analysis is shown through comparison between the pumps operating energy consumption cost and investment cost to implement the VFD control system.

The results of this thesis provides a potential energy efficiency/ saving for using VFD in Akaki well-field submersible pumps. The redesigned VSD control system provides low energy consumption in KWh, depends on the actual groundwater discharge capacity and economically viable to implement the variable speed drive control system to the existing pumps.

Keywords: Groundwater, Submersible Pumps, Energy Conservation, Variable Speed/Frequency Drives, Pulse Width Modulation, Affinity Laws, Matlab/Simulink Model

CHAPTER 1

1. INTRODUCTION

1.1 Introduction to Groundwater pumping System

Ground water is a fresh water available beneath the surface of the earth. It is used to replace the rain water and surface water. Less vulnerable for pollution due to ground formation and depth from the earth's surface [1]. To use the available water in the ground first from moderate to deep wells are drilled according to the water availability in the site and pumps are the main equipment to withdraw the water. This water needs to be pumped out of the well to the surface of the earth and deliver it under pressure to the place where it will be used.

A typical water pumping system includes pumps, piping system, fittings, valves, pressure and flow measuring devices, surge arresters, storage tanks or reservoirs, pump motor control system and remote control systems. A deep-well is the most common way to obtain a fresh water from ground. A well is basically a drilled hole in the ground, held open by a steel or PVC pipe casings that extends to an aquifer. A pump draws water from the aquifer to the reservoir for end use distribution through the piping system. The depth of the well is determined by factors such as water availability, the ground water quality and the geological conditions of the sight [2].

1.2 Ground Water Pumping System in Ethiopia

Rain water is the main source of water in Ethiopia, but it fluctuates from year to year. Currently groundwater is replacing rain water and surface water shortages. It is a source of freshwater for drinking, municipal use, livestock, industry and agricultural irrigation works in most parts of the country [3]. In Ethiopia, groundwater is obtained from shallow to moderately deep unconfined boreholes drilled using well drilling rigs.

Groundwater management has been given a very little attention in the country. It is a very necessary step towards evaluating and managing groundwater resources and withdrawal system, since excessive usage affect the natural groundwater formation system. The study in Hydro-geological and hydro-chemical framework of complex volcanic system in the Upper Awash River basin, Central Ethiopia, with special emphasis on inter-basins groundwater transfer between Blue Nile and Awash rivers [2]

result shows that groundwater movement could be connected to each other through the permeable and porous scoraceous lower basaltic aquifer all the way from the Blue Nile Plateau to the Awash River.

The study from the Ministry of water resources Ethiopia [3] in strategic framework for managed groundwater development, shows there is a need to scale up regulation of groundwater by clarifying responsibilities of different organizations at federal, regional and river basin level, and in the private and public sector and align all companies for managed groundwater development. In addition the study recommends that there should be a developed standard procedures to use groundwater.

The groundwater availability in the region relies heavily on the yearly recharge from annual rainfall, more than 90% of which occurs during the monsoon season, from June to September [3]. This recharge is the major source of freshwater during the dry season from October to May [3].

In general to mitigate the effects of the lack of recharging the groundwater due seasonal climate variability in the country and growing needs of water per year, resulting from increasing population, agriculture and industrial expansions, a carefully analyzed systems and new technologies should be adopted and manageable. Otherwise, this situation led to increase water problem in the region.

1.3 Pump

The focus of this thesis is, by studying the actual water pumping system from ground at Akaki well field, make energy efficiency analysis and financial or economic analysis for the groundwater pumping system, which is currently used fixed speed centrifugal submersible pumps by converting to variable speed drive pumps. Pumps are devices used to transfer liquids from low-pressure zone to high-pressure zones, or to move the liquids from a low elevation into higher elevation. There are many types of pumps used for many applications like for groundwater, wastewater and circulation of water in closed systems like heating, cooling, and air conditioning system [4].

In this thesis a centrifugal pumps used to withdraw Akaki ground water to the reservoir will be discussed. An increase in the fluid pressure from the pump inlet to the outlet is created when the pump is in operation. This pressure difference drive the fluid though the system. The centrifugal pump creates an increase in pressure by transferring mechanical energy from the motor to the fluid through the rotating impeller. The fluid flows from the inlet to the impeller center and out along its blades. The centrifugal force hereby increases the fluid velocity and consequently the kinetic energy is transformed into pressure [4].

Pumps are used widely in industry to provide cooling and lubrication services, to transfer fluids for processing and to provide motive force in hydraulic systems. Pumping system accounts 20% of the world's electric energy demand and range from 25-50% of energy usage in certain industrial plant operations. With raising energy costs, process plants are increasing focus on the amount of energy consumed by the equipment. An improper sized or poorly performing pump consumes unnecessary energy and money [5].

Water pumping systems are massive consumers of energy, which is consumed in each of the stages of the water production and supply chain. Water pumping and distribution systems are usually low-efficiency systems for energy consumption [6]. Furthermore, pressure reducing valves, which cause the mechanical dissipation of hydraulic energy, are often used in order to control the pressure regime in the system as well as to face topographical discontinuities during the pipeline path, to avoid high pressures in the network that can cause ruptures and water leakages.

1.4 Motor

3-phase induction motors are the prime movers for vast majority of pumps. These motor can be operated either directly from the main or from adjustable frequency drives. In modern industrialized countries, more than half of the total electrical energy used in those countries is converted to mechanical energy through AC induction motors [7]. The application for these motors covers every stages of manufacturing and processing. They are used to drive pumps, fans, compressor, mixers, agitators, mills, conveyors, crushers, machine tools, crane, etc [7].

Lately, it has become increasingly common practice to use 3-phase squirrel cage AC induction motors with variable frequency converters for variable speed drive (VSD) applications [8]. Clearly to understand how the VSD system works in induction motor, it is necessary to understand the principles of operation of this type of motor.

1.5 Variable Speed Drive in Water Pumping System

The main reason for employing variable speed drive control in water pumping system is related to energy saving and functionality of the application. When variable speed drive control system is used in pump applications, the pump adjust its rpm to a given set point and adjusting the flow of the system to the actual demand or capacity of the well and reduces power consumption of the pumping system [8].

There are many diverse reason for using variable frequency drives, using it in centrifugal pumps can give a benefit of energy saving in the system.

In general, variable speed drives are used to [8]:

- Match the speed of a drive to the system requirements.
- Match the torque of a drive to the system requirements.
- Save energy and improve efficiency.

1.6 Problem Statement

Groundwater pumping systems face many challenges, including groundwater variation due to seasonal change and drought, inefficient pumping system, lack of technical knowledge, aging infrastructure, increasing threats to aquifers, changing compliance and public health standards, shifts in population growth, and higher customer expectations etc.

Inefficient pumping system includes inefficient energy usage of pump motors. Energy efficiency/saving can play a role in addressing these challenges by understanding the energy consumption of the system and taking advantage of energy efficiency opportunities. The major share of energy consumption in water pumping system is associated with pump motor.

The benefit of energy saving in this study area are not fully appreciated by many users. Energy efficiency in water pumping system starts with motor speed control. When the input/output flow requirement fluctuate in any system an external means of adjustment is needed. In Ethiopia commonly used methods for flow control in water pumping system includes throttling which is a valve based control and add extra piping (riser pipes) in the system.

A decrease in availability of water in the ground of the site affect the output water capacity in the supply side and continuously on-off the pumps which lids to the pump motor failure and increase the maintenance cost of the system . Also, the pumps perform under the respective design efficiency and draw nearly full horsepower and consume maximum energy full time, since all the pumps currently used are fixed speed pumps.

Thus using variable frequency control of an induction motor in water pumping system in Akaki wellfield provides an economically sound and operationally effective for reducing power consumption, energy wastage and to save money.

1.7 Objectives

1.7.1 General Objective

The general objective of this thesis is to study the performance efficiency, improving energy efficiency and financial evaluation of deep-well groundwater pumping system in the Akaki well-field Phase-3A located in south east of Addis Ababa, which is owned by Addis Ababa Water Supply and Sewerage Authority (AAWSA), by implementing a variable speed drive (VSD) control to 10 deep-well submersible pumps.

1.7.2 Specific Objectives

Specific objectives include:

1. Select ten deep-well pumping stations from Akaki sites of Addis Ababa and collect their respective design documents and performance curves of each pump from Addis Ababa Water Supply and Sewerage Authority (AAWSA).
2. Assess if each of the ten pumping system are designed to operate at the best-efficiency points of the pumps. It is presumed that each pump unit is running at its constant speed.
3. Collect data on the water level variation of the deep-wells, the consequent actual flow rates obtained from each pumps and manufacturer characteristic curve of each pump. Besides, collect the data on variation of supply flow rate.
4. Evaluate the consequences of the change in the actual operating flow rates on the efficiencies of the pumps, and the consequent energy wastage of the system.
5. Consider minimizing energy wastage by fitting variable speed drives (VSD/VFD) and evaluate the merits by MATLAB/SIMULINK model.
6. Re-design each of the pumping systems and evaluate energy saving
7. Make economic evaluation of the re-designed system
8. Conclusion and recommendation that might be considered by a utility to improve incremental and overall energy efficiency

1.8. Scope of the Thesis

The analysis of this reaserch is based on the data provided by Addis Ababa Ground Water Study, Design, Construction and Supervision Project Office and Addis Ababa Water Supply and Sewerage Authority, and data collected from the CT2 site. The study focus on improving energy efficiency/saving of the pumps by implementing variable speed control.

Throttling, when the available flowrate from the wells is less or when the draw down in the system is high because of many factors the system face, is a common way of controlling the system and the key factor to give emphasis on this well-field pumps to consider enery efficiency/saving. It is possible to achieve significant energy savings through a systematic optimization process in this pumping system.

With the change from valve-based control in fixed speed pumping system to drive control in variable speed drive control unit in Akaki well-field Phase-3A water pumping system, we can observe a significant drop in power usage and run the pumps at its BEP. In addition, using variable speed pumping system keep the pumps to work in its BEP and minimize threats in the aquifers.

Energy efficiency/saving actions is presented that will enable water utilities to learn about, evaluate, and implement energy efficiency options that could reduce power consumption, run the pumps in its BEP and in the consequence save money.

1.9 Thesis Structure

The thesis consists of eight chapters. Chapter 1: Provides an introduction to the groundwater sources in Ethiopia, the method for pumping ground water by using centrifugal pump and VFD for conserving energy. Chapter 2: Literature review. Chapter 3: Studies types of pumps at Akaki well fields Phase-3A site and evaluate the pumps based on mechanical and electrical characteristic. Chapter 4: Studies the characteristic of induction motor and the possibility to save energy by using VFD and evaluate the merits by MATLAB/SIMULINK model. Chapter 5: Presents control method of water pumping system and re-design the pumping systems and evaluate energy saving. Chapter 6: Economic evaluation for using variable frequency convertor drive VFD of the system. Chapter 7: Presents the conclusion of this thesis and recommendation for future work.

CHAPTER 2

2. PUMPING SYSTEM ENERGY OPTIMIZATION

2.1 Literature Review

A comprehensive, detailed literature review was conducted to identify energy efficiency tools, practices, processes, and technologies associated with the design, construction, operation, optimization and measures to evaluate energy conservation methods of the water pumping system in groundwater. This research included energy efficiency practices associated with management tools, conservation practices, alternative energy, and pumping mechanisms. The requisite staff support and data collection as well as appropriate information necessary to optimize energy efficiency in water pumping system were identified. Since experimental studies are very expensive and time consuming, and also, because of the complex geometry, and analytical methods are lacking in this case, the perfect solution is using numerical methods. In other words, one of the suitable methods to evaluate energy efficiency of water pumping system by varying the pump motor speed is the numerical modeling. This research included review of academic researches, numerous water industry publications, pertinent water research foundation reports, presentations on energy efficiency conferences, and web-sites of energy related organizations and associations.

Andarge Yitbarek Baye [1] in 2009, study the Hydrogeological and Hydrochemical Framework of Complex Volcanic System in the Upper Awash River basin, Central Ethiopia, with special emphasis on inter-basins groundwater transfer between Blue Nile and Awash rivers. The result of the study showed that groundwater movement could be connected to each other through the permeable and porous scoraceous lower basaltic aquifer all the way from the Blue Nile Plateau to the study area. And concluded that groundwater monitoring has been given a very little and/or no attention in the country, but it is a very essential step towards evaluating and managing groundwater resources.

Ministry of Water Resources Ethiopia [2] in 2011, study strategic framework for managed groundwater development. The study shows there is a need to scale up regulation of groundwater, by clarifying responsibilities of different organizations at federal, regional and river basin level, and in the private and public sector and align all players for managed groundwater development. In addition standard procedures should be developed.

Rahul Gokhale and MilindSohoni [9] in 2015, evaluate the Data driven behavioral characterization of dry season groundwater level variation in India. The evaluation observed high variance of this coefficient points to significant variations in groundwater levels. It reveals that the typical groundwater user faces not only scarcity but also uncertainty in the access to such a key resource.

L.K Reynolds and S. Bunn [10] in 2010, study Improving energy efficiency of pumping systems through real-time scheduling systems. The result shows the variable speed drive operates over a very wide range of efficiency from 8% to 78% efficiency with an average of 47%. If this were a fixed speed pump they would expect a gain of 14%. Thus they concluded that, because this is a variable speed drive, the potential savings potential will be much greater.

Hamad Raad Salih1, Ali Abdulwahhab Abdulrazzaq, Basarab Dan Guzun [11] in 2015, study a new modeling and dynamic design for pump drive system utilizing MATLAB /SIMULINK Program to control the speed of motor. The result shows using VFD can save energy according to affinity law, so that a small reduction in speed can save a large amount of energy, it is a good solution for improving the response and control precision of hydraulic motor. And their research shows that, using this type of control will increase the cost of the drive system and control complexity, but achieves the expected energy savings target.

The article written by Robin Priestley [12] in 2014, on energy saving using variable speed drives, by applying the affinity laws to the centrifugal pump shows, the power consumption of 100KW motor @50% speed is 12.3 KW and @ 85% speed of 100HP pump motor, since the pump speed is limited, the power consumption is 61HP. Also shows the potential annual energy cost saving of using variable speed system.

Muhammed H Al-Khalifah and Gregory K. McMillan [13] in 2012, study Control valves verses speed drive for flow control. By using affinity laws and typical VFD Simulink model, they state the drawback of control valve pump control system, the substantial energy saving of using VFD control system and measure taken during VFD application to the system.

Mr. Ankur P. Desai, Mr. Rakesh. J. Motiyani and Dr. Ajitsinh R. Chudasama [14] in 2014, study Energy conservation using VFD in pumping application using Matlab simulation and experimental methods. The result shows VFD offers a very good response in energy conservation in pumping system. Reducing the pump flow by VFD control, motor consume a very less power.

In other paper Poul Waide and Conrad U. Brunner [15] in 2011, study Energy efficiency policy opportunities for electric motor driven system, focusing on general purpose medium size (0.75KW-375KW) industrial AC squirrel-cage induction motors and less DC motors, using a top-down and a bottom-up approach method. The conclusion shows, if available state-of-art efficiency measures are systematically applied to pump system 40%-75% energy efficiency/saving can be achieved in industrial pumps and state factors needed consideration during new system installation on the existing system.

M. Ishtiaque Rahman and Khosru M. Salim [16] June 2015, study Comparison of Conventional Induction Motor-Pump System with One Containing a Variable Frequency Drive in a Quantitative Performance Analysis in Low-Voltage Conditions. These findings suggest that a VFD enables the motor pump system to maintain its efficiency at a high level throughout a range of voltages lower than the rated voltage. Furthermore, it provides lower power to a system, when required, without having a significant impact on the efficiency of the system. They accomplishes this by proper Volts/Hz control of the induction motor. Also, in contrast they shows providing lower output power using the conventional system by reducing the input voltage, it reduces the efficiency appreciably and it becomes dangerous to operate the motor at such low efficiencies, as the excessively high copper loss might overheat and burn the stator windings of the induction motor. And concluded that, a conventional system is unable to adjust its power consumption according to system needs.

The article compiled by ABB Ltd [17] in 2011, on Energy saving in submersible system, briefly states VSD control system are less common in submersible pump application because of its difficulties during implementation, but worth this efforts since a massive energy saving can be achieved. Also this article shows, using this drives in submersible pumps can offer energy efficiency/saving of 30% - 50% when there is a need for flow, head or velocity of the system variation.

Based on this research's and input and outcomes, the following broad categories were identified and formed the framework for identifying and presenting information on energy efficiency practices.

- Groundwater hydrogeological study and survey
- Water pumping system
- Pumping system optimization
- Energy Conservation
- Variable frequency/speed drives controllers

The discussion on each of these topics includes an introduction to the topic area, a description of the various practices, the energy savings realized, and references and resources.

2.2. Water Pumping System

A proper discussion of pumping considers not just the pump, but the entire pumping system and how the system components interact. The recommended systems approach to evaluation and analysis includes both the groundwater flow demand, availability of the water in the aquifers and supply sides of the system.

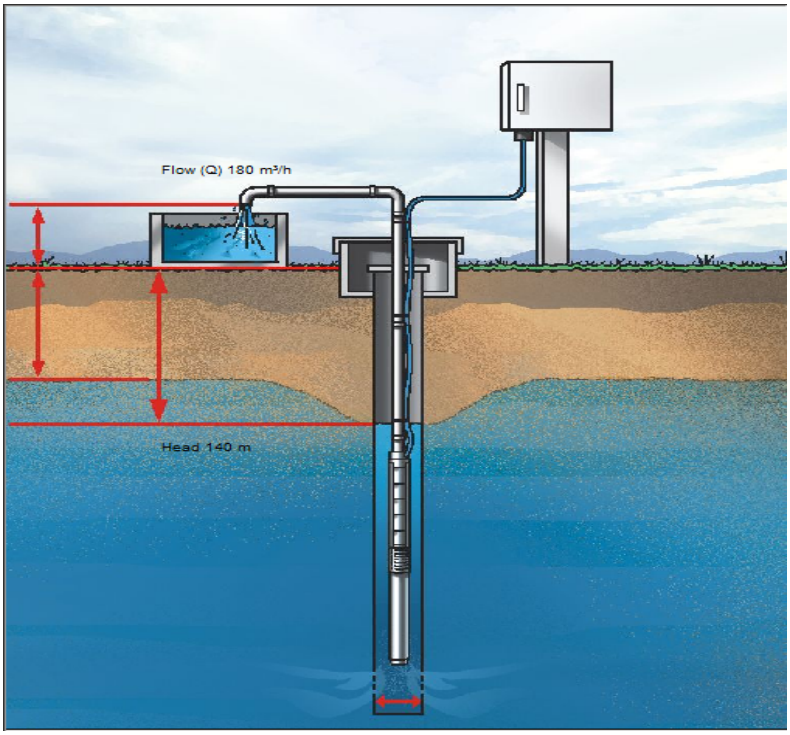

Figure 2.1: Hydraulic pumping system (From Grundfos pump selection tutorial)

In a water pumping system, the objective is either to transfer a water from a source to a required destination, filling a high level reservoir where this thesis takes place, or to circulate water around a system. Pressure is needed to make the water flow at the required rate and this must overcome losses in the system. Losses are of two types which is static or elevation and friction head [18].

Static head, in its most simple form, is the difference in height of the supply and destination of the water being moved. Friction head sometimes called dynamic head loss, is the friction loss on the water being moved, in pipes, valves, and other equipment in the system. Static or elevation is the main head since it is the difference between the suction point and delivery point of the system.

2.3 Pump System Theory

Pumps are broadly classified as kinetic or positive displacement. One of the sub-classifications of the kinetic pump branch is the centrifugal type. It consists of a wet end and a drive end. The wet end consists of a rotating impeller within a casing with inlet and outlet connections. It is coupled to either a constant or variable speed drive [18]. Of all of the types of pumps, the centrifugal pump is the most commonly used.

Liquid is transferred by the centrifugal pump by virtue of the kinetic energy imparted to the liquid by the rotating impeller. For a given diameter impeller at a given speed, a finite amount of energy is transferred to each amount of liquid pumped regardless of the weight or density of the liquid. This fact gives rise to the maxim that the resulting fluid height produced from this pumping operation.

A pressure reduction occurs when the liquid moves from the pump inlet to the point at which it receives energy from the impeller. In pump hydraulics, suction refers to the inward movement of liquid through a conduit, such as a section of pipe, into the pump and ultimately to the eye of the impeller [19]. The basic pump parameters can be divided into hydraulic aspects and in rotational nature.

2.3.1. The Hydraulic Variables Consist Of Head, Capacity/Flow, and Efficiency

The capacity of a pump is the amount of liquid conveyed per unit time. It is actually the volumetric rate of flow. Other common terms for capacity are flow rate and discharge rate.

Head is simply a pressure unit that is commonly used in hydraulic engineering that is expressed in meter of pumped fluid. That is to say, it is the pressure that is exerted from the weight of a height of a given liquid. There are numerous forms and references to hydraulic head, such as,

- Fluid friction head
- Static suction head
- Pump discharge head

When centrifugal pumps are used in a system, the advancing elevation pressure to ensure a certain flow rate in piping is often called the system head, and it is marked with H. This resembles the head which the pump must overcome to deliver the certain amount of flow rate, often marked with Q, in the current system. The system head can be described as a sum of the geodetic difference between the suction and discharge fluid levels, the differential pressure in suction and discharge fluid levels, the

friction head in piping, valves, fittings, etc., and the difference in the velocity heads in the inlet and outlet section of the system. Thus, the system head can be expressed with equation [18].

$$H = H_{geo} + \frac{p_a - p_e}{\rho g} + \frac{V_a^2 - V_e^2}{2g} + \sum_{i=1}^{n} H_r \quad \text{..... (Eq. 2.1)}$$

Where;

H- Total head,

p_a- Pressure to the outlet section,

p_e - Pressure to the inlet section,

ρ- Density,

g- Gravitational constant,

V_a- outlet section velocity of the pumped liquid,

V_e- inlet section velocity of the pumped liquid,

H_{geo}- Geodetic difference,

H_r- Head loss conducted by friction in the system.

The system head can be divided into the static part and dynamic part as shown in figure 2.2. The static part includes the geodetic head and the pressure difference between the inlet and outlet sections of the system and the dynamic part consists of the velocity head difference and the friction head [18]. Thus, the static head H_{st} can be written as

$$H_{st} = H_{geo} + \frac{p_a - p_e}{\rho g} \quad \text{..... (Eq. 2.2)}$$

Correspondingly, the dynamic head H_{dyn} is

$$H_{dyn} = \frac{V_a^2 - V_e^2}{2g} + \sum_{i=1}^{n} H_r \quad \text{..... (Eq. 2.3)}$$

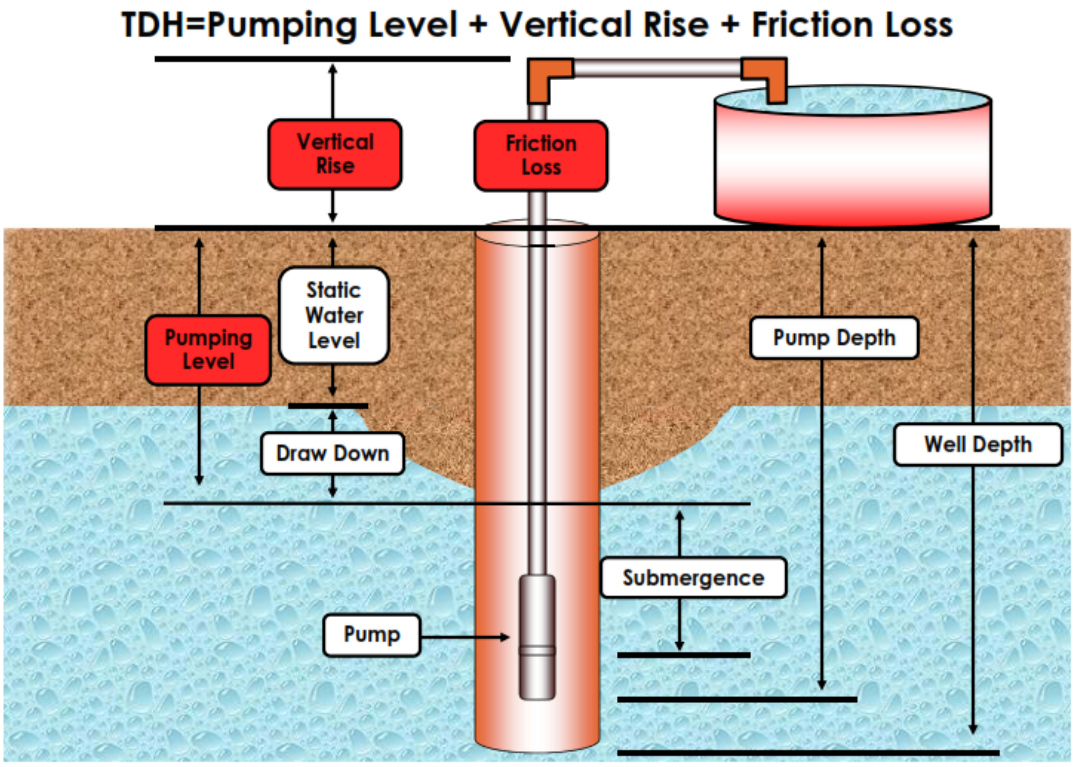

Figure 2.2: Hydraulic pumping system [4].

The system head is usually illustrated with system head curve or just system curve in the QH axis. The pressure difference between the inlet and outlet sections is relevant in closed systems having pressurized reservoirs. In open-loop systems, this difference is insignificant and therefore usually ignored. Also, the velocity head in the dynamic part is often considered very small compared with the total system head. Therefore, the velocity head in equation (2.3) can be ignored to simplify the system modeling. The friction head (or the dynamic head in the simplified case) depends on the flow rate. In practice, the dynamic head in the system is [20]:

$$H_{dyn} = kQ^2 \quad \text{(Eq. 2.4)}$$

Where, k can be described as a liquid-based coefficient depending also on the characteristics of the piping.

Using the above equations, the system head is often simplified to

$$H = H_{st} + kQ^2 \quad \text{(Eq. 2.6)}$$

Where;

H- System head,

H_{st} - Static head

k - Constant describing the total system characteristics

Q- Flow rate

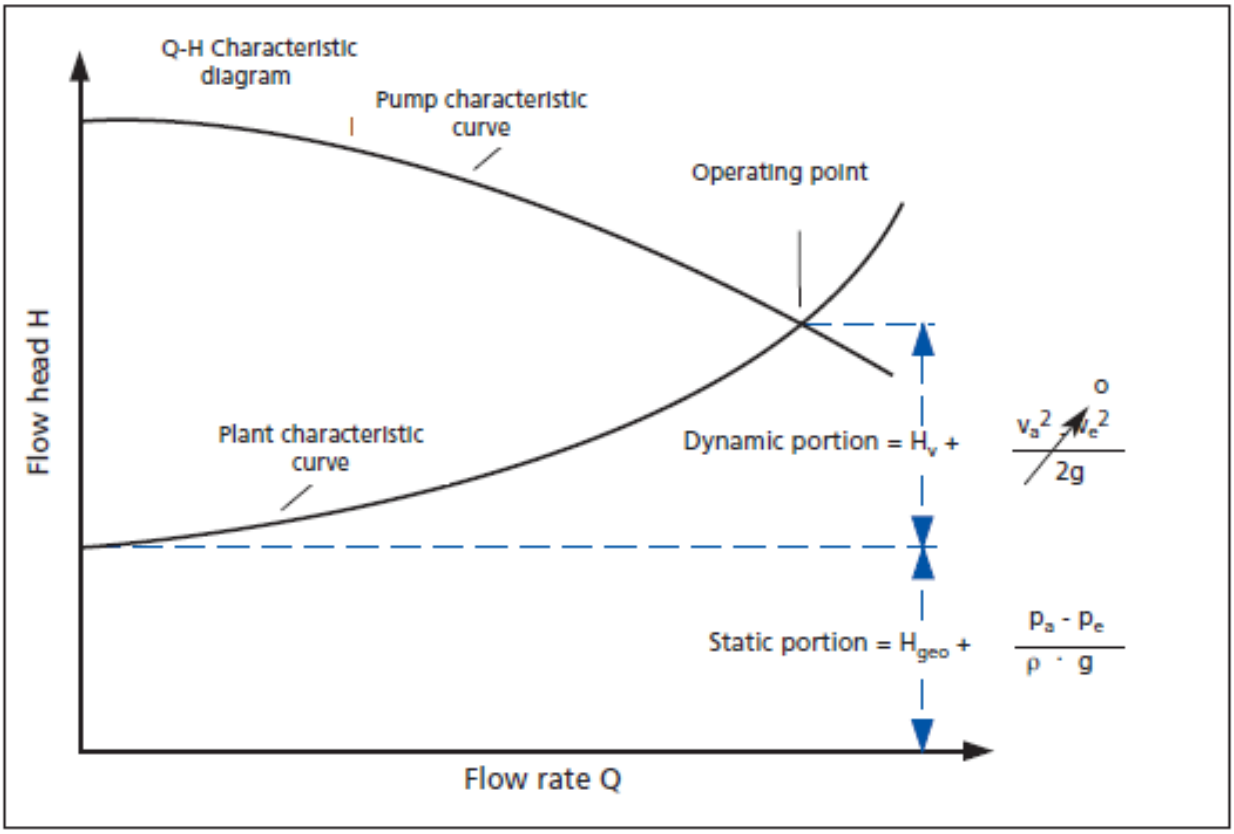

Figure 2.3 Q-H Characteristic diagram [20]

The graphical representation of the flow head of a system (H), in dependence of the flow rate (Q), is the characteristic curve of a pipe or the system. It consists of a static portion that is independent of the flow rate and a dynamic portion in square with rising flow rate.

The behavior of the pump under different operation conditions is indicated with pump characteristic curves. Typically, the curves are given for the produced head H, power input P, and efficiency η as a function of flow rate Q at constant rotational speed n [18]. In addition to the QH curve, QP curve, and Qη curve, the pump manufacturers often present the NPSHr (Net Positive Suction Head) as a function of the flow rate. The NPSHr curve illustrates the required head at the suction of the pump to avoid harmful operation of the pump, such as cavitation.

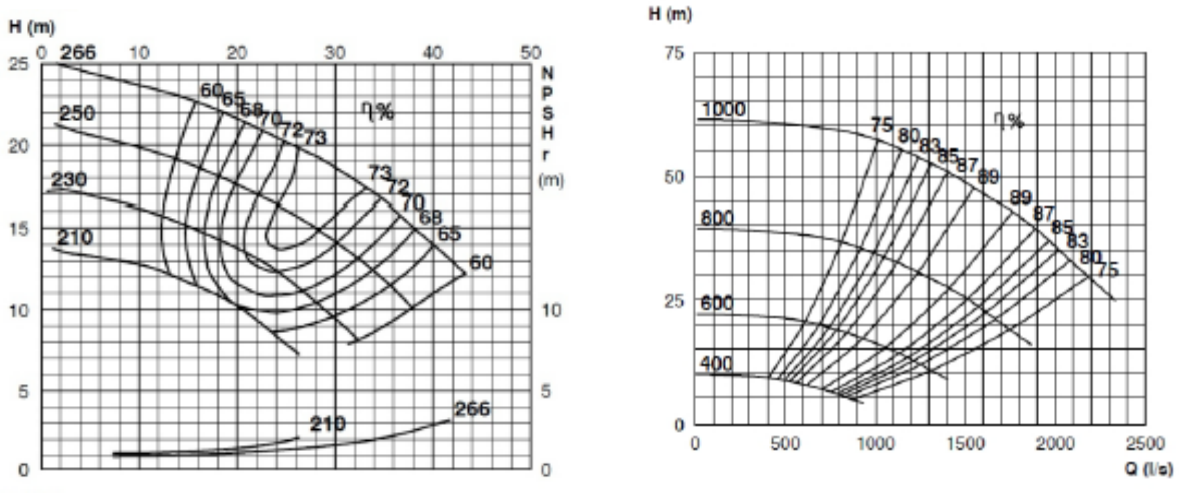

Figure 2.4 Characteristic curves for the centrifugal pump at the (a, left) constant and (b, right) varying rotational speed [18].

Efficiency is a measure or indication of the amount of loss. We must be careful when we discuss efficiency because there are no less than four efficiencies involved in centrifugal pump systems.

These are hydraulic efficiency, mechanical efficiency, and drive efficiency. The overall pump operational efficiency is the product of the three preceding efficiencies [18].

Mechanical efficiency is a measure of the losses between the drive output shaft and shaft input side of the impeller. Also, frictional losses in couplings would be a contributing factor to lower mechanical efficiency. Relatively speaking, mechanical losses are small and are usually ignored. Drive efficiency refers to the effectiveness of the pump driver motor [21].

2.3.2 The Rotational Variables: Power, Speed, and Impeller Diameter

In the field of engineering, power is defined as the ability to do work. Units for power are the horsepower (HP) and the kilowatt (KW). In centrifugal pump system there are three different powers involved. These are hydraulic horsepower, brake horsepower, and drive or motor horsepower. Hydraulic horsepower, is the power imparted to the liquid by the pump. It is defined by the following formula [19].

$$P_{Hyd} = \frac{Q.\rho.g.H}{3.6*10^3} \quad \text{..... (Eq. 2.7)}$$

Where,

P_{Hyd} = hydraulic power (KW)

q = flow capacity (m^3/h)

ρ = density of fluid (kg/m^3)

g = gravity (9.81 m/s^2)

h = differential head (m)

The hydraulic Horse Power can be also calculated as:

$$P_H(HP) = \frac{P_H(KW)}{0.746} \quad \text{(Eq. 2.8)}$$

or can be multiply kilowatts by 1.341 to obtain horsepower.

To provide a certain amount of power to the liquid a larger amount of power must be provided to the pump shaft to overcome inherent losses. The hydraulic efficiency is a measure of these losses and is the comparison of power input to the pump shaft to that of the power transferred to the liquid. The power delivered to the pump shaft is known as absorbed power P_a is defined by the following formula,

$$P_a = \rho \frac{QH}{102 .\eta} \text{ [KW]} \quad \text{(Eq. 2.9)}$$

Where,

Pa = absorbed power, kw

Q = flow rate, l/s

H = head, m

η = efficiency

ρ = Density, Kg/m^3

Rotational speed is the scalar quantity of the dynamics term known as angular velocity. Rotational speed is generally referred to simply as speed. The unit of revolutions per minute (rpm) is used in conjunction with speed. Centrifugal pumps are generally driven by AC induction motors and therefore have speed multiples at or near 60 depending on a consideration known as the slip factor [18]. Variable frequency AC drives have gained in popularity and allow for variable pump speeds and improved efficiencies [19].

Impellers are basically discs with outwardly radiating vanes which when rotated impart the motive centrifugal hydraulic force to the fluid being pumped. The impeller is mounted on the pump shaft and within the pump casing. Impeller diameter is 2X the distance of a line passing through the pump shaft center to the impeller periphery.

What is important about the diameter variable is that the peripheral velocity, which is directly proportional to the diameter, is directly relatable to the pump head developed. The impeller diameter is variable by virtue of the fact that the maximum dimension can be turned down or trimmed to produce a smaller diameter and thereby result in a lesser amount of centrifugal force delivered to the fluid. On the other hand, a pump operating with an undersized impeller can be retrofitted with a larger impeller up to the maximum that can be accommodated by the casing geometry [19].

2.4. Net Positive Suction Head

NPSH (Net Positive Suction Head) is the international dimension for the calculation of the supply conditions. The Net positive suction head is the actual positive pressure at the pump inlet over and above the vapour pressure of the liquid at the pumping temperature. The NPSH of the pump is called NPSH required, and that of the system is called NPSH available. The $NPSH_{avl}$ should be greater than the $NPSH_{req}$ in order to avoid cavitation [20].

$NPSH_{avl} > NPSH_{req}$

For safety reasons another 0.5 m should be integrated into the calculation, i.e.:

$NPSH_{avl} > NPSH_{req} + 0.5m$

Trouble free operation of centrifugal pumps is given as long as steam cannot form inside the pump, in other words, if cavitation does not occur. Therefore, the pressure at the reference point for the NPSH must be at least above the vapour pressure of the pumped liquid. The reference level for the NPSH is the center of the impeller so that for calculating the $NPSH_{avl}$ according to the equation below, the geodetic flow head in the supply mode ($H_{z,geo}$) must be set to positive and in the suction mode ($H_{s,geo}$) to negative.

$$NPSH_{avl} = \frac{p_e + p_b}{\rho g} + \frac{p_D}{\rho g} + \frac{V_e^2}{\rho g} + H_{v,s} + H_{s,geo} \ldots\ldots\ldots\ldots\ldots \text{(Eq. 2.10)}$$

Where:

p_e = Pressure at the inlet cross section of the system

p_b = Air pressure in N/m2 (consider influence of height)

p_D = Vapour pressure

ρ = Density of the fluid

g = Acceleration of the fall

V_e = Flow speed

$H_{v,s}$ = Sum of pressure drops

$H_{s,geo}$ = Height difference between liquid level in the suction tank and center of the pump suction socket

NPSH does not take into account the velocity head at the suction. There are two values of NPSH for any given set of conditions:

- Available NPSH calculated by the equation above
- Required NPSH decided by the manufacturer of the pump

Obviously, the Available NPSH must never be less than the required NPSH if cavitation is to be avoided. [18].

Cavitation arises when the velocity head of the liquid being accelerated in its passage through the pump reduces its absolute pressure. Owing to the high specific volume of vapour compared with liquid, the effect of the implosions is evident in the rapid wear of the pump walls which cause a substantial drop in efficiency. It's not easy to predict the onset of cavitation from general rules so the manufacturer's recommendation should be followed.

2.5. Pressure Drops

Essential for the design of a pump are not only the NPSH, flow head and flow rate, but also pressure drops. Pressure drops H_v of the plant can be determined by help of tables and diagrams. Basis are the equations for pressure drops in pipes used for fluid mechanics that will not be handled any further [20].

Pressure drops of a plant may be caused by pressure drops in the pipe system and installed components like valves, bends, inline measurement instruments, etc.

Pressure drop of the plant can be calculated from

$$H_A = H_{geo} + \sum H_V \quad \text{(Eq. 2.11)}$$

$$H_{geo} = H_{d,geo} + H_{z,geo} \quad \text{(Eq. 2.12)}$$

$$\sum H_V = H_{v,s} - H_{v,d} \ldots\ldots\ldots\ldots\ldots\ldots\ldots\ldots\ldots \textit{(Eq. 2.13)}$$

Where:

H_v = Pressure drop

$H_{v,s}$ = Total pressure drop - suction pipe

$H_{v,d}$ = Total pressure drop - delivery pipe

$H_{s,geo}$ = Geodetic head - suction pipe

$H_{z,geo}$ = Geodetic head - supply pipe

$H_{d,geo}$ = Geodetic head - delivery pipe

$H_{v,s}$= Pressure drop - suction pipe

$H_{v,d}$= Pressure drop - delivery pipe

2.6 The Affinity Laws for Variable Speed Pumping

The affinity laws are mathematic relationships that allow for the estimation of changes in pump performance as a result of a change in one of the basic pump parameters [19].

Pump variables are changed to change pump performance. For instance, it would make little sense to completely replace a given pump in order to simply reduce the head in a system. It may be more efficient to simply turndown the impeller, i.e., change the diameter variable, to produce the desired result. In so doing, how the flow rate may be affected with this new impeller diameter have to be known.

With the advent of the variable speed drive, a pump rotational speed is easily and conveniently adjusted over a broad range. This is an excellent method of controlling the flow rate of material streams in processes that require variability.

What changes in head and flow might occur with the manipulation of a pump speed using a variable drive. In another way, it may become necessary to estimate the performance of a centrifugal pump whose impeller diameter or speed may not be indicated on a standard performance curve. The approximate curves for a new impeller diameter or new speed could be determined by means of the affinity laws. In short, the affinity laws can come to the rescue of an innovative Engineer.

The premise of the first set of affinity laws is:

"For a given pump with a fixed diameter impeller, the capacity will be directly proportional to the speed, the head will be directly proportional to the square of the speed, and the required power will be directly proportional to the cube of the speed" [19].

In other word, the Affinity Laws state that: flow will change directly when there is a change in speed or diameter, heads will change as the square of a change in speed or diameter, and HP will change as the cube of a change in speed or diameter. As formula, Affinity Laws are expressed as follows [19].

For a Speed Change ($N_1 \rightarrow N_2$)

$$Q_2 = Q_1 (N_2 / N_1) \quad \textit{(Eq. 2.14)}$$

Flow rate (Q) is directly proportional to speed.

$$H_2 = H_1 (N_2 / N_1)^2 \quad \textit{(Eq. 2.15)}$$

Head (H) is proportional to the square of speed.

$$P_2 = P_1 (N_2 / N_1)^3 \quad \textit{(Eq. 2.16)}$$

Power (P) is proportional to the cube of speed.

$$NPSH_{R2} = NPSH_{R1} (N_2 / N_1)^2 \quad \textit{(Eq. 2.17)}$$

2.7. Measures for Pumping System Effectiveness

The effectiveness of a single pump is often observed with the pump efficiency [7].

$$\eta_{pump} = \frac{P_{Hyd}}{P_{in}} \quad \textit{(Eq. 2.18)}$$

Where, $P_{Hyd}(\text{kw}) = \frac{\text{Q.}\rho\text{.g.H}}{3.6*10^3}$

P_{in} represents the total input power to the pump drive train. The wire-to-water system efficiency can also be written:

$$\eta_{sys} = \eta_{pump} \cdot \eta_{motor} \cdot \eta_{VSD} \quad \textit{(Eq. 2.19)}$$

Where:

η_{motor} = the motor efficiency,

η_{vsd} = the efficiency of the VSD.

In addition to the system efficiency, the effectiveness of a pumping task can be evaluated using the specific energy consumption, which describes the energy used per pumped volume [22]. The specific energy consumption is given by;

$$E_S = \frac{P_{in}.t}{V} = \frac{P_{in}}{Q} = \frac{\rho.g.H}{\eta_{sys}} \quad \text{(Eq. 2.20)}$$

Where:

E_s = the specific energy consumption,

P_{in} = the input power,

t = time,

V = the pumped volume, and

Q_{tot} = total flow rate.

Since the delivered flow rate is often the control variable in parallel pumping, the specific energy can be seen as a justified metrics to evaluate the energy efficiency in different pumping control strategies.

The specific energy consumption in closed-loop systems or systems without static head is primarily dependent on the losses in the piping system and the system efficiency. In systems with the static head, the minimum value of specific energy is also dependent on the amount of static head and the coefficients ρ and g [22].

2.8. Pump Performance Curves and Adjusting the Output of Pumping System

Centrifugal pump basic parameters are plotted on manufacturer's performance curves. The data generated is produced by conducting operational tests of the pump with water. The presentation of these parameters is somewhat standardized on a rectangular coordinate plane. Performance curves are generated for constant speed and multiple impeller diameters represented as a family of essentially parallel decaying parabolic plots that characterize the relationship of head versus flow. Other data presented on the curves are Efficiency, BHP and $NPSH_R$

The operating point of a pump is the intersection point of the water system resistance curve and the pump Q-H curve as shown in figure 2.5 below [23]. Efficient operation is achieved when the efficiency curve is at its maximum point. However, system demand changes daily and seasonally. The working point for a fixed speed pump would shift from this optimal point to non-efficient working points and might reach to shut-off. To handle operation against these varying conditions, different pump unit

combination will be operated or pumps will be operated against partially closed valves to reduce through put.

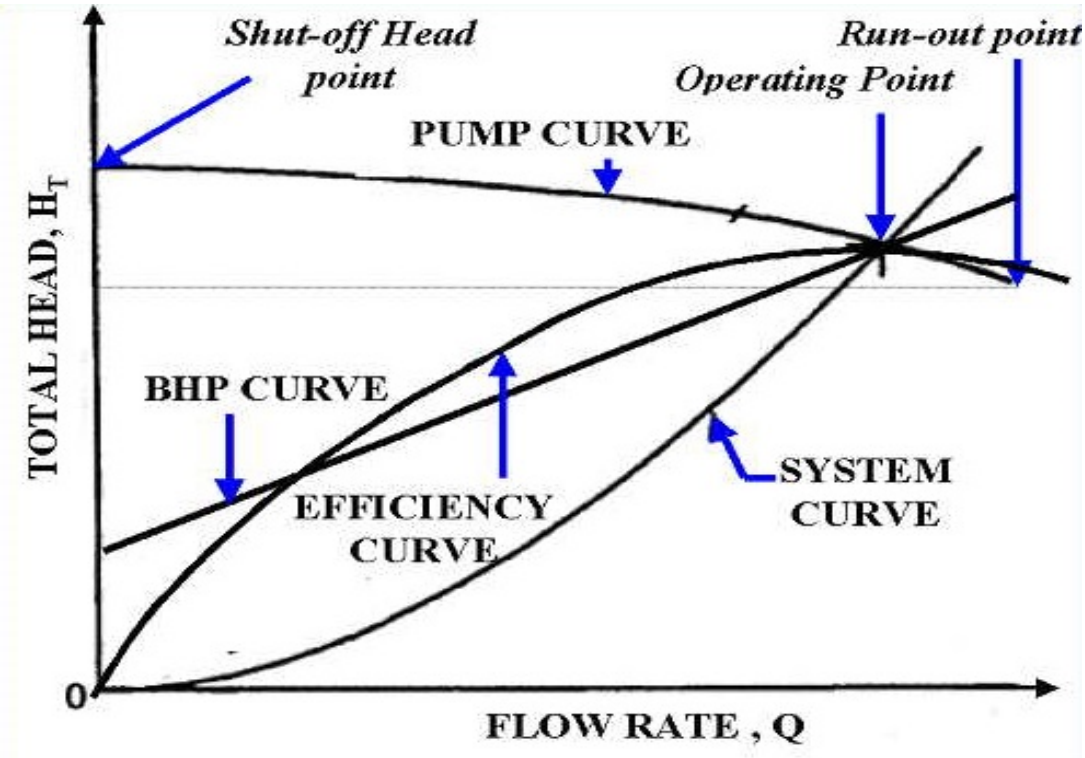

Figure 2-5 Performance curves of pump [23].

In general, the selected control method of the pumping system should be based on the process needs. The available solutions like throttling, by-pass, and rotational speed control can be evaluated, for instance in terms of a possibly varying flow or head requirements, the necessity of accurate flow adjustment, and the spread of the output requirements in the operating time span [17].

Typical methods to control the output of pumping systems are for instance the on-off method, throttling, and rotational speed control. The use of the on-off method is usually justified for applications having a tank or a reservoir and no need for accurate control of the flow rate. In pumping systems with a regular need for flow adjustment, the throttling method or rotational speed control are commonly used. The effect on the pump operation point when adjusting the output with throttling, rotational speed control, and on-off control is illustrated in Figure 2.6, which plots the QH curve of the pump and the system curve in the QH axis.

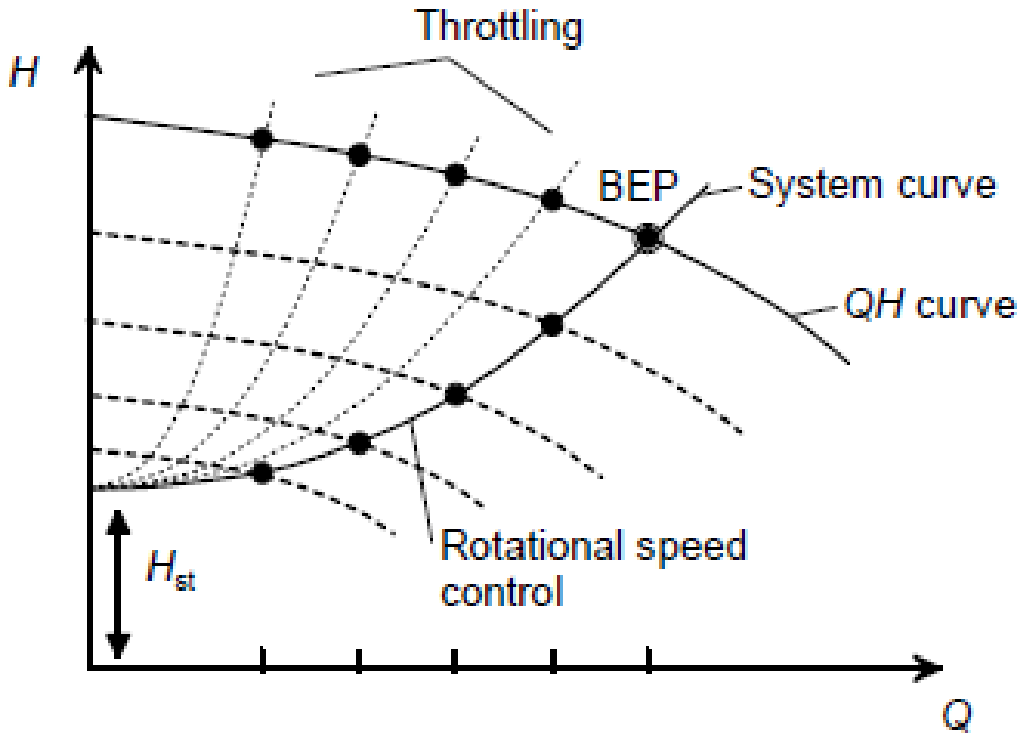

Figure 2.6: Operation points using basic flow adjustment methods [22].

In the on-off control, the pump is operating at the BEP. Reducing the output of the pump with throttling shifts the operation points along the QH curve. Correspondingly, when the output is adjusted with rotational speed control, the operation points are found along the system curve [22].

The pump is operated only at a single operation point when using the on-off control, which in this is located at the BEP as shown in Figure 2.6. Adjusting the output of the pump with throttling valve changes the dynamic head in the system causing that the system curve intersects the QH curve in new operation points. Thus, throttling the output of the pump reduces the flow rate, but the pump is forced to produce increased head. If the output of the pump is reduced with rotational speed control, the piping system characteristics remain unchanged. Instead, the pump characteristics moves down in accordance with the speed change and the operation points are found at new intersections with system curve shown in Figure 2.6 above.

The benefit of the rotational speed control is that the efficiency of the pump usually drops much less compared to the throttling adjustment, and also less energy is wasted at increased head when reducing the output of the pump [24]. This has a positive effect on the energy efficiency of pumping system, as the amount of hydraulic losses in the piping system decreases with the lower flow velocity. The amount of static head has a strong influence on the pump energy efficiency when using rotational

speed control. Figure 2.7 illustrates the operation points of the rotational speed controlled pump in two different system scenarios. In both cases, the pump operation point is located in BEP when the pump is running at nominal speed, but the static head of the system is different. As it can be seen from Figure 2.7, in the case of high static head H_{st1}, the pump has to overcome more head compared with the low static head case H_{st2}. Also, the operation points in the low static head system are located close on the line of constant best efficiency marked q' in Figure 2.7, and as a result, the efficiency of the pump remains on a good level during the adjustment. It should be noted that the line q' is a theoretical efficiency line based on the affinity laws [24].

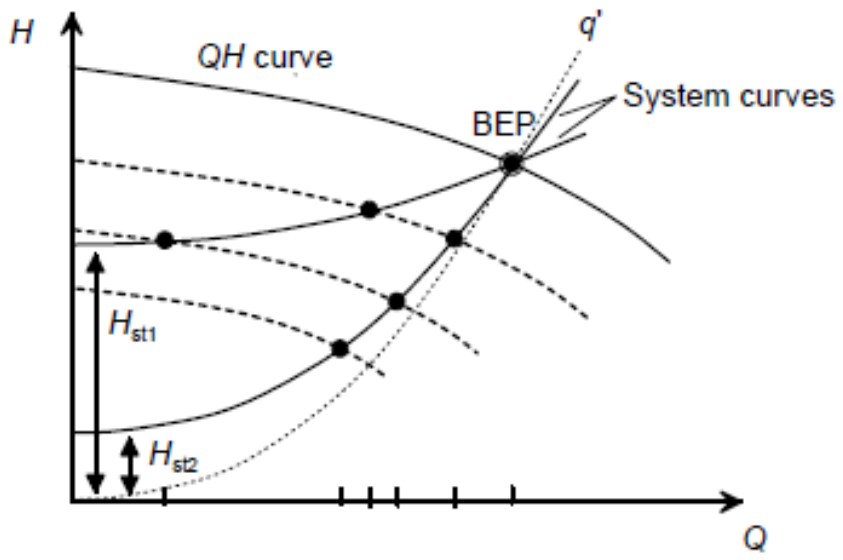

Figure 2.7. Operation points when the output of the pump is adjusted with rotational speed control in high static head and low static head systems [24].

In both system scenarios, the pump operation point is located in BEP when running the pump at nominal rotational speed. The plotted line q' illustrates the line of constant efficiency according to affinity laws [24].

In other word, Variable speed drive (VSD) for pump provides significant flexibility and improves the operation efficiency. VSD for pumps enables maintaining fixed pressure vs changing flow conditions or inversely, flow vs pressure. This flexibility reduces the number of pump start and pump stops and consequently the number of water hammers in the distribution system and the number of pipe breaks [23]. It would also enable more efficiency operation, this efficiency response provides an essential cost advantage. Keeping the operating efficiency as high as possible across variations in the system flow demand can reduce the energy and maintenance costs of the pump significantly.

2.9 Characteristics of Induction Motor

An induction or asynchronous motor is an AC electric motor in which the electric current in the rotor needed to produce torque is induced by electromagnetic induction from the magnetic field of the stator winding.

Induction motors are the most industrial plants since they are rugged, inexpensive, and less maintenance. About a third of the world's electrical energy is consumed by electric motors. Improving energy efficiency in electric device is important for economic saving and for environmental pollution reduction [25].

Induction motors have high efficiency at rated speed and torque. Energy saving can be achieved by proper section of the flux level in the motor [25]. Like any other electrical motors induction motor also have two main parts namely rotor and stator. Stator is a stationary part of induction motor, and the rotor is a rotting part of the induction motor. The rotor is connected to the mechanical load through the shaft.

Induction motors are classified into single-phase and three-phase motors according to the using power source. Single-phase induction motors are simple in construction, reliable and economical for small power rating. Also singe-phase induction motors are not self-starting, low capacity, low starting torque and less efficiency compare to three-phase induction motor. The three-phase induction motor has simpler connection, not require any starting device, higher efficiency and reliable than single-phase induction motor.

Three-phase induction motor is popular as a general purpose motor. The power source for this motors are (220V, 380/400V, 440V, 50/60HZ) [7]. The circuit diagram of three-phase induction motor and speed vs torque curve are shown in figure 2.8.

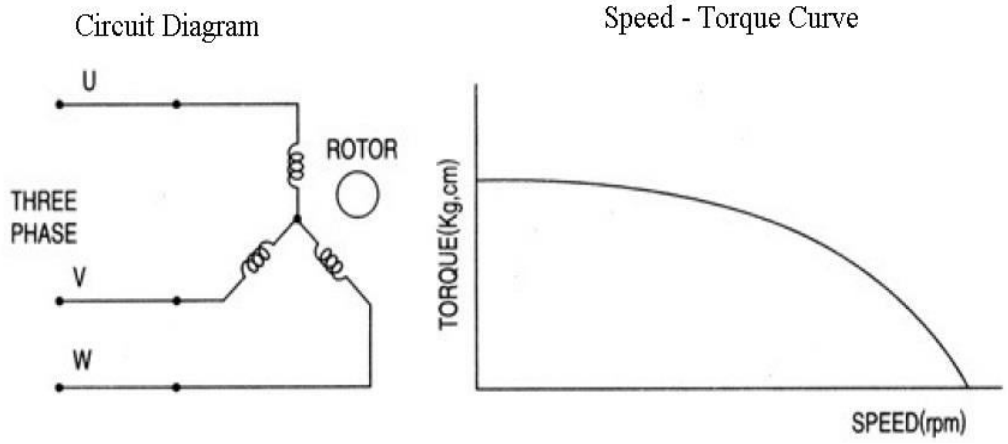

Figure 2.8 Speed-Torque curve of induction motor [25].

For a three-phase AC induction motor, the rotating magnetic field must rotate faster than the rotor to induce current in the rotor. When power is first applied to the motor with the rotor stopped, this difference in speed is at its maximum and a large amount of current is induced in the rotor. After the motor has been running long enough to get up to operating speed, the difference between the synchronous speed of the rotating magnetic field and the rotor speed is much smaller. This speed difference is called slip. Slip is expressed as a percentage of the synchronous speed [25].

$$S = \frac{n_{sync} - n_{async}}{n_{sync}} 100 \quad \text{..... (Eq. 2.21)}$$

Slip is necessary to produce torque. Slip is also dependent on load. An increase in load causes the rotor to slow down, increasing slip.

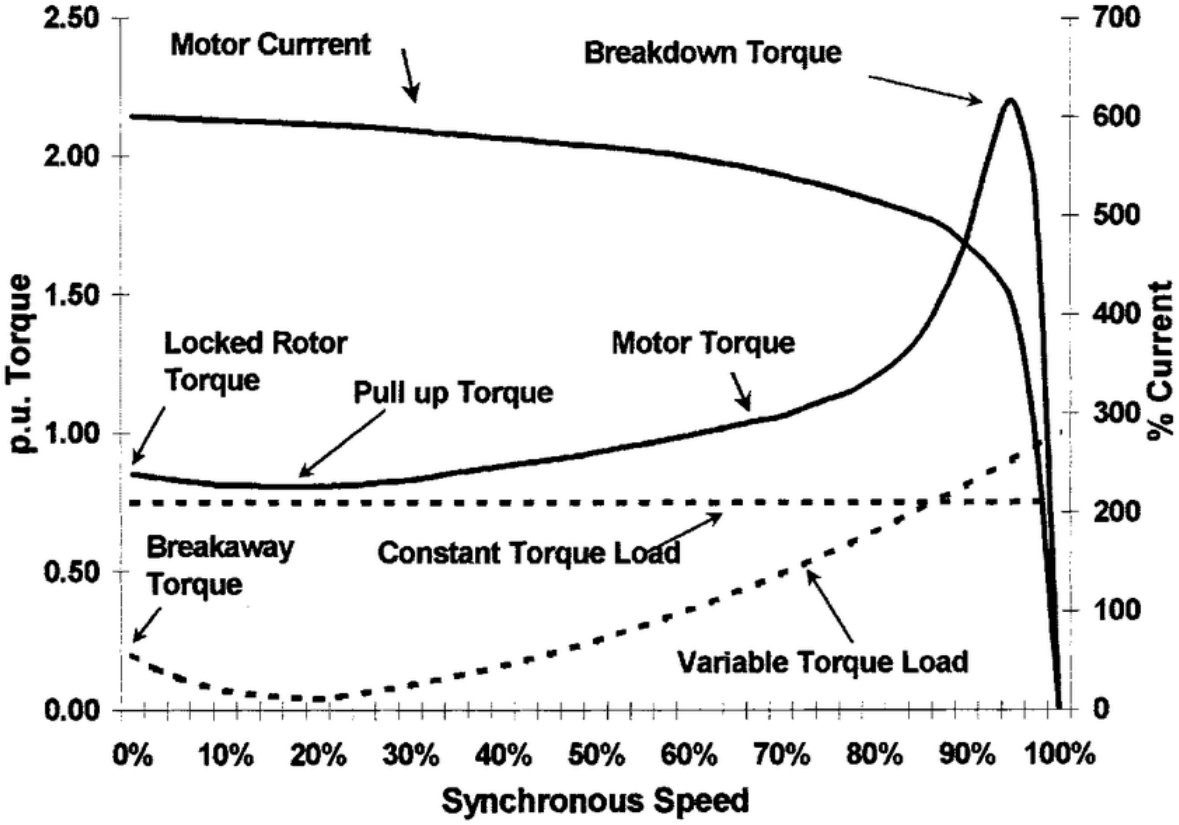

Figure 2.9 Typical Speed-Torque Curve of Three-Phase AC Induction Motor

Table 2.1 Operation of induction motor [26]

Approximate Electrical Motor Speed (RPM)				
No. Poles	Speed with Rated Load		Synchronous Speed (no Load)	
	60 HZ	50 HZ	60 HZ	50 HZ
2 Pole	3450	2850	3600	3000
4 Pole	1725	1425	1800	1500

6 Pole	1140	950	1200	1000
8 Pole	850	700	900	750

2.10 Torque Effect on Characteristics of Induction Motor

In real application, there are various kinds of load exist with different torque-speed curves, which is constant torque variable speed load, variable torque variable speed load, constant power load, constant power constant torque load and high breakaway or starting torque followed by constant torque load. The motor load system is said to be stable when the developed motor torque is equal to the required torque load. The motor will operate in a steady state at a fixed speed. The response of the motor to any disturbance gives an idea to the user about the stability of the load system. This concept will help in quickly evaluating the selection of the motor drive in a particular load.

Constant torque with variable speed

The torque required by this type of load is constant regardless of the speed. On the other hand the power is linearly proportional to the speed. Figure 2.10 shows the characteristic of Constant torque with variable speed [26].

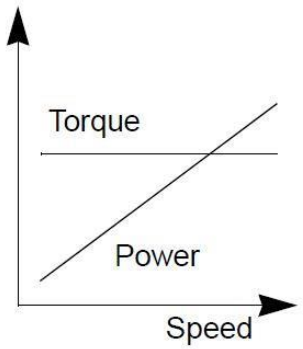

Figure 2.10: Constant torque with variable speed load.

Variable torque with variable speed

Constant torque with variable speed load motor are commonly found in industry and known as quadratic torque load. The torque is the square of the speed, while the power is the cube of the speed. This is the typical torque vs speed of pump [26].

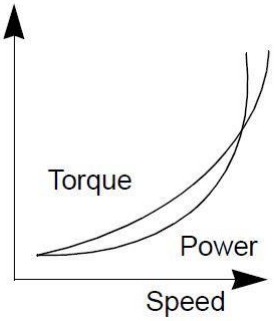

Figure 2.11: Variable torque with variable speed load.

Constant Power Load

The power remains constant while the torque varies. This type of load is rare and sometime found in industries. The torque is inversely proportional to the speed. This type of load requires high torque at low speed for the initial acceleration and then much reduced torque at running speed [26].

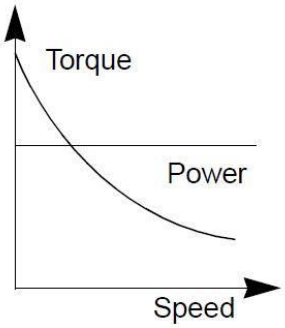

Figure 2.12: Constant Power load.

Constant Power constant Torque Load

In this type of load as speed increases the torque is constant with the power linearly increasing, when the torque start to decrease the power remains constant [26].

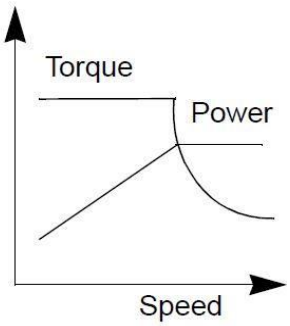

Figure 2.13: Constant Torque with Constant Power load.

2.11 Method of Starting of Induction Motor

In general, there are five basic methods of starting induction motors, these includes [7]:

- Direct on line starting (DOL)
- Star-Delta starting (Wye-delta starting)
- Autotransformer starting
- Soft starting
- Variable frequency converter

This thesis discusses using variable frequency converter for electrical deep-well submersible pumps compared with fixed speed/frequency pumps installed at Akaki Phase-3A pumping station and discuss the economic analysis of the systems. So, the focus will be particularly in two starting method which is Star-Delta starting method which is a current pumping stations starting method, and variable frequency/speed converter starting method.

2.11.1 Star-Delta/WYE-delta starting method

Star-Delta or Wye-delta starting involves connecting the motor windings first in wye during the starting period and then in delta after the motor has begun to accelerate (Figure 2.14). Wye-delta starters can be used with three-phase AC motors where all six leads of the stator windings are available, on some motors only three leads are accessible. Connected in a wye configuration, the motor starts with a significantly lower inrush current, than if the motor windings had been connected in a delta configuration [7].

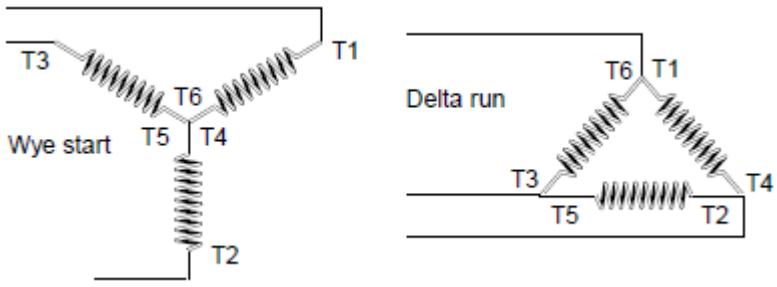

Figure 2.14: Star/Wye and delta motor winding connections.

Figure 2.15 shows a typical star-delta/wye-delta starting circuit. Transition from wye to delta is made using three contactors and a timer. The two contactors that are closed during run are often referred to

as the main contactor (M1) and the delta contactor (M2). The third contactor (S) is the wye contactor and that carries wye current only while the motor is connected in wye.

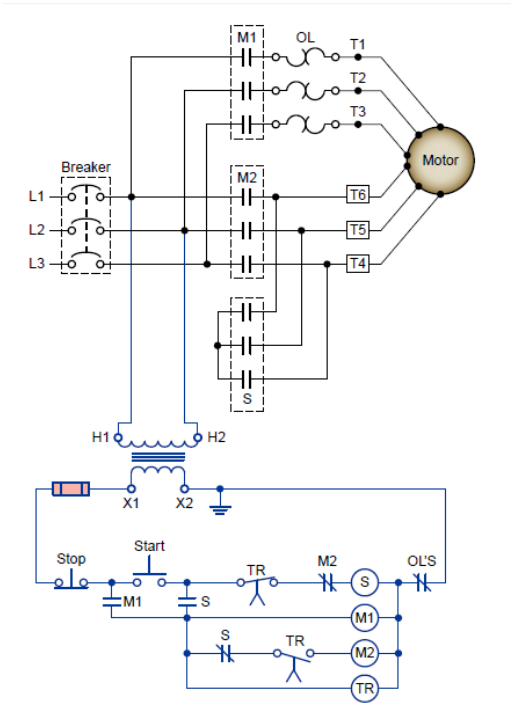

Figure 2.15: Typical star-delta/wye-delta starting circuit.

Operation of the circuit can be summarized as follows [7]:

- When the start push button is pressed, contactor S coil is energized.
- The S main power contacts close to connect the motor windings in a wye (or star) configuration.
- The normally open S auxiliary contact closes to energize timer coil TR and contactor coil M1
- The M1 main power contacts close to apply voltage to the wye-connected motor windings.
- Normally open auxiliary contacts S and M1 close to seal in and maintain timer coil S.
- After the time delay period has elapsed, the TR contacts change state to de-energize contactor coil S and energize contactor coil M2.
- S main power contacts, which hold the motor windings in a wye arrangement, open.
- The M2 contacts close and cause the motor windings to be connected in a delta configuration. The motor then continues to run with the motor connected in a delta arrangement.
- In most wye-delta starters, contactors S and M2 are electrically and mechanically interlocked. If both contactors were to be energized at the same time, the result would be a line-to-line short.

- With this type of open transition starter, there is a very short period of time where no voltage is applied to the motor during transition from wye to delta connections. This condition can cause current surges or disturbances to be fed back into the main power source. The magnitude of the surges is proportional to the phase difference between the voltage generated by the running motor and the power source. These transients can in some instances affect other equipment that is sensitive to current surges.

2.11.2 Variable Speed/Frequency Converter starting method

2.11.2.1 Variable speed drive (VSD) Description

Squirrel-cage induction motors are the most common three-phase motors. The preferred method of speed control for squirrel-cage induction motors is to alter the frequency of the supply voltage. Since the basis of the drive's operation is to vary the frequency to the motor in order to vary the speed. The best suited name for the system is the variable frequency drive (VFD). However, other names used to reference this type of drive include adjustable-speed drive (ASD), adjustable-frequency drive (AFD), variable-speed drive (VSD), and frequency converter (FC).

A VFD controls the speed, torque, and direction of an AC induction motor. It takes fixed voltage and frequency AC input and converts it to a variable voltage and frequency AC output. Figure 2.16 shows the block diagram of a typical three-phase variable-frequency drive controller [7].

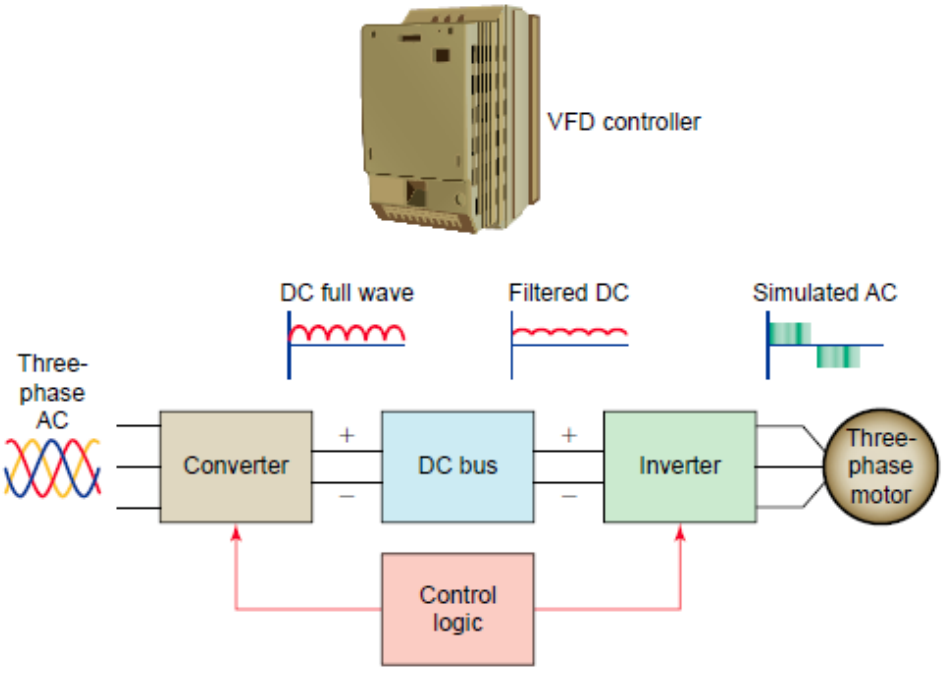

Figure 2.16 Block diagram of a typical three-phase variable-frequency drive [7].

The function of each block is as follows:

Converter: A full-wave rectifier that converts the applied AC to DC.

DC bus: Also referred to as a DC link, connects the rectifier output to the input of the inverter. The DC bus functions as a filter to smooth the uneven, rippled output to ensure that the rectified output resembles as closely as possible pure DC.

Inverter: The inverter takes the filtered DC from the DC bus and converts it into a pulsating DC waveform. By controlling the output of the inverter, the pulsating DC waveform can simulate an AC waveform at different frequencies.

Control logic: The control logic system generates the necessary pulses used to control the firing of the power semiconductor devices such as and transistors. Fairly involved control circuitry coordinates the switching of power devices, typically through a control board that dictates the firing of power components in the proper sequence. An embedded microprocessor is used for all internal logic and decision requirements.

Sometimes called the front end of the VFD, the converter is commonly a three-phase, full-wave bridge rectifier. However, one of the advantages of variable frequency drives is being able to operate a three-phase AC motor from a single-phase AC supply. The key to this is process is the rectification of the AC input to a DC output. At this rectification point, the DC voltage has no phase characteristics; the VFD is simply producing a filtered pulsating DC waveform. The drive inverts the DC waveform into three different pulse-width modulated waveform signatures that duplicate an AC three-phase waveform.

AC input voltage levels that are different from that required to operate the motor require the converter section to raise or lower the voltage to the proper operating level of the motor. As an example, an electric motor drive supplied with 115 V AC that must deliver 230 V AC to the motor requires a transformer capable of stepping up the input voltage [7]. The VFD offers an alternative to other forms of power conversion in areas where three-phase power is unavailable.

Since it converts incoming AC power to DC, the VFD really doesn’t care if its source is single or three phase. Regardless of the input power, its output will always be three phase. Drive sizing, however, is a factor since it must be capable of rectifying the higher-current, single-phase source. As a rule of thumb, most manufacturers recommend doubling the normal three-phase capacity of a drive that will be operating on a single-phase input.

Figure 2.17 shows a simplified diagram of the three sections of a variable-speed drive. The control logic and inverter section control the output voltage and frequency to the motor. Six switching transistors are used in the inverter section. The control logic uses a microcontroller to switch the transistors on and off at the proper time. The main objective of the VFD is to vary the speed of the motor while providing the closest approximation to a sine wave for current [23].

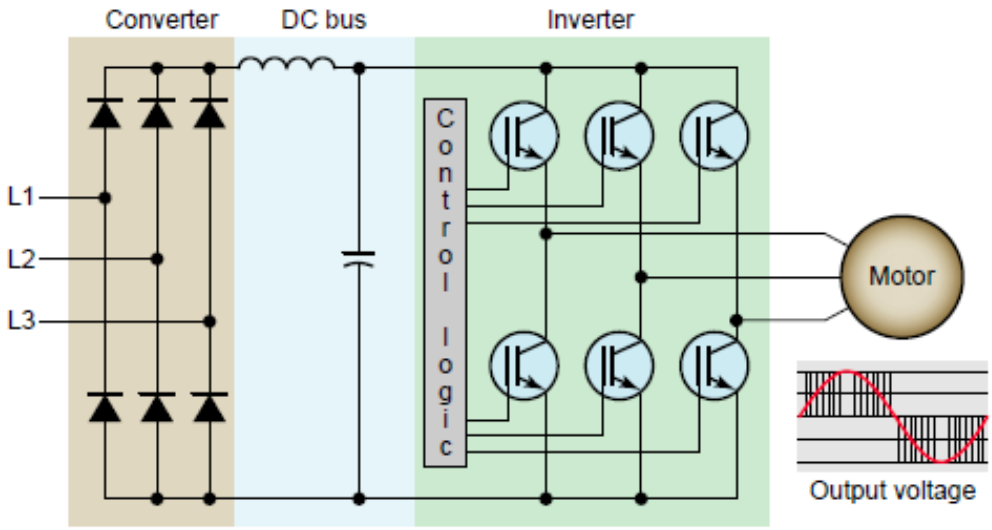

Figure 2.17: A simplified diagram of the three sections of a variable-speed drive [23].

In the simplest circuit implementation, two IGBTs are placed in series across the DC supply and are switched on and off to generate one phase of the three phases for the motor. Two other identical circuits generate the other two phases.

2.11.2.2 How Drive Changes Motor Speed

As the drive provides the frequency and voltage of output necessary to change the speed of a motor, this is done through Pulse Width Modulation Drives. Pulse width modulation (PWM) inverter produces pulses of varying widths which are combined to build the required waveform [23].

Figure 2.18 shows a simplified circuit of a pulse width modulation (PWM) inverter. Switches are used to illustrate the way that the transistors are switched to produce one phase (A to B) of the three-phase output. The output voltage is switched from positive to negative by opening and closing the switches in a specific sequence of steps.

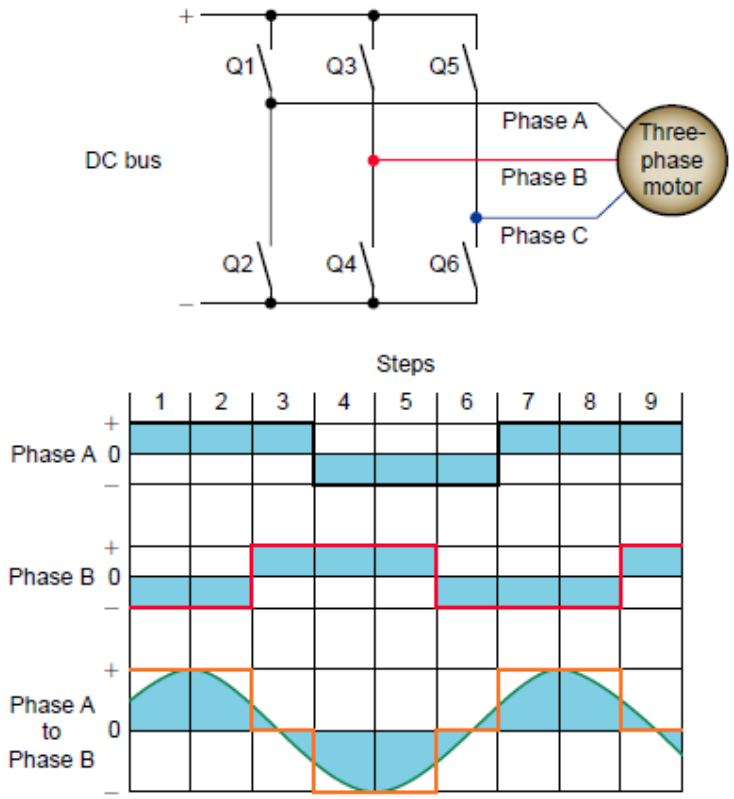

Figure 2.18: A simplified circuit of a pulse-width modulation (PWM) inverter [23].

The operation can be summarized as follows:

- During steps 1 and 2, transistor switches Q1 and Q4 are closed.
- The voltage from phase A to B is positive.
- During step 3, transistor switches Q1 and Q3 are closed.
- The difference in voltage between phase A and phase B is zero, resulting in zero output voltage.
- During steps 4 and 5, transistor switches Q2 and Q3 are closed.
- This results in a negative voltage between phases A and B.
- The other steps continue in a similar manner.
- Output voltage is dependent on the state of the switches (open or closed), and the frequency is dependent on the speed of switching.

CHAPTER 3

3. Studies Types of Pumps used and Evaluate the Current Pumps Based on Mechanical and Electrical Characteristic

3.1. Introduction to the Water Wells

In this chapter a description of the design system of the well field and evaluation of the pumping system will be presented with all the necessary information that is needed to understand the design system and current system working performance.

Water well is a hole used for the purpose of extracting groundwater from the ground. This thesis focused on vertical water production deep wells commonly used to supply water for the half of Addis Ababa city for domestic and municipal propose. Seventeen vertical deep wells in Akaki Phase-3A project, which is a new project and actively demanding water to the city, were conducted.

Figure 3.1: Well layout of Akakai Phase 3A project.

3.2 Well Field Pumping System

In Akaki well field Phase-3A project pumping system 17 high discharge and high head capacity submersible pumps has been used to pump the water from deep well as shown in the site layout diagram figure 3.2 and the table design data of the wells and proposed pumps and piping for the system. The installation system of all boreholes are open tank type, which is the groundwater is pumped directly to the reservoir by supply system piping network.

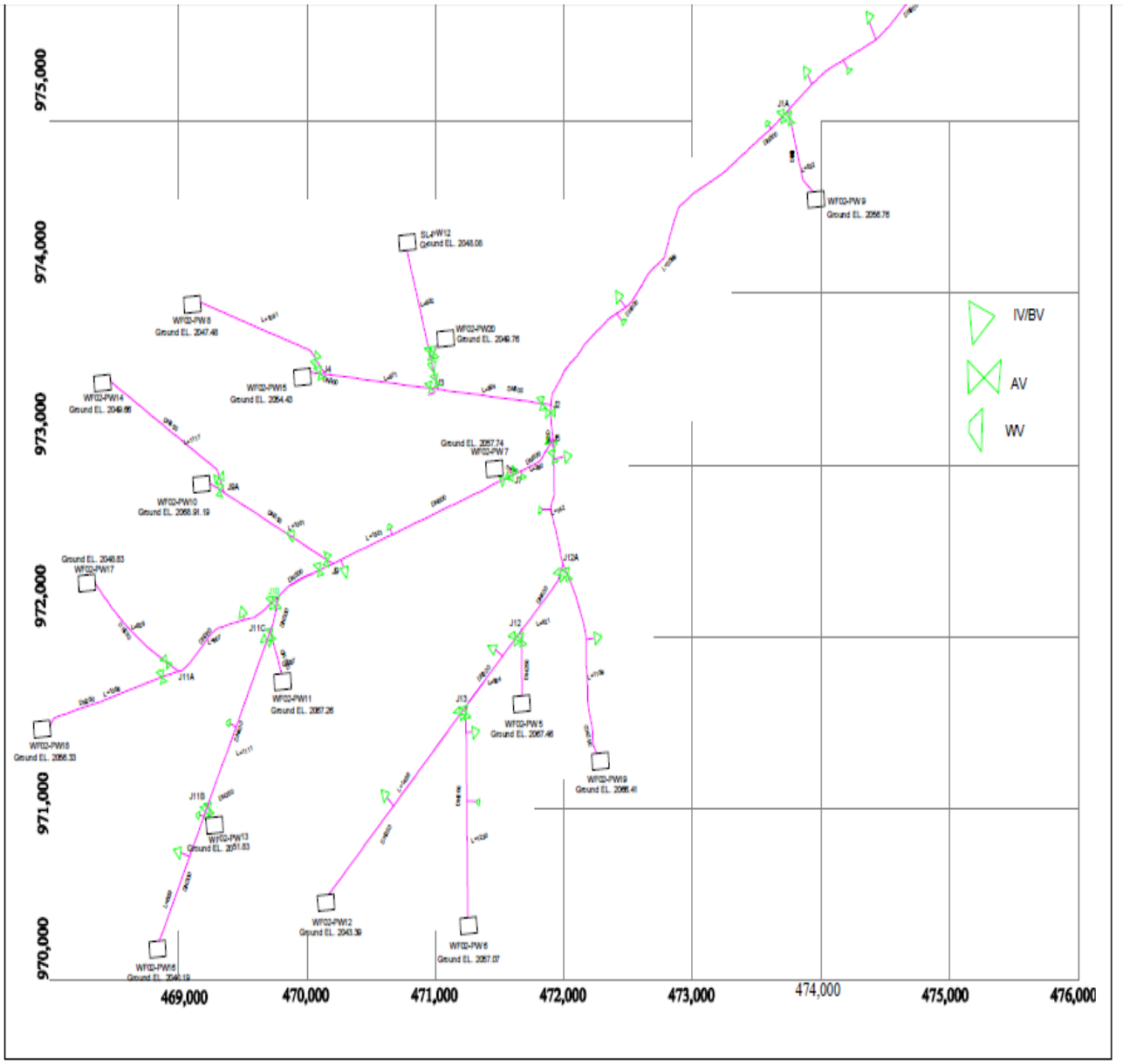

Figure 3.2: Site layout of Akakai Phase-3A project.

Table 3.1 Pumping System Wells Design

N°	Site Name	Ground Level (m)	Casing Dia (inch)	Well Depth (m)	Static Level (MASL)	Dynamic Level (MASL)	Pump Position (m)	Proposed Pump Size					Steel Riser Pipe dia (mm)
								Pump model	Motor Power (KW)	Discharge (L/S)	Head (m)	Eff (%)	
1	WF02-PW5	2,046.00	12”	498.6	1,965.90	1,963.61	130	PN 104-5a + MI10-740/2	140	50	140	75	DN 150
2	WF02-PW6	2,067.00	12”	500	1,993.16	1,957.66	120	PN 101-7a + MI10-490/2	90	30	170	75	DN 150
3	WF02-PW7R	2,057.00	14”	550	2,003.28	1,909.29	190	QN 102-8a + VNI12-110/2	250	80	200	76	DN 200
4	WF02-PW8	2,063.00	14”	502	2,017.26	1,959.70	120	PN 104-5a + MI10-740/2	140	50	140	74	DN 150
5	WF02-PW9	2,064.00	14”	505	2,013.27	1,992.44	120	QN 102-6a + MI10-960/2	190	80	140	75	DN 200
6	WF02-PW10	2,071.00	14”	500	1,986.25	1,962.36	132	PN 104-6 + MI10-880/2	75	50	180	75	DN 150
7	WF02-PW11	2,075.00	14”	341	1,991.60	1,970.00	130	QN 102-6a + MI10-880/2	170	70	140	75	DN 200
8	WF02-PW12	2,048.00	12”	520	1,986.80	1,953.20	150	QN 101-7a + MI10-880/2	170	60	170	74	DN 150
9	SL-PW-12	2,046.00	14”	320	1,996.55	1,990.05	81	QN 102-6a + MI10-960/2	190	80	140	75	DN 200
10	WF02-PW13	2,066.00	14”	342	2,001.19	1,994.96	110	QN 102-6a + MI10-880/2	170	70	140	75	DN 200
11	WF02-PW14	2,062.00	14”	500	2,008.60	1,978.56	120	QN 102-6a + MI10-960/2	170	70	150	75	DN 200
12	WF02-PW15	2,064.00	14”	540	2,011.27	1,931.91	150	QN 103-8 + VNI12-120/2	270	100	170	76	DN 200
13	WF02-PW16	2,064.00	14”	493	2,008.95	1,982.59	110	QN 102-6a + MI10-960/2	190	80	140	75	DN 200
14	WF02-PW17	2,061.00	14”	480	1,999.38	1,971.89	120	QN 102-7a + MI10-1070/2	210	80	160	75	DN 200
15	WF02-PW18	2,066.00	14”	496	2,008.20	1,963.95	120	QN 102-6a + MI10-880/2	170	70	140	75	DN 200
16	WF02-PW19	2,067.00	14"	550	1,984.30	1,892.40	200	PN 101-7a + MI10-490/2	110	30	190	75	DN 150
17	WF02-PW20	2,056.00	12	379	2,012.00	1,997.80	100	QN 102-7a + MI10-1070/2	210	80	160	75	DN 200

The supply network consists of a pipe network and different pumping stations and water collector reservoirs until the water delivered to the demand side. These pumping stations are operationally the most important and needed high more focuses of all the pumping stations. In general, the pumping station consists of head work pipes and pumps. Head work pipe work of pumping stations consists of riser pipes and head work and pump installation include shut-off and back-pressure valves, flow measuring equipment (electromagnetic flow meter), pressure valves, pressure measuring pressure gauge and remote controlling system. In submersible pumps the suction pipes is not needed.

The operation of the pumps in the system is based on all duty configuration for the submersible pumps and duty-stand by configuration for the surface pumps. The start and stop levels for operation of pumps are specified at design stage. When the service water reservoir tank in the network is start to drop from the start level, the pumps start to operate. Correspondingly, when the level of the reservoirs exceed to the stop level, the pump stops. This makes the pumps to operate according to the different level of collector reservoirs on the system.

Controlling the operation system and collector reservoir level in the network is based on sensor providing information. The typical methods for controlling the every station are electro-magnetic flow meter, float switches, pressure transmitters and computer based SCADA system as shown in figure 3.3 below.

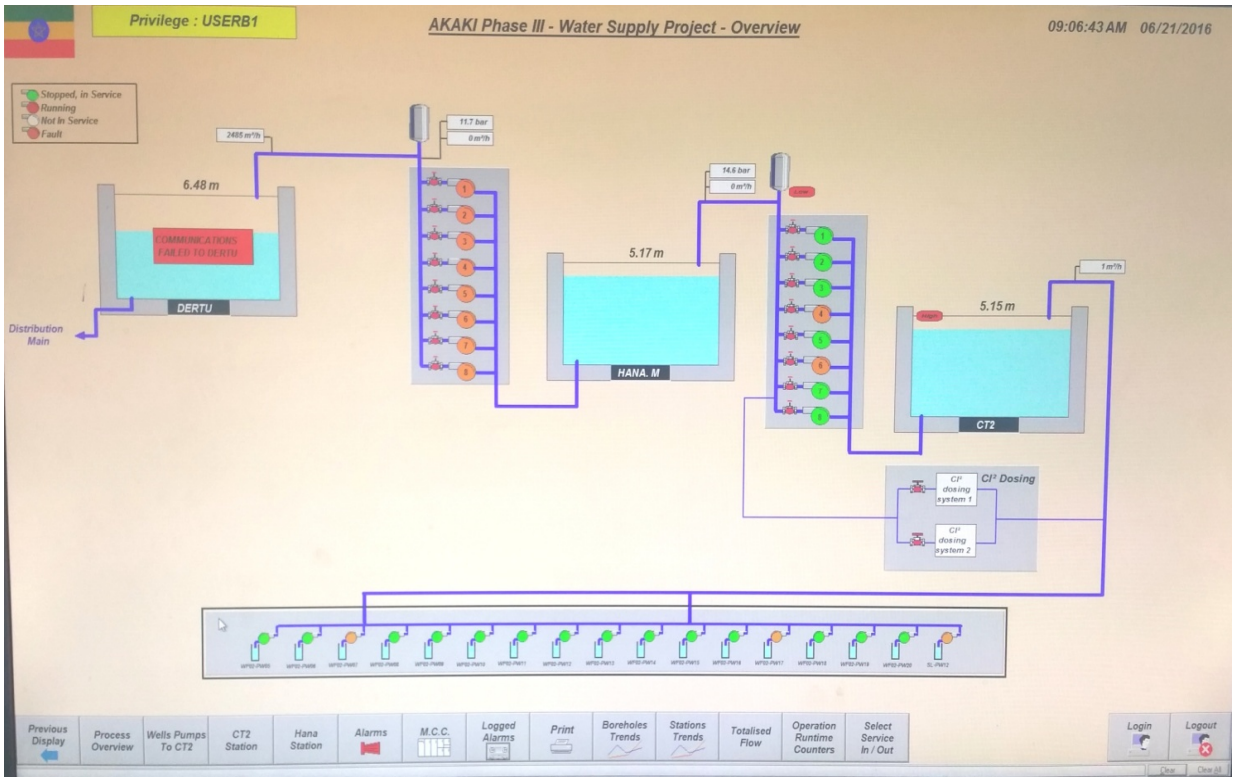

Figure 3.3: SCADA system overview of Akakai Phase 3A project.

3.3. Types of Pump Used

The submersible pumps are manufactured by Flowserve Hamburg GmbH as per the design requirements. Appendix A. figures shows the technical data and individual pump performance characteristics curve [37].

3.4. Performance Evaluation of Pumps

17 submersible pumps works together by one piping system networking in Phase-3A well field water pumping system. In this thesis, 10 submersible pumps will be selected, according to the availability of full design and operation data, and conducted for performance evaluation of the water pumping system at Akaki well-field. From manufacturer characteristic curve evaluation of the actual system deep-wells discharge and pumps design discharge for each submersible pumps will be discuss in detail graphically and also effectiveness of pumps are often observed with the pump efficiency equations.

WF02-PW05 well, design data of pump model PN 104-5a + MI10-740/2, discharge Q= 180m^3/hr, total head H=140 m, power P=140 kw and maximum pump efficiency η =75%.

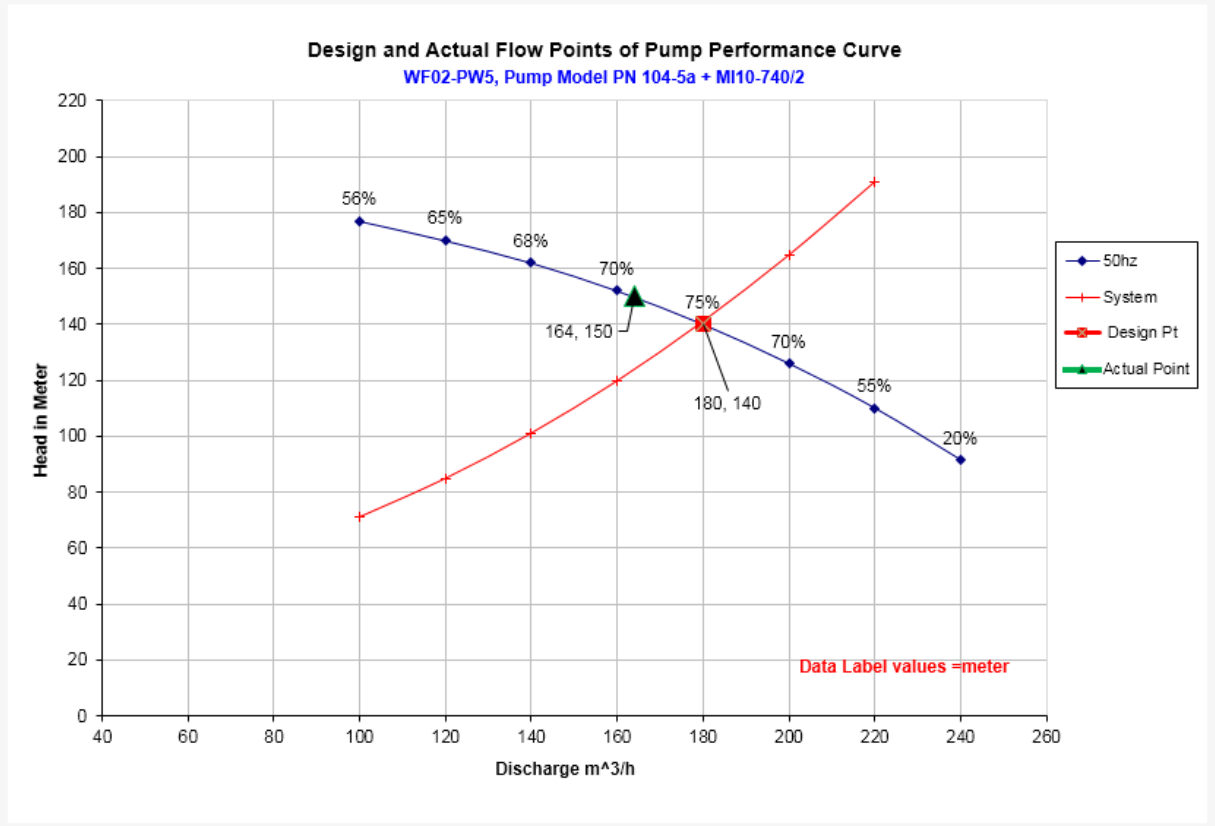

Figure 3.4 Performance Evaluation curve for well name WF02-PW05

Characteristic curve range of head and quantity delivered shall be capable of operating the pump against maximum run out conditions.

The actual flow rate delivered to the system from this pump is lower by 16m^3/hr than design flow rate. The efficiency at this flow rate as shown in manufacturer curve are less than 70% and Head H=148m.

And also the effectiveness of a single pump is often observed with the pump efficiency from equation 2.18 and equation 2.7,

$$\eta_{pump} = \frac{P_{Hyd}}{P_{in}}$$

Where: $P_{Hyd} = \frac{Q.\rho.g.H}{3.6*10^3}$

Pin = Input power, (kw)

Q = flow rate, m^3/h

H = head, m

η = efficiency

g = gravity (9.81 m/s^2)

ρ = Density of water, (1000Kg/m^3)

Power convert to watt, hour=60s * 60m = 3.6 x 10^3

Using pumping system data collected from SCADA telemetry system and borehole site efficiency of this pump can be calculated as:

The measurement data of pump motor model M10 740-2, are power P=140 Kw, Rated Current I=275 A and voltage V=400V +10/-10%

The actual pumping process data of the motor are as follows. The three phase voltage from EEU line read from the switch gear read V=380V and the motor starting current I= 285A. Where average pump head are the sum of line pressure read from the pressure gauge 65m of pump position 120m, static water level 80.10m,and draw down 2.29m, H=148 m and flow read from electromagnetic flow meter Q = 164 m^3/hr.

The input power can be calculated as: AC three-phase motor

$$P_{in} = V\ x\ I\ x\ cos\emptyset\ (w),$$

Where cosφ = 0.8, power input P_{in} = 91,200 W or 92 Kw

Therefore, Pump Efficiency

$$\eta_{pump} = \frac{2.275x164x148}{91200} x\ 100\% = 60.54\%$$

Where, $2.275 = \frac{\rho x g}{3.6\ x\ 10^3} = \frac{1000x9.81}{3.6\ x\ 10^3}$

WF02-PW07 well, design data of pump model QN 102-8a + VNI12-110/2, discharge Q = 288m^3/hr, total head H=200 m, power P=250kw and maximum pump efficiency η =76%.

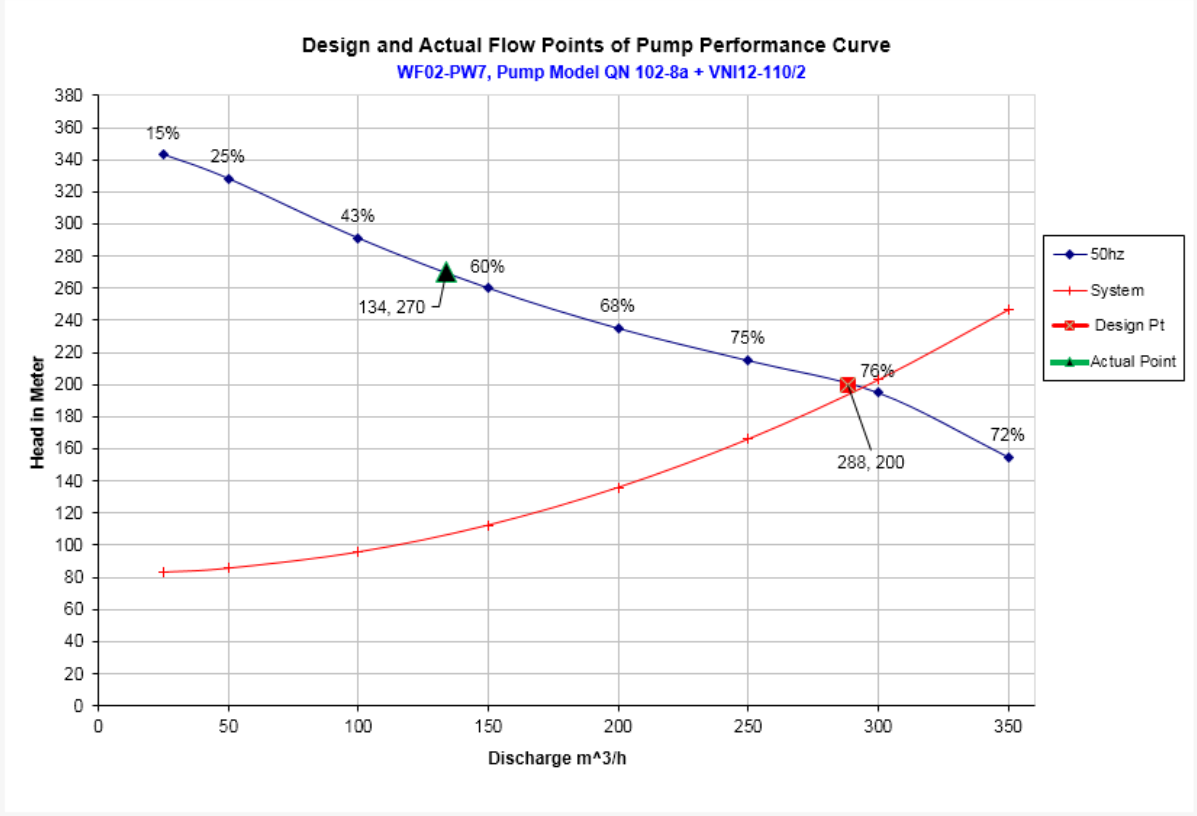

Figure 3.5 Performance Evaluation curve for well name WF02-PW07

The actual flow rate delivered to the system from this pump is lower by 150 m^3/hr than design flow rate. The efficiency at this flow rate as shown in manufacturer curve are less than 60% and Head H=270m.

The measurement data of pump motor model VNI 12-110/2, are power P=250 Kw, Rated Current I=460 A and voltage V=400V +10/-10%

The actual pumping process data of the motor are as follows. The three phase voltage from the utility line read from the switch gear read V=400V and the motor starting current I= 473A. Where average pump head are the sum of line pressure read from the pressure gauge 76m of pump position 230m, static water level 53.72m, draw down 93.99m, H=270m and flow read from electromagnetic flow meter Q = 134 m^3/hr.

The input power can be calculated as: AC three-phase motor

$$P_{in} = V\ x\ I\ x\ cos\emptyset\ \ (w),$$

Where cosφ = 0.8, power input P_{in} = 151,360 W or 152 Kw

Therefore, Pump Efficiency

$$\eta_{pump} = \frac{2.275x134x270}{151360}\ x\ 100\% = \ 54.38\%$$

Where, $2.275 = \frac{\rho x g}{3.6\ x\ 10^3} = \frac{1000x9.81}{3.6\ x\ 10^3}$

WF02-PW08 well, design data of pump model PN 104-5a + MI10-740/2, discharge Q= 180m^3/hr, total head H=140 m, power P=140 kw and maximum pump efficiency η =74%.

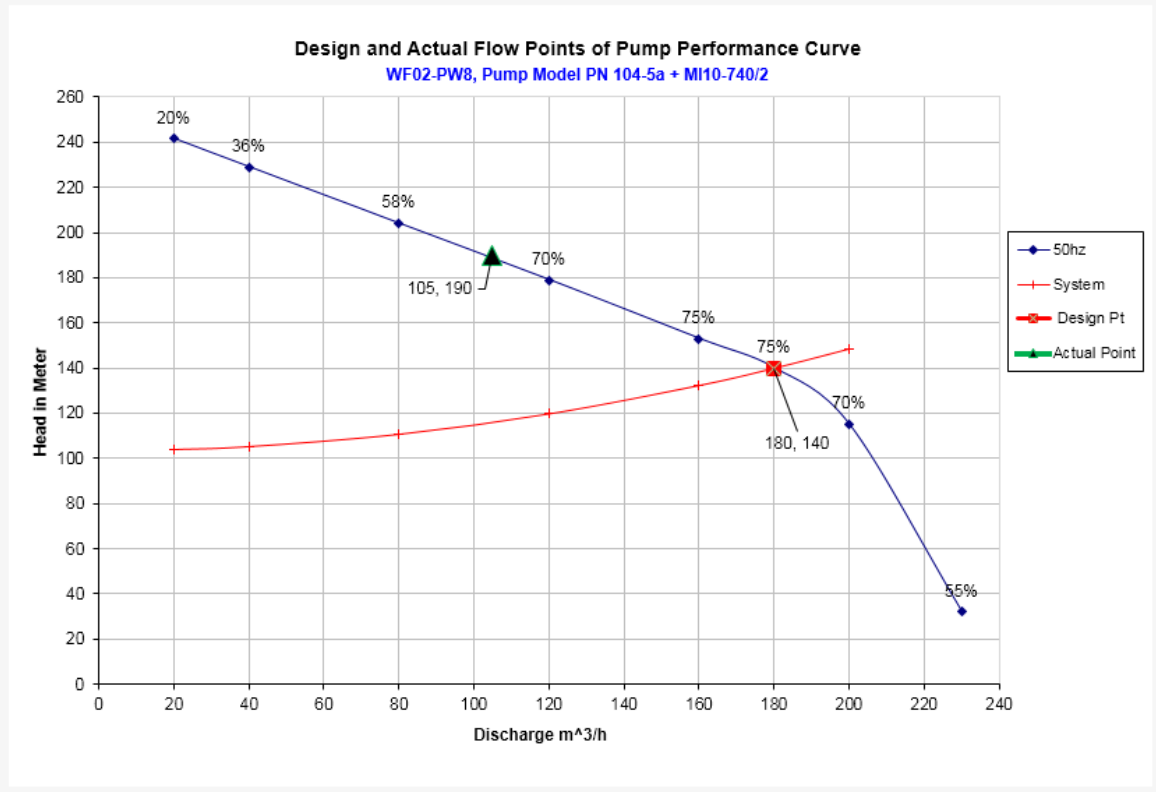

Figure 3.6 Performance Evaluation curve for well name WF02-PW08

The actual flow rate delivered to the system from this pump is lower by 75m^3/hr than design flow rate. The efficiency at this flow rate as shown in manufacturer curve are less than 60% and Head H=190m.

The measurement data of pump motor model MI10-740/2 are power P=140 Kw, Rated Current I=275 A and voltage V=400V +10/-10%

The actual pumping process data of the motor are as follows. The three phase voltage from the utility line read from the switch gear read V=400V and the motor starting current I= 280A. Where average pump head are the sum of line pressure read from the pressure gauge 72m of pump position 128m, static water level 45.74m, draw down 57.59m, H=190 m and flow read from electromagnetic flow meter Q = 105 m^3/hr.

The input power can be calculated as: AC three-phase motor

$$P_{in} = V\ x\ I\ x\ cos\emptyset\ \ (w),$$

Where cosφ = 0.8, power input P_{in} = 89,600 W or 90 Kw

Therefore, Pump Efficiency

$$\eta_{pump} = \frac{2.275x105x190}{89600} x\ 100\% = 50.65\%$$

Where, $2.275 = \frac{\rho x g}{3.6\ x\ 10^3} = \frac{1000x9.81}{3.6\ x\ 10^3}$

WF02-PW09 well, design data of pump model QN 102-6a + MI10-960/2, discharge Q = 288m^3/hr, total head H=140 m, power P =190 kw and maximum pump efficiency η =75%.

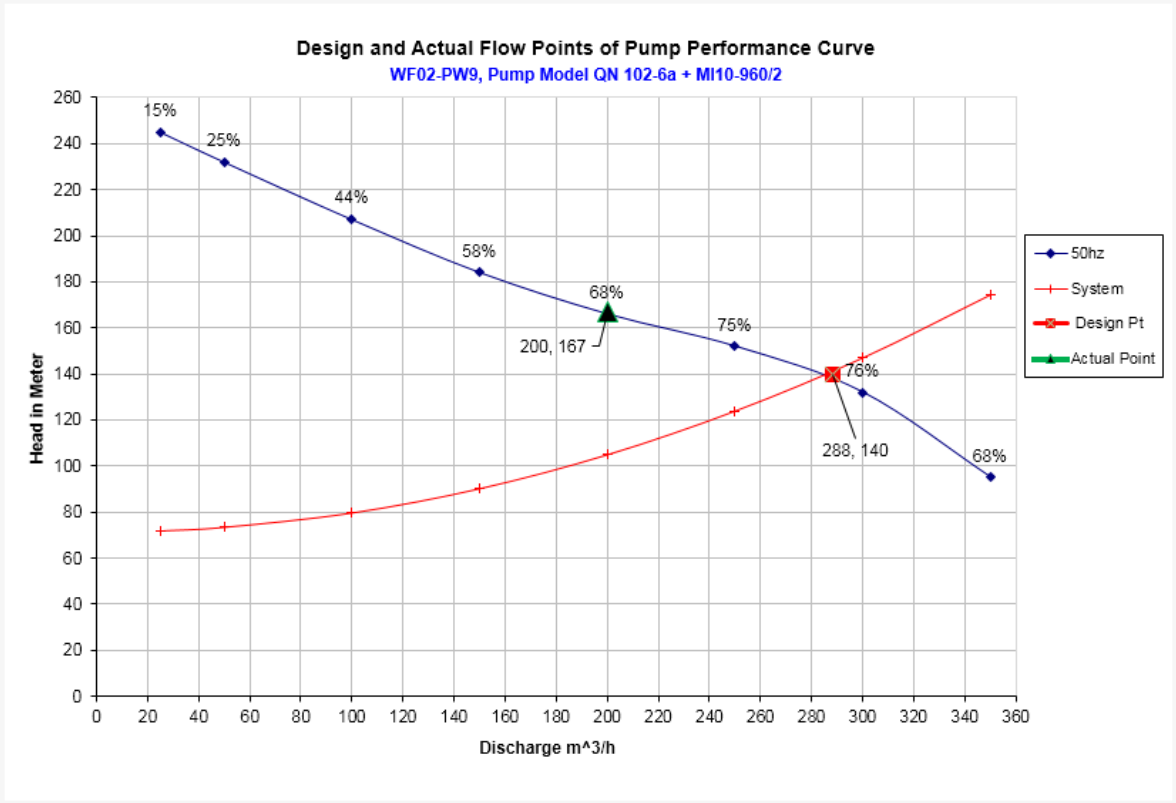

Figure 3.7 Performance Evaluation curve for well name WF02-PW09

The actual flow rate delivered to the system from this pump is lower by 88m^3/hr than design flow rate. The efficiency at this flow rate as shown in manufacturer curve are less than 60% and Head H=167m.

The measurement data of pump motor model MI10-960/2 are power P=190Kw, Rated Current I=370 A and voltage V=400V +10/-10%

The actual pumping process data of the motor are as follows. The three phase voltage from EEU line read from the switch gear read V=400V and the motor starting current I= 385A. Where average pump head are the sum of line pressure read from the pressure gauge 70m, pump position 90m, static water level 50.73m, draw down 20.83m, H=167 m (it have a throttling device) and flow read from electromagnetic flow meter Q = 200 m^3/hr.

The input power can be calculated as: AC three-phase motor

$$P_{in} = V\ x\ I\ x\ cos\emptyset\ \ (w),$$

Where cosφ = 0.8, power input P_{in} = 123,200 W or 124 Kw

Therefore, Pump Efficiency

$$\eta_{pump} = \frac{2.275x200x167}{123200} x\ 100\% = 61.67\%$$

Where, $2.275 = \frac{\rho x g}{3.6\ x\ 10^3} = \frac{1000x9.81}{3.6\ x\ 10^3}$

WF02-PW11 well, design data of pump model QN102-6a + MI10-880/2, discharge Q = 252m^3/hr, total head H=140 m, power P =170kw and maximum pump efficiency η =75%.

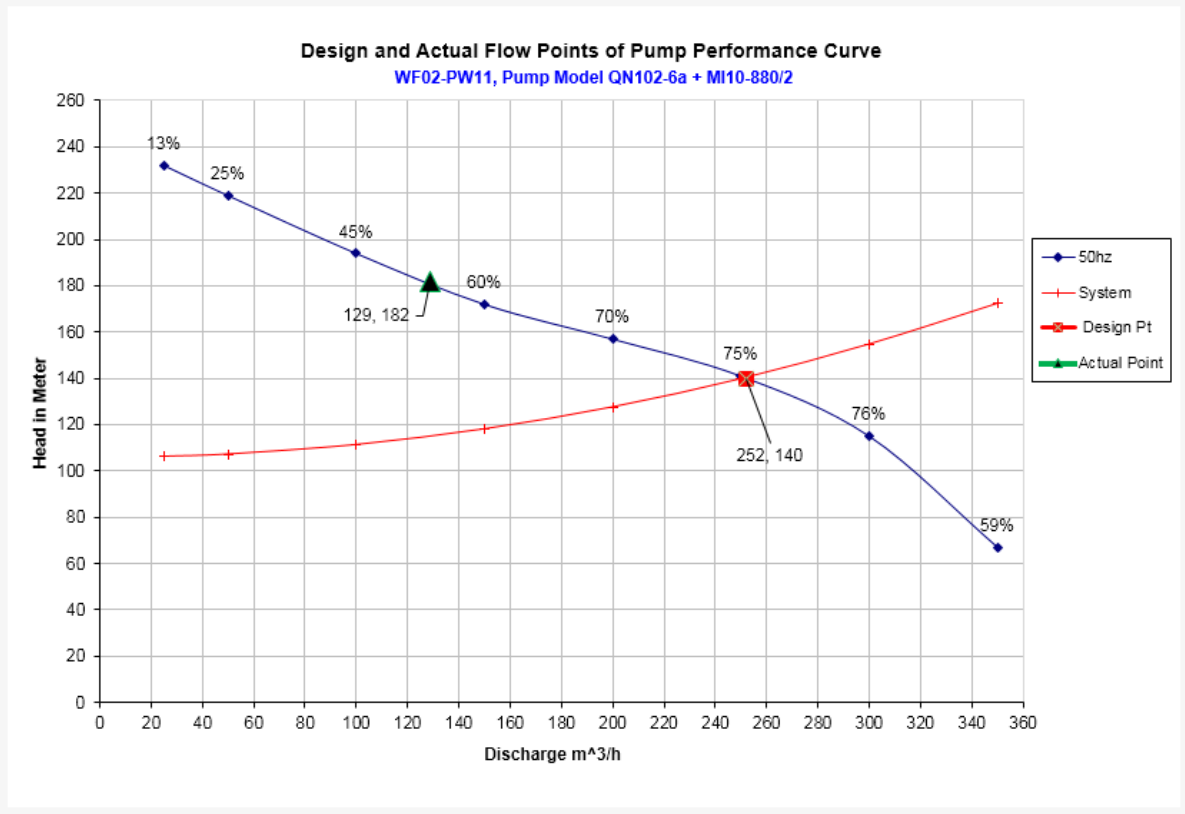

Figure 3.8 Performance Evaluation curve for well name WF02-PW11

The actual flow rate delivered to the system from this pump is lower by 123m^3/hr than design flow rate. The efficiency at this flow rate as shown in manufacturer curve are less than 60% and Head H=182m.

The measurement data of pump motor model MI10-880/2are power P=170Kw, Rated Current I=330 A and voltage V=400V +10/-10%

The actual pumping process data of the motor are as follows. The three phase voltage from the utility line read from the switch gear read V=400V and the motor starting current I= 340A. Where average pump head are the sum of line pressure read from the pressure gauge 72m, pump position 130m, static water level 83.40m, draw down 22.42m, H=182m and flow read from electromagnetic flow meter Q = 129 m^3/hr.

The input power can be calculated as: AC three-phase motor

$$P_{in} = V\ x\ I\ x\ cos\emptyset\ \ (w),$$

Where cosφ = 0.8, power input P_{in} = 108,800 W or 110 Kw

Therefore, Pump Efficiency

$$\eta_{pump} = \frac{2.275x129x182}{108800}\ x\ 100\% = 49.09\%$$

Where, $2.275 = \frac{\rho xg}{3.6\ x\ 10^3} = \frac{1000x9.81}{3.6\ x\ 10^3}$

WF02-PW12 well, design data of pump model QN101-7a + MI10-880/2, discharge Q = 216m^3/hr, total head H=170 m, power P =170kw and maximum pump efficiency η =73.5%.

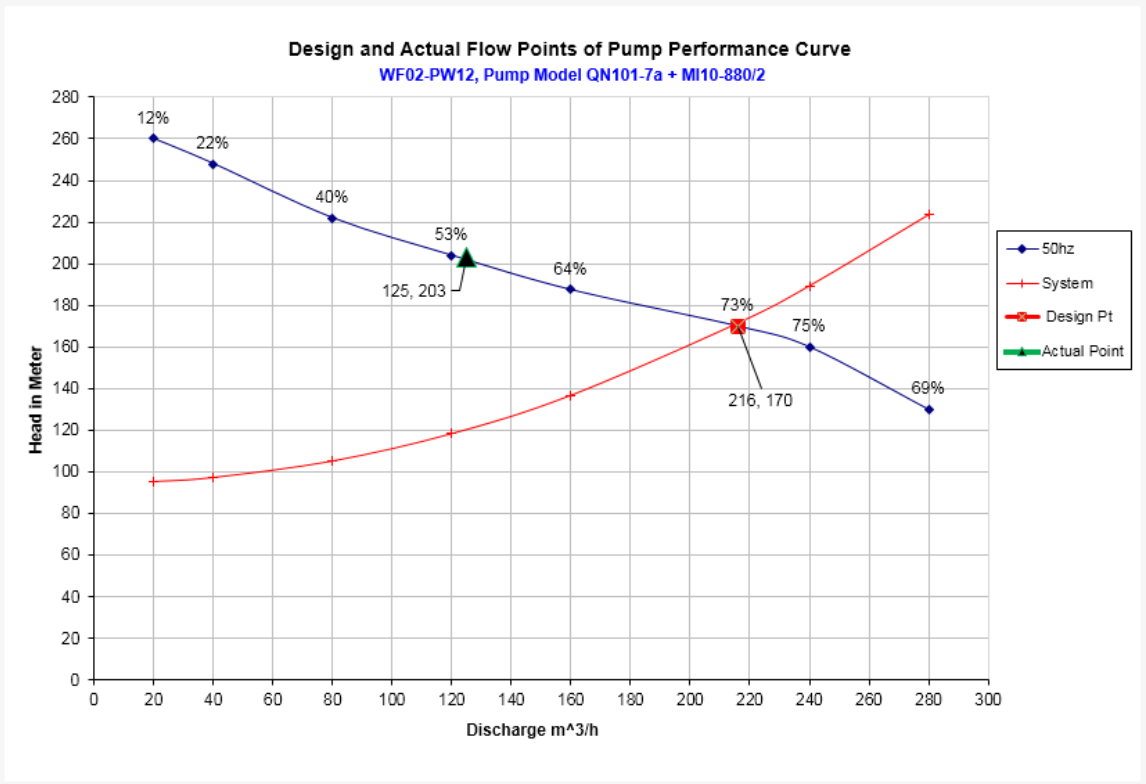

Figure 3.9 Performance Evaluation curve for well name WF02-PW12

The actual flow rate delivered to the system from this pump is lower by 91m^3/hr than design flow rate. The efficiency at this flow rate as shown in manufacturer curve are less than 60% and Head H=203m.

The measurement data of pump motor model MI10-880/2 are power P=170Kw, Rated Current I=330 A and voltage V=400V +10/-10%

The actual pumping process data of the motor are as follows. The three phase voltage from the utility line read from the switch gear read V=400V and the motor starting current I= 340A. Where average pump head are the sum of line pressure read from the pressure gauge 79m, pump position 110m, static water level 61.20m, draw down 33.56m, H=203 m and flow read from electromagnetic flow meter Q = 125 m^3/hr.

The input power can be calculated as: AC three-phase motor

$$P_{in} = V\ x\ I\ x\ cos\emptyset\ \ (w),$$

Where cosφ = 0.8, power input P_{in} = 108,800 W or 110 Kw

Therefore, Pump Efficiency

$$\eta_{pump} = \frac{2.275x125x203}{108800}\ x\ 100\% = 53.06\%$$

Where, $2.275 = \frac{\rho x g}{3.6\ x\ 10^3} = \frac{1000x9.81}{3.6\ x\ 10^3}$

WF02-PW13 well, design data of pump model QN102-6a + MI10-880/2, discharge Q = 252m^3/hr, total head H=140 m, power P =170kw and maximum pump efficiency η =75%.

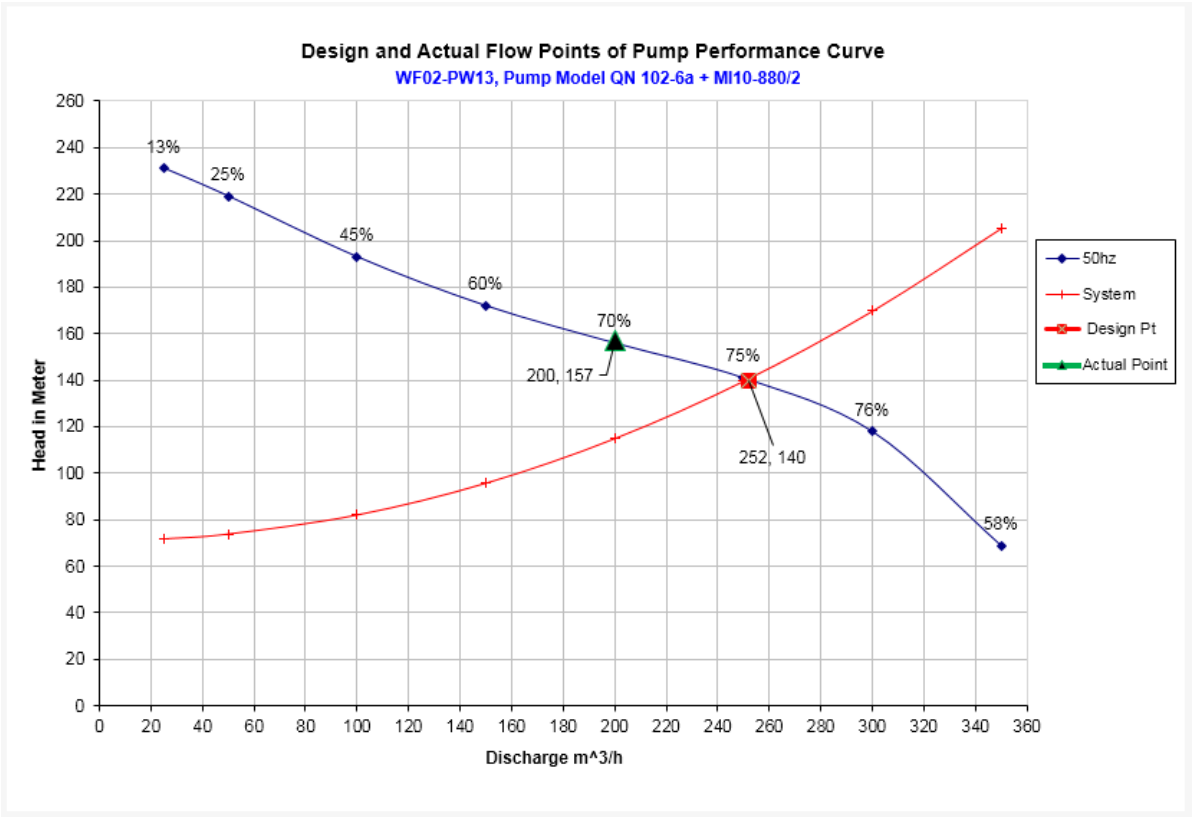

Figure 3.10 Performance Evaluation curve for well name WF02-PW13

The actual flow rate delivered to the system from this pump is lower by 52m^3/hr than design flow rate. The efficiency at this flow rate as shown in manufacturer curve are less than 70% and Head H=157m and power P=170 kw.

The measurement data of pump motor model MI10-880/2 are power P=170Kw, Rated Current I=330 A and voltage V=400V +10/-10%

The actual pumping process data of the motor are as follows. The three phase voltage from EEU line read from the switch gear read V=400V and the motor starting current I= 338A. Where average pump head are the sum of line pressure read from the pressure gauge 75m, pump position 113m, static water level 64.81m, draw down 6.23m, H=157 m and flow read from electromagnetic flow meter Q = 200 m^3/hr.

The input power can be calculated as: AC three-phase motor

$$P_{in} = V\ x\ I\ x\ cos\emptyset\ \ (w),$$

Where cosφ = 0.8, power input P_{in} = 108,160 W or 108 Kw

Therefore, Pump Efficiency

$$\eta_{pump} = \frac{2.275x200x157}{108160} x\ 100\% = 66.04\%$$

Where, $2.275 = \frac{\rho x g}{3.6\ x\ 10^3} = \frac{1000x9.81}{3.6\ x\ 10^3}$

WF02-PW14 well, design data of pump model QN102-6a + MI10-880/2, discharge Q = 252m^3/hr, total head H=150 m, power P =170kw and maximum pump efficiency η =75%.

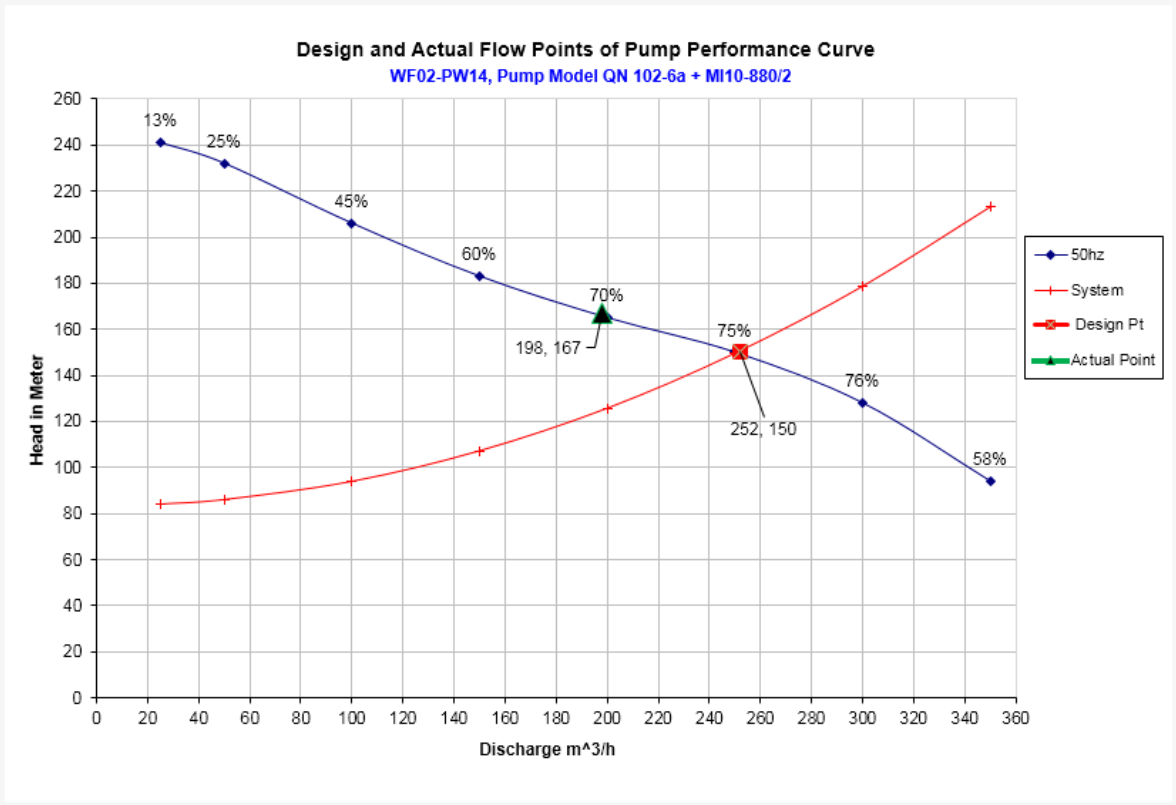

Figure 3.11 Performance Evaluation curve for well name WF02-PW14

The actual flow rate delivered to the system from this pump is lower by 54m^3/hr than design flow rate. The efficiency at this flow rate as shown in manufacturer curve are below 70% and Head H=167m and power P=190 kw.

The measurement data of pump motor model MI10-880/2 are power P=170Kw, Rated Current I=370 A and voltage V=400V +10/-10%

The actual pumping process data of the motor are as follows. The three phase voltage from EEU line read from the switch gear read V=400V and the motor stating current I= 385A. Where average pump head are the sum of line pressure read from the pressure gauge 78m, pump position 120m, static water level 53.40m, draw down 30.04m, H=167 m and flow read from electromagnetic flow meter Q = 198 m^3/hr.

The input power can be calculated as: AC three-phase motor

$$P_{in} = V\ x\ I\ x\ cos\emptyset\ \ (w),$$

Where cosφ = 0.8, power input P_{in} = 123,200 W or 124 Kw

Therefore, Pump Efficiency

$$\eta_{pump} = \frac{2.275x198x167}{123200}\ x\ 100\% = 61.05\%$$

Where, $2.275 = \frac{\rho x g}{3.6\ x\ 10^3} = \frac{1000x9.81}{3.6\ x\ 10^3}$

WF02-PW15 well, design data of pump model QN 103-8 + VNI12-120/2, discharge Q = 360m^3/hr, total head H=170 m, power P =270kw and maximum pump efficiency η =76%.

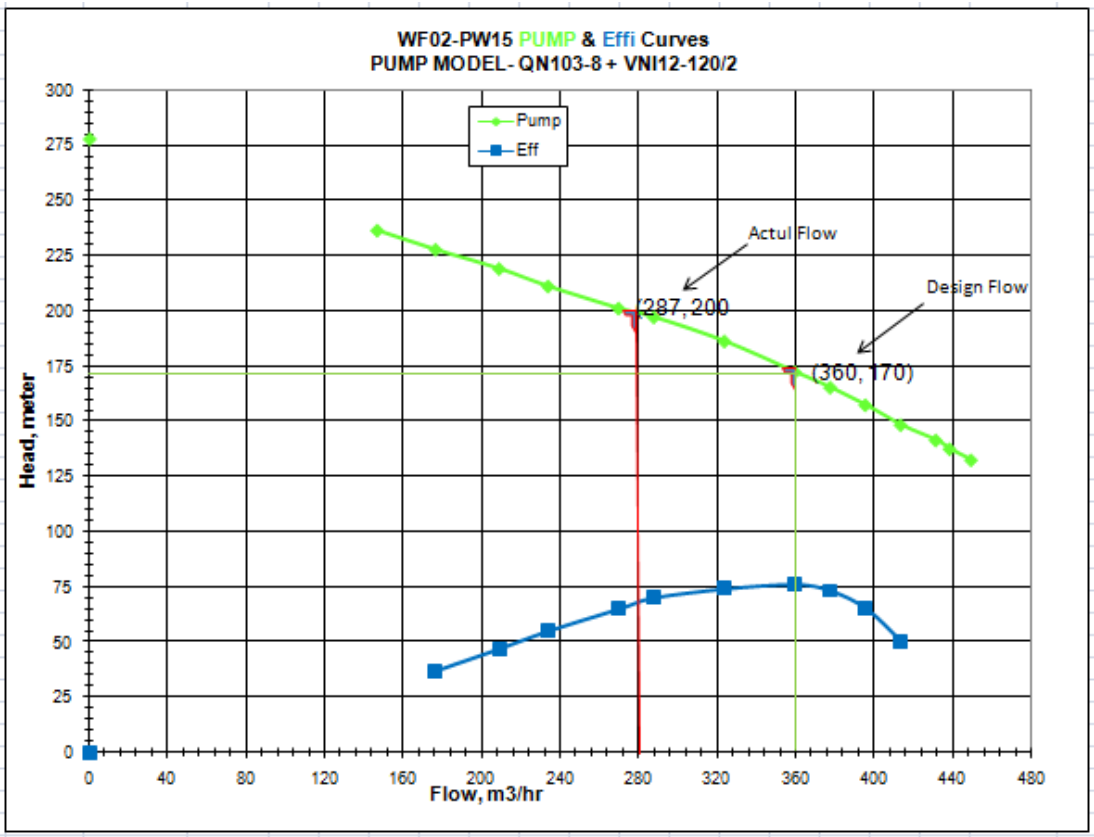

Figure 3.12 Performance Evaluation curve for well name WF02-PW15.

The actual flow rate delivered to the system from this pump is lower by 73m^3/hr than design flow rate, The efficiency at this flow rate as shown in manufacturer curve are below 70% and Head H=200m power P=270 kw.

The measurement data of pump motor model VNI12-120/2are power P=270Kw, Rated Current I=575 A and voltage V=400V +10/-10%

The actual pumping process data of the motor are as follows. The three phase voltage from the utility line read from the switch gear read V=400V and the motor starting current I= 594A. Where average pump head are the sum of line pressure read from the pressure gauge 60m, pump position 180m, static water level 52.73m, draw down 79.3m, H=200 m and flow read from electromagnetic flow meter Q = 287 m^3/hr.

The input power can be calculated as: AC three-phase motor

$$P_{in} = V\ x\ I\ x\ cos\emptyset\ \ (w),$$

Where cosφ = 0.8, power input P_{in} = 190,080 W or 191 Kw

Therefore, Pump Efficiency

$$\eta_{pump} = \frac{2.275x287x200}{190080}\ x\ 100\% = 68.70\%$$

Where, $2.275 = \frac{\rho x g}{3.6\ x\ 10^3} = \frac{1000x9.81}{3.6\ x\ 10^3}$

WF02-PW19 well, design data of pump model PN 101-7a + MI10-490/2, discharge Q = 108m^3/hr, total head H=190 m, power P =110 kw and maximum pump efficiency η =75%.

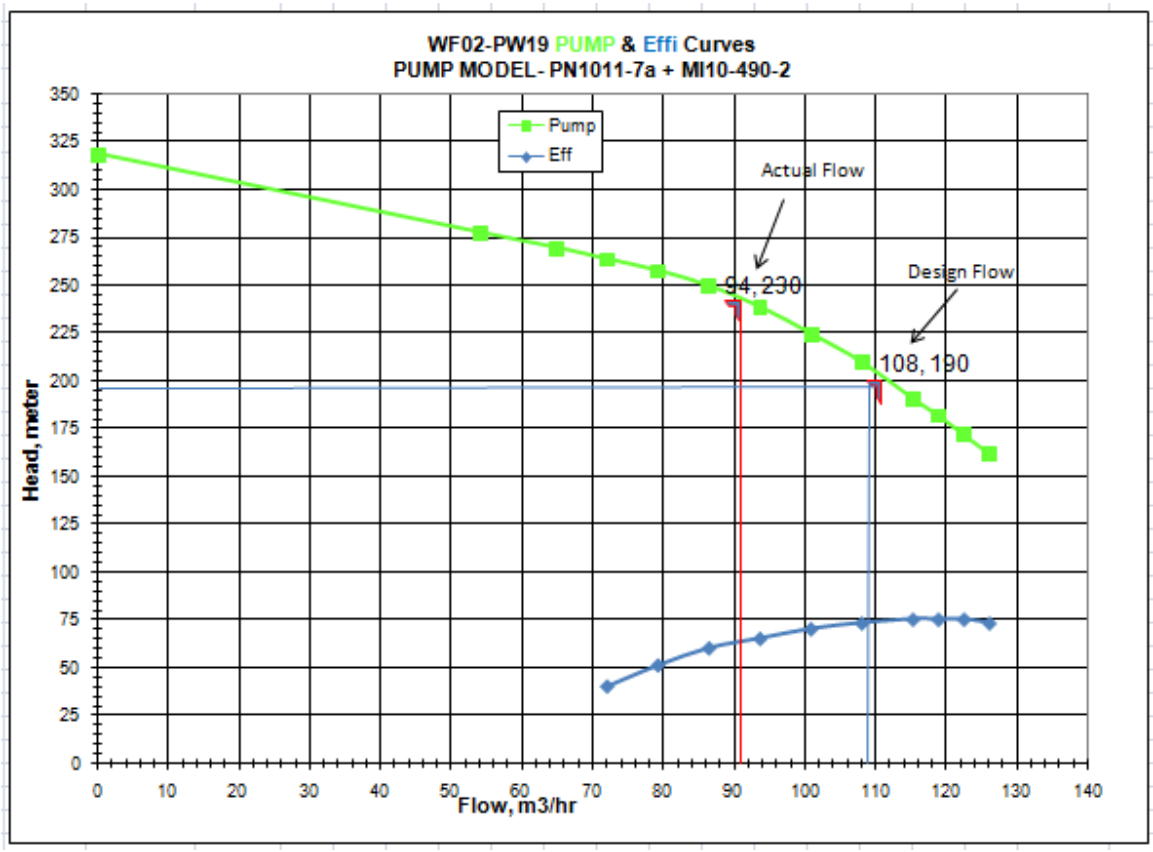

Figure 3.13 Performance Evaluation curve for well name WF02-PW19

The actual flow rate delivered to the system from this pump is lower by 14m^3/hr than design flow rate. The efficiency at this flow rate as shown in manufacturer curve are less than70% and Head H=230m and power P=110 kw.

The measurement data of pump motor model MI10-490/2 are power P=110Kw, Rated Current I=213 A and voltage V=400V +10/-10%

The actual pumping process data of the motor are as follows. The three phase voltage from the utility line read from the switch gear read V=400V and the motor starting current I= 230A. Where average pump head are the sum of line pressure read from the pressure gauge 52m, pump position 180m, static water level 82.1m, draw down 92.5m, H=230 m and flow read from electromagnetic flow meter Q = 94 m^3/hr.

The input power can be calculated as: AC three-phase motor

$$P_{in} = V\ x\ I\ x\ cos\emptyset\ \ (w),$$

Where cosφ = 0.8, power input P_{in} = 73,600 W or 74 Kw

Therefore, Pump Efficiency

$$\eta_{pump} = \frac{2.275x94x230}{73600} x\ 100\% = 66.83\%$$

Where, $2.275 = \frac{\rho x g}{3.6\ x\ 10^3} = \frac{1000x9.81}{3.6\ x\ 10^3}$

WF02-PW20 well, design data of pump model QN102-7a + MI10-1070/2, discharge Q = 288m^3/hr, total head H=160 m, power P =210kw and maximum pump efficiency η =75%.

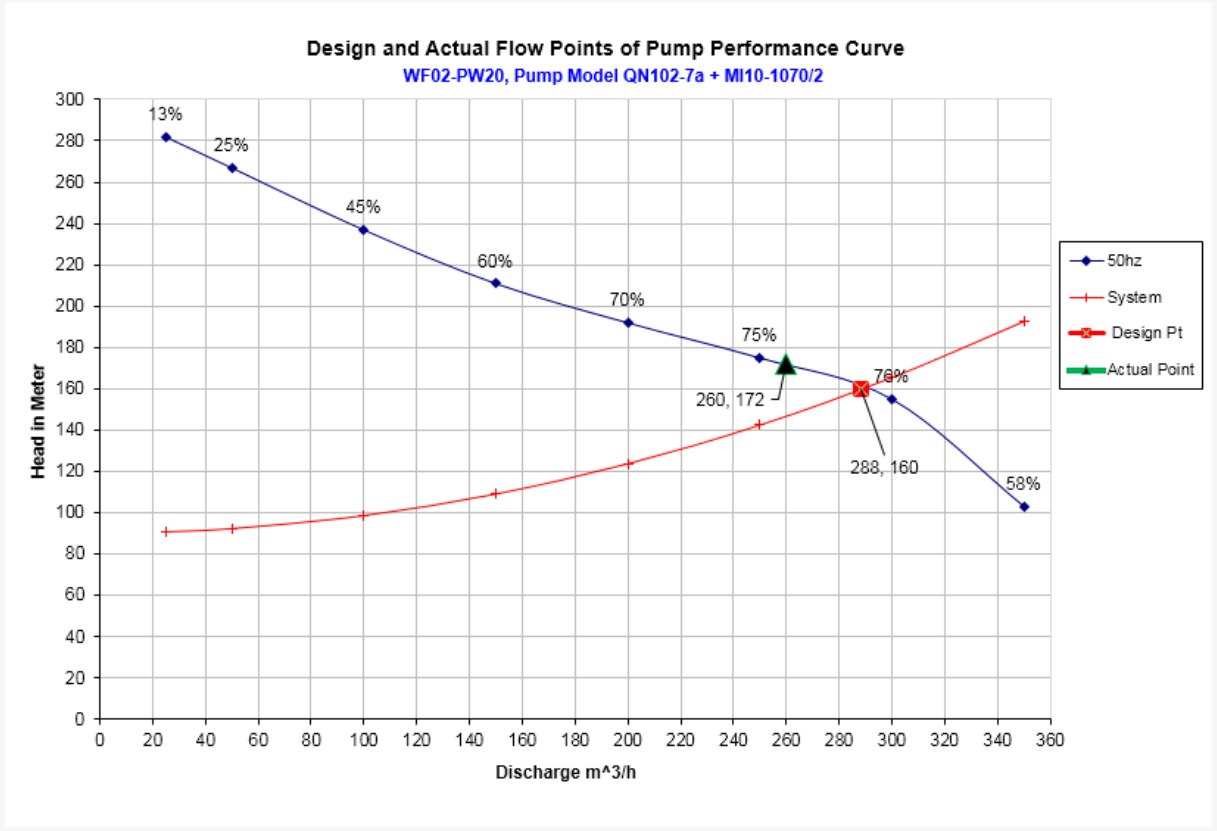

Figure 3.14 Performance Evaluation curve for well name WF02-PW20

The actual flow rate delivered to the system from this pump is lower by 29m^3/hr than design flow rate. The efficiency at this flow rate as shown in manufacturer curve are less than 60% and Head H=172m and power P=210 kw.

The measurement data of pump motor model MI10-1070/2 are power P=210Kw, Rated Current I=410 A and voltage V=400V +10/-10%

The actual pumping process data of the motor are as follows. The three phase voltage from EEU line read from the switch gear read V=400V and the motor starting current I= 420A. Where average pump head are the sum of line pressure read from the pressure gauge 60m, pump position 100m, static water level 44.0m, draw down 14.0m, H=160m (throttled) and flow read from electromagnetic flow meter Q = 261 m^3/hr.

The input power can be calculated as: AC three-phase motor

$$P_{in} = V\ x\ I\ x\ cos\emptyset\ \ (w),$$

Where cosφ = 0.8, power input P_{in} = 134,400 W or 135 Kw

Therefore, Pump Efficiency

$$\eta_{pump} = \frac{2.275x261x160}{134400}\ x\ 100\% = 70.04\%$$

Where, $2.275 = \frac{\rho x g}{3.6\ x\ 10^3} = \frac{1000x9.81}{3.6\ x\ 10^3}$

Using pumping system data collected from SCADA telemetry system and borehole site, input power and efficiency of this pumps calculated.

Following from the actual pumps efficiency of the pumping system of the field, from a reading of manufacturer curve and efficiency calculation using the actual flowrate read from electromagnetic flow meter, the energy conservation measures for the pumping system is essential to save energy wasted and to run the pumps at its best efficiency point. In addition as the calculation indicated for some pumps in the system oversized motors are used.

Actual pumping system performance, test result of the system and design data of the wells including pumps model summarized as the shown in the table below. For actual system, the flowrate data is taken from the actual pumping system, head is read directly from the manufacturer curve as per the actual flowrate and also the effectiveness of a single pump is often observed from the pump efficiency equation taking hydraulic power and input power to the pumps.

Table 3.2 Design, test and actual pumping system evaluation table

N°	Well Index	Pump model	Design Data				pump test result					Actual system data			
			Motor Power (KW)	Q (L/S)	H (m)	Eff (%)	Static Level	Dynamic Level	Q (L/S)	Pump Position	Draw down	Motor Power (KW)	Q (L/S)	H (m)	Eff (%)
1	WF02-PW5	PN 104-5a + MI10-740/2	140	50	140	75	*80.1*	*82.39*	*50*	*120*	*2.29*	140	45.6	148	60.54%
2	WF02-PW7R	QN 102-8a + VNI12-110/2	250	80	200	76	*53.72*	*147.71*	*75*	*230*	*93.99*	250	37.2	270	54.38%
3	WF02-PW8	PN 104-5a + MI10-740/2	140	50	140	74	*45.74*	*103.33*	*50*	*128*	*57.59*	140	29.2	190	50.65%
4	WF02-PW9	QN 102-6a + MI10-960/2	190	80	140	75	*50.73*	*71.56*	*70*	*90*	*20.83*	190	55.6	167	61.67%
5	WF02-PW11	QN 102-6a + MI10-880/2	170	70	140	75	*83.4*	*105.82*	*70*	*130*	*22.42*	170	35.8	182	49.09%
6	WF02-PW12	QN 101-7a + MI10-880/2	170	60	170	73.5	*61.2*	*94.76*	*46*	*110*	*33.56*	170	34.7	203	53.06%
7	WF02-PW13	QN 102-6a + MI10-880/2	170	70	140	75	*64.81*	*71.04*	*61*	*113*	*6.23*	170	55.6	157	66.04%
8	WF02-PW14	QN 102-6a + MI10-960/2	170	70	150	75	*53.4*	*83.44*	*60*	*120*	*30.04*	170	55.0	167	61.05%
9	WF02-PW15	QN 103-8 + VNI12-120/2	270	100	170	76	*52.73*	*132*	*142*	*180*	*79.3*	270	79.7	200	68.70%
10	WF02-PW19	PN 101-7a + MI10-490/2	110	30	190	75	*82.1*	*174.6*	*26.3*	*180*	*92.5*	110	26.1	230	66.83%
11	WF02-PW20	QN 102-7a + MI10-1070/2	210	80	160	75	*44*	*58*	*90*	*100*	*14*	210	72.5	160	70.42%

CHAPTER 4

4. Model Evaluation of Variable Speed Drive Motor Using Simulink

This thesis discusses using variable frequency converter for electrical deep-well submersible pumps compared with fixed speed/frequency pumps installed at Akaki Phase-3A pumping station and discuss the economic analysis of the systems. So, the focus will be particularly in two starting method which is star-delta starting method (current pumping stations starting method) and variable frequency/speed converter method.

4.1 Modeling of Pump Drive System MATLAB/SIMULINK

Driving the pumps with fixed speed motors and controlling them at partial loads either by throttling or mechanically by fluid coupling decreases the plant efficiency tremendously. When large flows must be controlled and motor energy consumption is significant, varying the motor speed is the answer. Controlling pumps by adjusting speed avoid wasting energy, reduce maintenance cost and improve the plant efficiency [20, 27].

At variable speed control strategy, the VFD changes the three-phase AC sinusoidal voltage into DC voltage, the harmonics generated during the AC - DC conversion are filtered out and send to inverter unit, which comprises six insulated gate bipolar transistors (IGBT) where the filtered DC supply is being converted into quasi-sinusoidal wave of AC supply and supplies to the induction motor. Therefore by varying the frequency of the power supply through VFD, the speed of the motor can be controlled. The controller circuit receives feedback information from the driven motor and sensor to adjust the output voltage or frequency to the selected values. Usually the output voltage is regulated to produce a constant ratio of voltage to frequency (V/Hz) [11].

Modeling diagram in SIMULINK is shown in figure 4.1.and figure 4.2. The model includes a three phase voltage source, a controller connected to three phase squirrel cage induction motor [11].

The SIMULINK model illustrates the use of the Asynchronous Machine block in motor mode. It consists of an asynchronous machine in an open-loop speed control system.

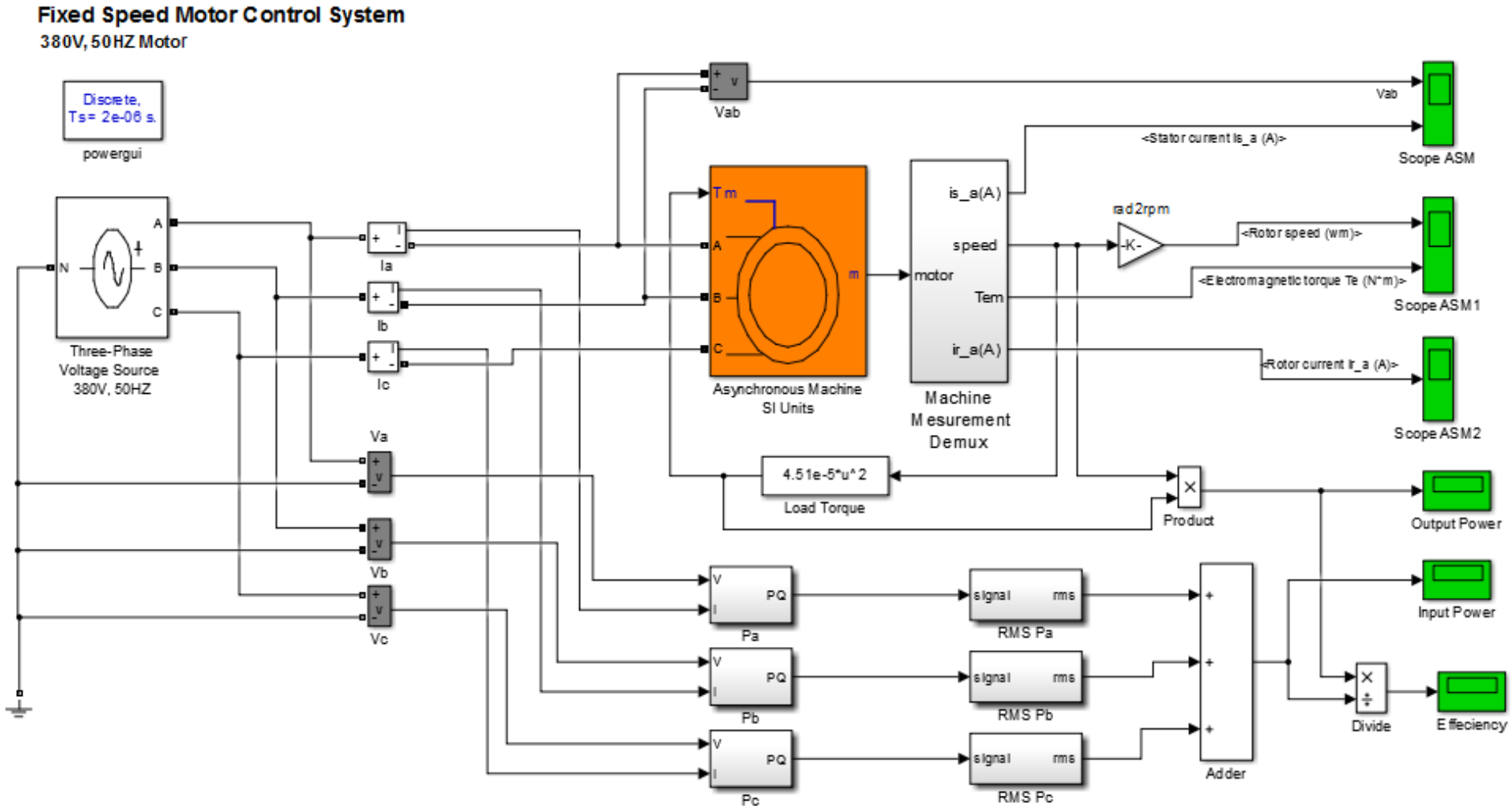

Figure 4.1: The corresponding modeling diagram representation of the conventional motor-pump system in SIMULINK

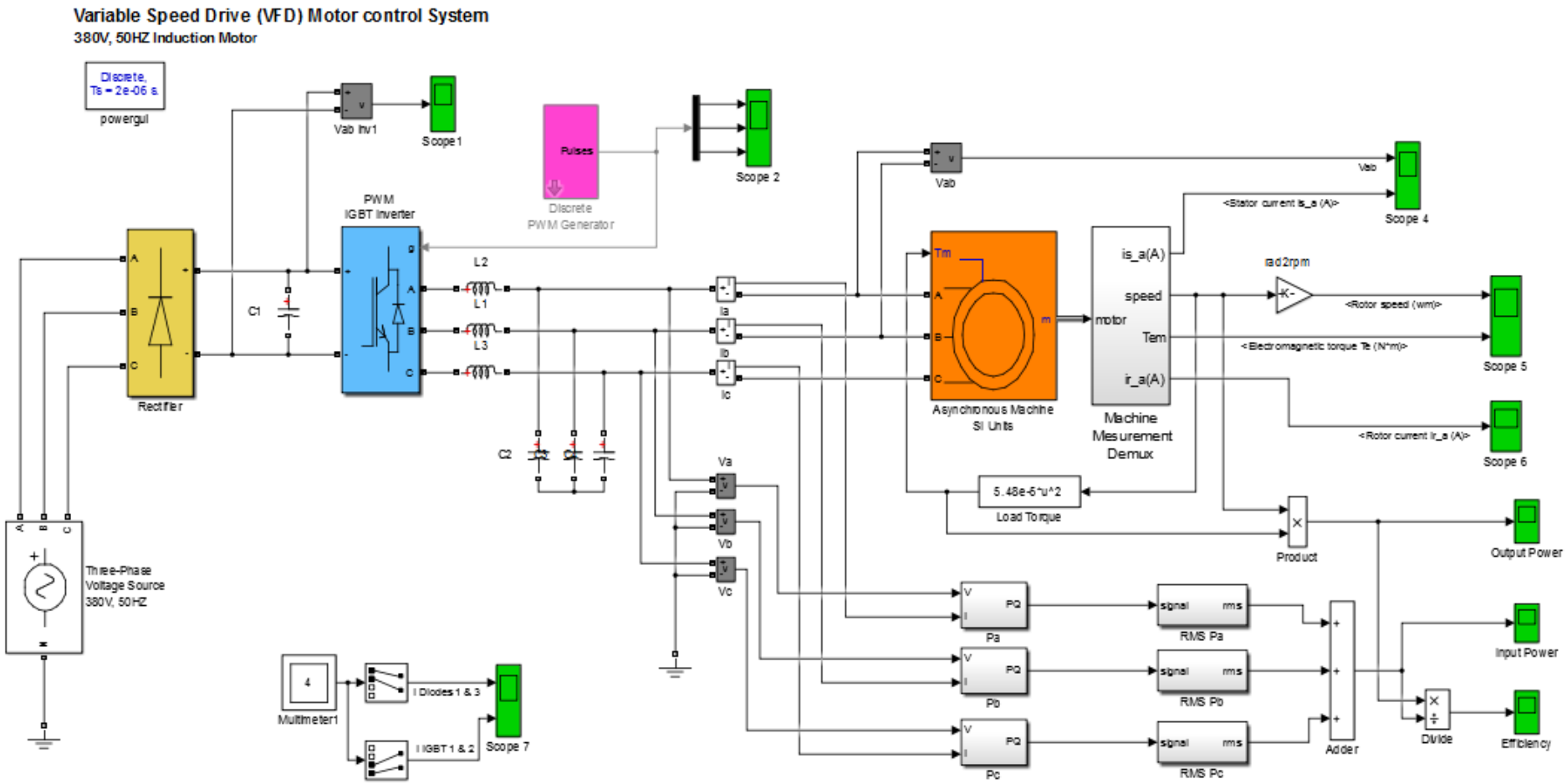

Figure 4.2: The corresponding modeling diagram representation of the VFD motor-pump system in SIMULINK

Motor-Pump System without VFD

The first system is composed of a three phase, star configured voltage source connected to a squirrel cage induction motor, as shown in Fig. 4.1. Using the bus selector block, the stator current for one of the phases is chosen to be viewed on the scope, along with the rotor speed and electromagnetic torque. Assuming a centrifugal pump as the load, we can use equation (4.1) to (4.8) in order to describe the relationships between various motor parameters [27]. For pump type load, the torque is proportional to the square of speed, as shown.

$$T = k\omega^2 \quad \text{…….. (Eq. 4.1)}$$

Where:

T = the electromagnetic torque produced by the motor,

ω = the speed of the rotor and

k = a constant of proportionality.

Hence, the value of *k* in equation 4.1 is found to be 4.73×10^{-4}Nms^2. This value of *k* is multiplied with the square of the rotor speed and fed back to the torque input of the motor, thus creating a model for a centrifugal pump type load.

Since supply frequency is 50Hz, the synchronous speed for the 2 pole machine is found using equation (4.2) [28].

$$N_s = \frac{120f}{P} \quad \text{…….. (Eq. 4.2)}$$

Where:

Ns = the synchronous speed of the motor,

f = the frequency of the supply voltage and

p = the number of poles.

Thus the synchronous speed is 3000rpm, or 314.16rad/s. We can now calculate the nominal torque of the motor as shown in equation (4.3) below. This yields a value of 445.7Nm for the 140 KW motor or 190HP motor.

$$T_n = \frac{P_n}{\omega_n} \quad \text{…….. (Eq. 4.3)}$$

Where:

T_n = the nominal torque,

P_n = the horsepower rating and

ω_n = the synchronous speed of the motor.

The total input power, P_{in}, at each voltage is calculated by summing the power delivered at each individual phase, as shown in equation 4.4. The output power, P_{out}, is found from the product of load torque, T_{load}, and rotor speed, ω_r, as shown in equation 4.5 [29].

$$P_{in} = V_{Ph(a)}I_{Ph(a)} + V_{Ph(b)}I_{Ph(b)} + V_{Ph(c)}I_{Ph(c)} \quad \text{..... (Eq. 4.4)}$$

$$P_{out} = T_{Load}\omega_r \quad \text{..... (Eq. 4.5)}$$

VFD Controlled Motor-Pump System

The second system, shown in Figure 4.2, incorporates a VFD between the supply and the induction motor. The fundamental components of a VFD are the rectifier, DC link and inverter. The rectifier converts supply AC voltage to DC voltage. A bank of electrolytic capacitors constitutes the DC link, which stores electrical energy for the inverter to draw against and function properly. Finally the inverter converts the DC link voltage back into AC voltage whose frequency and magnitude can be changed according to system requirements [30].

Since the loading of the motor in this system is identical to that of Figure 4.2, equation 4.1 to 4.8 are applicable for this system as well. However, the percentage of rated voltage applied to the motor is varied using the modulation index, m, of the pulse width modulated (PWM) inverter according to equation 4.6.

$$V_{rms,line} = \frac{m}{2}\sqrt{\frac{3}{2}}V_{DC} = m * 0.612 * V_{DC} \quad \text{..... (Eq. 4.6)}$$

$$V_{DC} = \frac{3}{\pi}\sqrt{2}V_{phase\ to\ phase} = 1.35V_{phase\ to\ phase}$$

The value of V_{DC} is kept constant while calculating the modulation index for each value of percentage rated voltage. For the purpose of investigation, the percentage of rated voltage is varied keeping the Volts/Hertz ratio constant. At rated condition, line voltage is 400V and frequency is 50Hz. Consequently, the frequency is varied using equation 4.7. Finally, the efficiency, η, is calculated using equation 4.8 [11].

$$f = \frac{3}{11} * V_{rms\ line} \quad \text{..... (Eq. 4.7)}$$

$$\eta = \frac{P_{out}}{P_{in}} * 100\% \quad \text{..... (Eq. 4.8)}$$

The simulation result of the pump drive is done by MATLAB/SIMULINK are presented below.

The motor starts and reaches its steady-state speed of 2888 rpm after 0.5s. At starting, the magnitude of the 50 Hz current reaches a peak and back to its steady-state value. As expected, the magnitude of the 50 Hz voltage contained in the chopped wave stays at 400V.

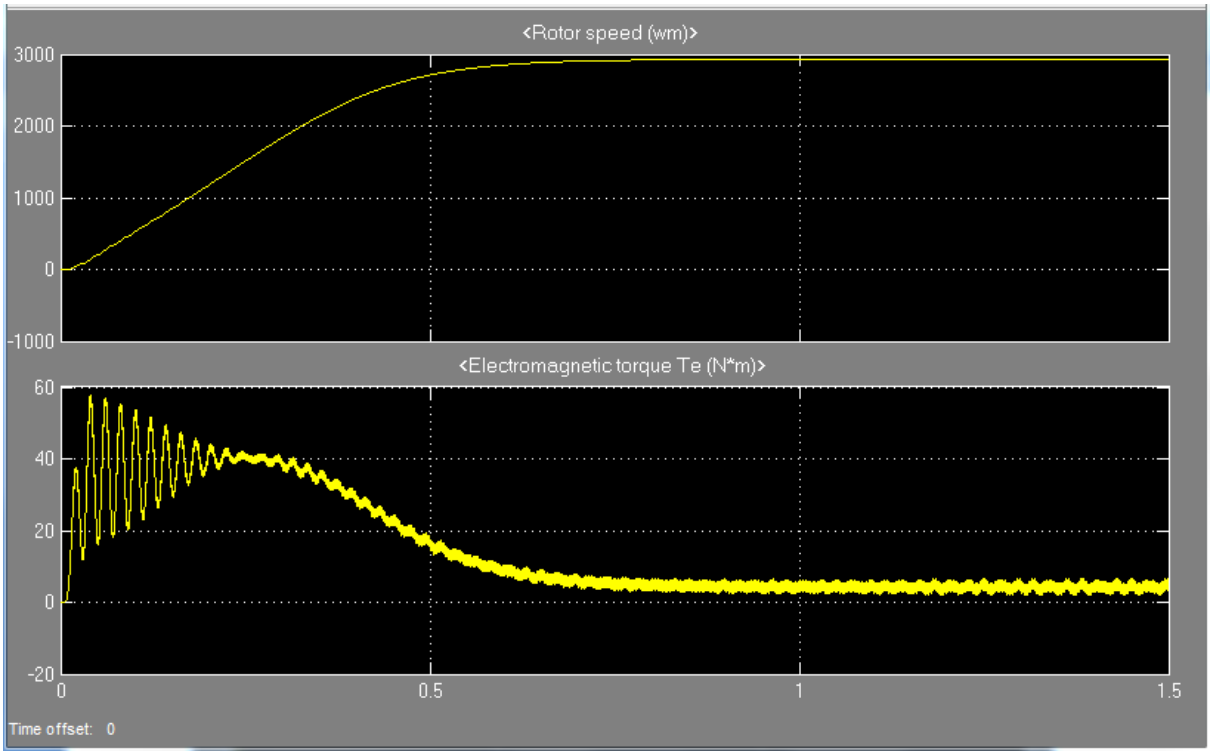

Figure 4.3: Motor speed and electromagnetic torque

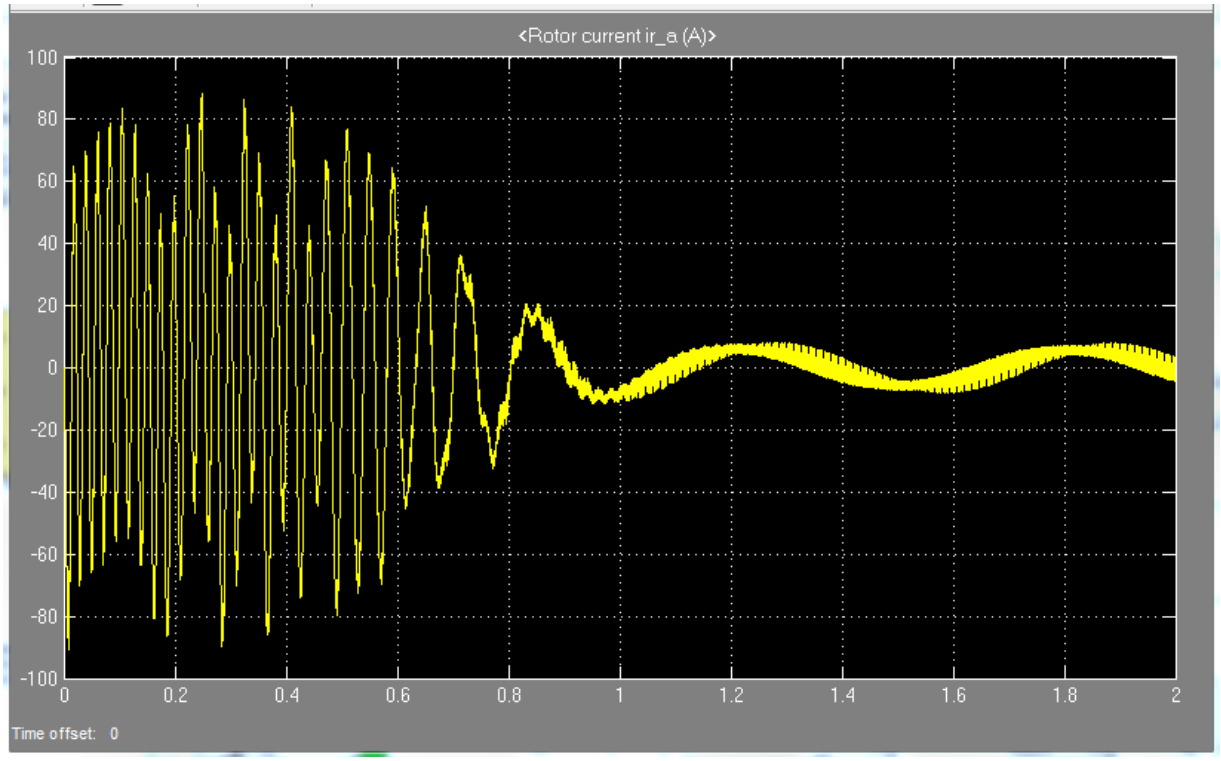

Figure 4.4: Rotor Current

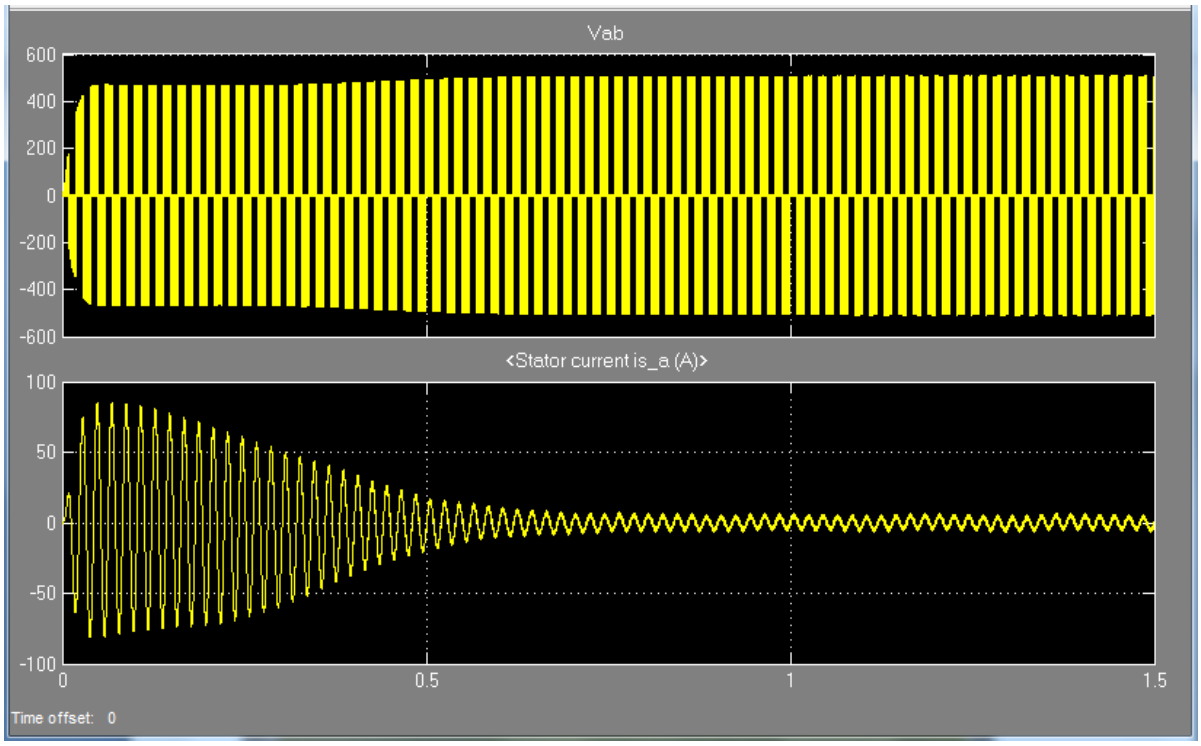

Figure 4.5: Stator Current and voltage wave form

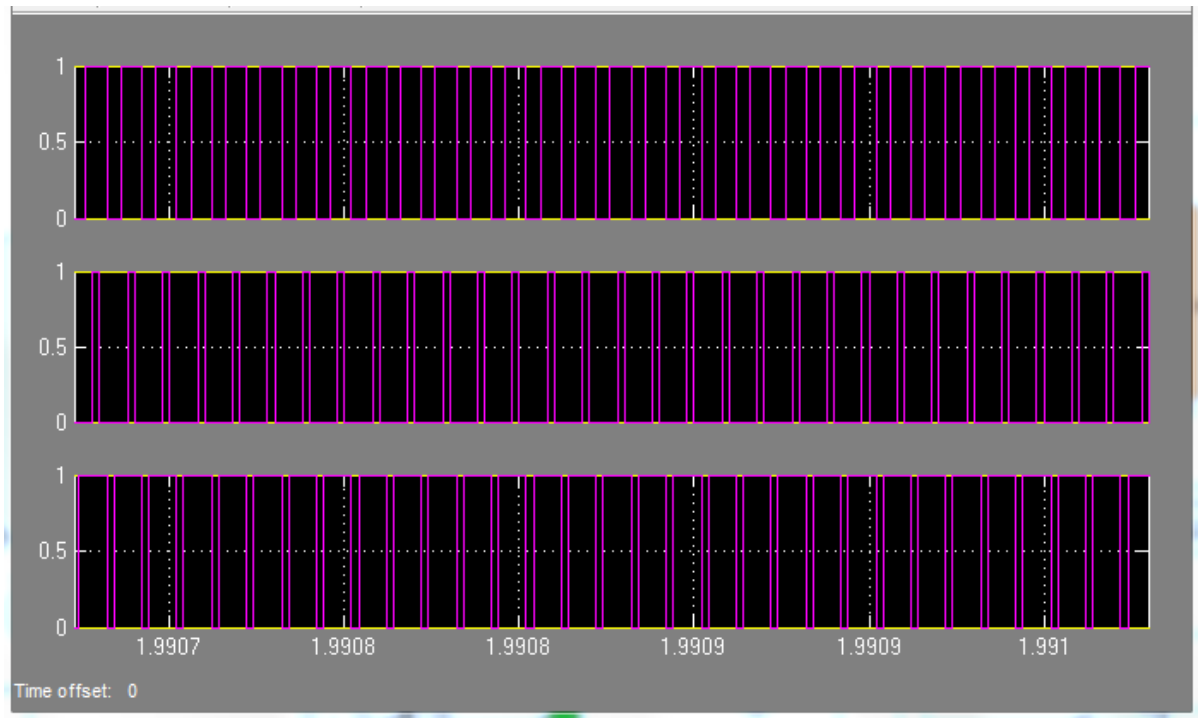

Figure 4.6: Pulse width modulator (PWM) generator signals

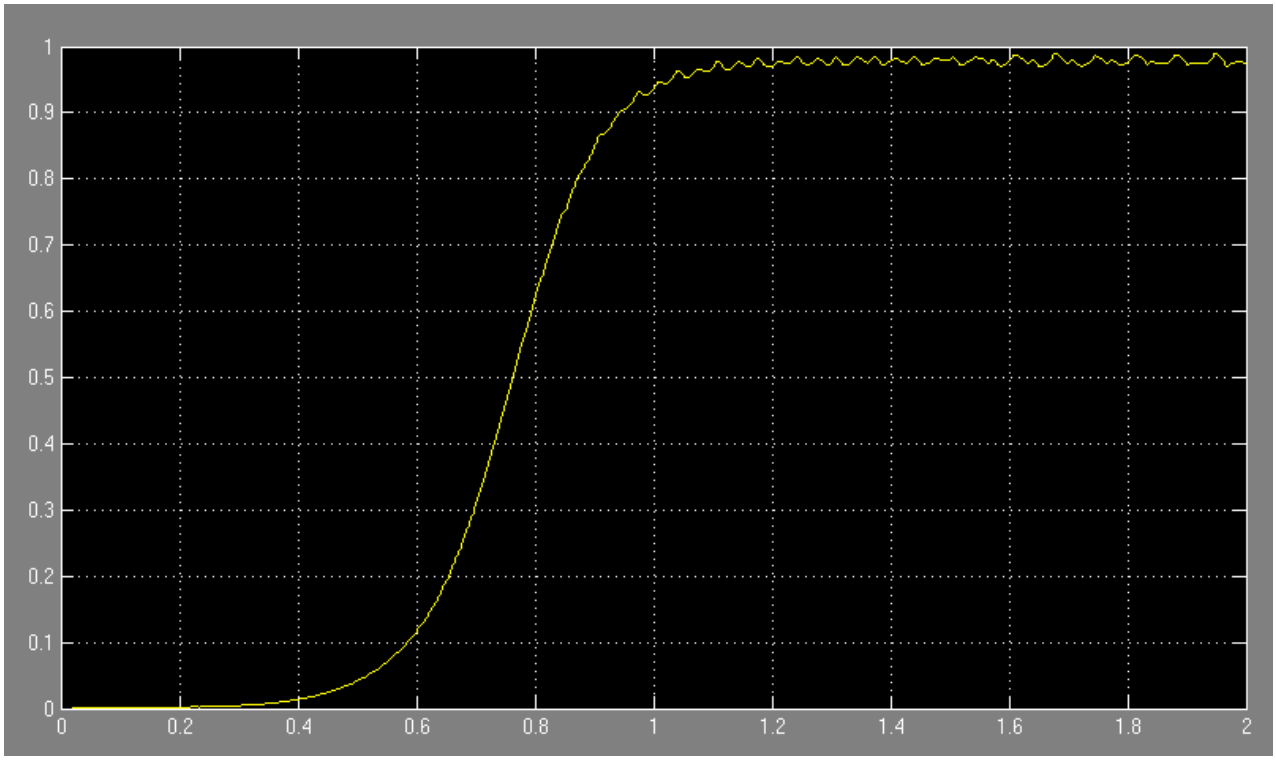

Figure 4.7: Efficiency Curve of the Motor

4.2 Technical Data of the Motors and the Simulation Results

Parameters used for 140 KW, three-phase, 50HZ, 2 pole, induction motors from the manufacturer are as follows:

Table 4.1 Parameters for 140 KW motor for direct and star-delta start [30]

P_N	KW	140	Dir.		Y	
I_N	A	275	M_A/M_N	1.7	M_A/M_N	0.4
M_N	Nm	465	M_K/M_N	2.8	M_K/M_N	0.8
$\cos\varphi_A$		0.44	I_A/I_N	5.7	I_A/I_N	1.6

The following figure 4.8 will show the corresponding torque and stator current vs speed curve of the manufacturer specifications for 140 kw, 2880 rpm, 2 pole pump motor with star-delta staring method.

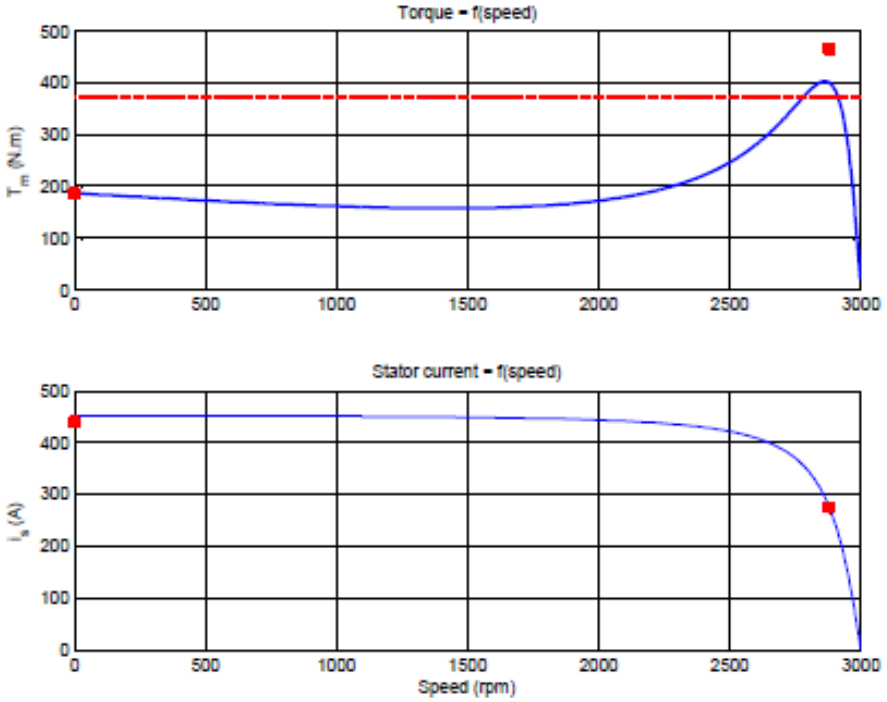

Figure 4.8: The corresponding torque and stator current vs speed curve of the motor

By varying the Frequency applied from 50HZ to 40HZ and the modulation index m of the PWM Generator the power, efficiency and speed of the systems were obtained while the supply voltage was kept unchanged. The results from the VFD system after it reaches the steady-state are presented in Table below.

Table 4.2 Results For VFD Motor-Pump System at steady-state

Frequency (HZ)	Input Power	Output Power	Efficiency (%)	Speed (RPM)
50	1335.3	1301.5	97	2929
49	1281.8	1230.6	96	2875
48	1190	1138.2	96	2801
47	1100.9	1075.1	97	2748
46	1029.8	984.9	96	2669
45	951.3	929.9	97	2618
44	886.7	849.9	95	2531
43	822.9	790.7	96	2482
42	766.6	750.2	96	2437
41	696.9	679.1	97	2358
40	650.3	634.5	97	2306

The voltage is increased/decreased by increasing/decreasing modulation index and speed also increases/decrease when frequency increases/decrease. Due to inherent control from inverter and using PMW techniques voltage is sinusoidal. As frequency increase/decrease, speed also increase/decrease. Power being equal to speed cubed for variable torque load, reduces total power consumption of motor. Voltage and current levels are high during starting of motor to be able to supply enough torque needed by the motor. These then reduce in magnitude to a certain point where they become constant. Electromagnetic torque, rotor speed and stator current are high and sinusoidal during starting of motor. They then maintain a certain magnitude after a few seconds. Torque ripples are reduced as motor moves from starting to running state. The parameters are initially ramping in nature till they got settled at the peak value. It is seen that the VFD has succeeded in increasing the nominal speed of the motor from using the nominal frequency of 50Hz. Initially the speed of the motor rises from zero and increases to the nominal speed, it experiences some transients and then settles to a stable level within few milliseconds.

These findings suggest that a VFD enables the motor pump system to maintain its efficiency at a high level. Furthermore, it provides lower power to a system, when required, without having a significant impact on the efficiency of the system. It accomplishes this by proper Hz control of the induction motor. In contrast, if we attempt to provide lower output power using the conventional (fixed speed) pumping system by reducing the input voltage, it reduces the efficiency significantly. It becomes dangerous to operate the motor at such low efficiencies, as the excessively high copper loss might overheat and burn the stator windings of the induction motor. Therefore, a conventional system is unable to adjust its power consumption according to system needs.

CHAPTER 5

5. Re-Design the Pumping Systems and Evaluate Energy Saving

5.1 Conservation of Energy Using Variable Frequency

The standard practice to design a pump is to operate the pump most efficiently at the maximum flow rate and head conditions at a constant pump speed. This study introduces a novel approach to lower the operating points by varying the motor speed with the help of a variable frequency drive in contrast to the commonly used fixed speed approach. By varying the speed of the motor, the required minimum pivot point pressure can be provided at any required flow rate and position in a field.

Usually, the fixed speed of the motor or pump makes it difficult to adjust the pump design conditions to the required operating conditions. Pump behavior is governed by its performance curve and is unable to change the design pressure without a corresponding change in speed. However, maintaining the minimum required system operating pressure regardless of operating conditions can achieve optimum efficiency. This optimum efficiency can be achieved by employing a Variable Frequency Drive (VFD) which can vary the frequency of power supplied to the motor. This change in frequency will alter the pump speed based on the ratio of adjusted frequency to unadjusted frequency. A reduction in the speed of the motor will also reduce the pressure delivered to the center pivot and horsepower demand of the pump, specifically focusing on the opportunity to save energy and therefore reduce operating costs [17].

A VFD can provide a wide range of speeds to match a particular situation by sending a controlled modulating signal into the motor. The VFDs can be programmed to change the speed of the pump according to the required parameters which are directly related to the rotational speed of the pump [31].

The equations known as Affinity Laws show the relation of the pump performance parameters; flow rate, head, and required brake power with the pump speed. For a Speed Change (N1 → N2) as shown in equation 2.14 to equation 2.17.

$$Q_2 = Q_1 (N_2 / N_1),\ H_2 = H_1 (N_2 / N_1)^2,\ P_2 = P_1 (N_2 / N_1)^3$$

Where: Q = flow rate, H = head or pressure, BHP = brake horsepower or kilowatt, rpm =rotational shaft speed (revolutions per minute)

The factors that need to be considered in installing VFD are motor efficiency, motor loading and VFD efficiency. The rule of design to prevent the motor from inefficient operation is to operate motor greater than 50% of maximum speed [32]. The VFD is also not 100% efficient resulting from energy losses due to heat and other harmonic losses. Typical efficiencies of VFD are in the range of 95- 98% [32].

5.2 Re-Design Pumping System for Each Pump in the Well-Field and Energy Saving

A good approach to assessing and improving the pumping system is to take a whole-system approach, meaning that look at the entire pumping system from need to delivery or the efficiency of converting electricity into movement of fluid.

The main opportunities are, when an existing pumping system is being modified to solve a system problem or to implement a flow rate change for best efficiency point and new pumping system is being designed and installed [33].

These are both ideal times to create an energy efficient system. There are two general approaches to assessing existing pumping systems. The first consists of observing the operation of the pumping system and the second consists of collecting system data and performing detailed calculations.

The first approach relies on observations of the system; the second deals with creating an accurate model of the system and then calculating the flow rate and system head within the model.

Observing the operating system over a period of time allows the observer to view how the actual system is working during a range of operating conditions. In many cases, system operational requirements limit the range of operating conditions that can be explored.

By developing a model of the system, a comparison can be made between the system resistance curve and the pump characteristic curves to determine the operating point of the pump. Regardless of the approach adopted, the objective is to gain a clear picture of how the system operate and to see where improvements can be made to optimise the operation of the system.

When we think of VFD control, the first thing that comes to mind is energy savings. The potential energy savings available through variable speed control depends, upon the pumps In this application, the control valve is removed and a VFD is employed to control pump speed and system flowrate across the same range of head/pressure.

Comparing energy consumption between the design point and best efficiency point BEP according to current pumping capacity of the pumps from the well field are conducted, and a very important result of this comparison is the fact that a relatively small change in speed can result in a much larger reduction in power.

Follow the steps below to view the operating characteristics and potential power savings of a pump under VFD control.

5.2.1 Variable Speed Pump Analysis for WF02-PW05 well field

Design data of pump model PN 104-5a + MI10-740/2, discharge Q= 180m^3/hr, total head H=140 m, power P=140 kw and maximum pump efficiency η =75%.

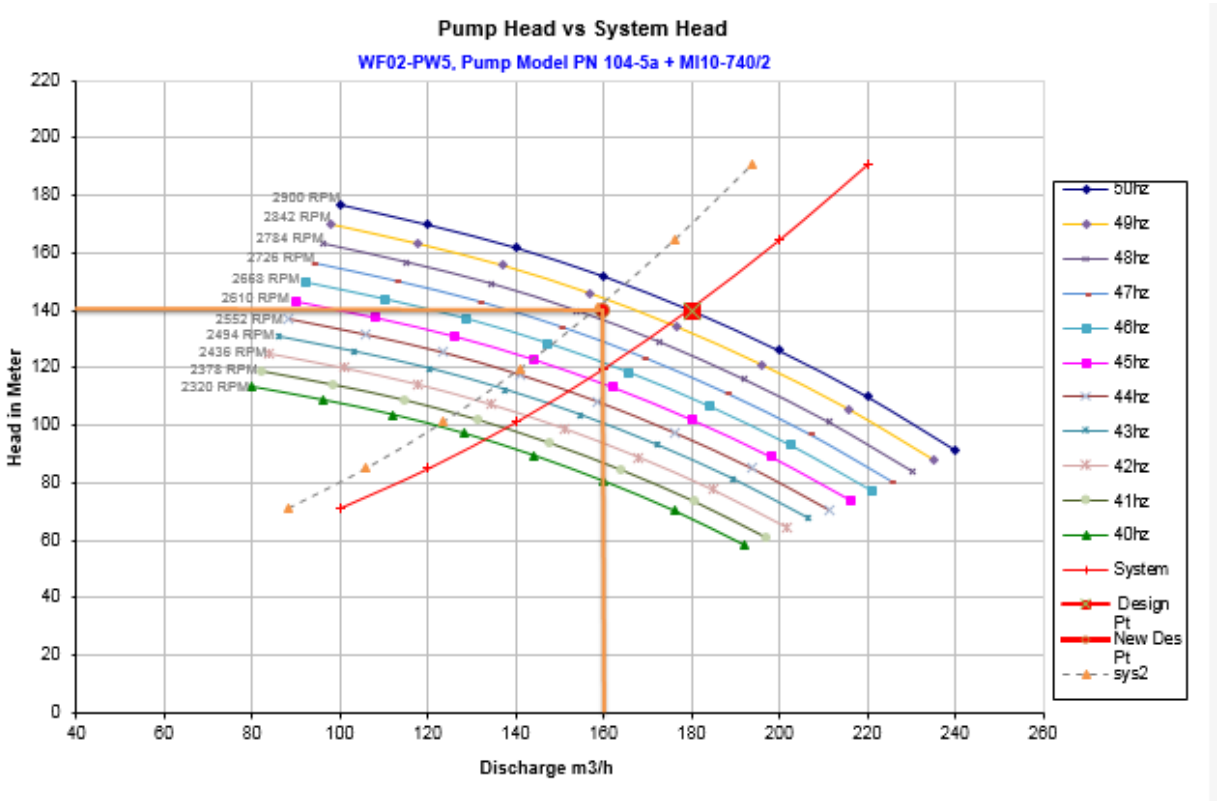

Figure 5.1. Pump head versus system head

Figure 5.1 shows how pump flow is reduced with RPM reduced which exactly leads to best efficiency point (BEP). The main difference between a variable frequency (speed) drive and a discharge valve is that a VFD changes a pump curve, while a valve changes a system curve. A pump operates at the intersection between its H-Q curve and a system curve, and a change in either moves the operating point to a new intersection.

Figure 5.2 shows the pump hydraulic efficiency versus system head across the range of flow. It also shows the slope of the efficiency isomers as pump speed (frequency hz) is reduced and how they intersect the system curve.

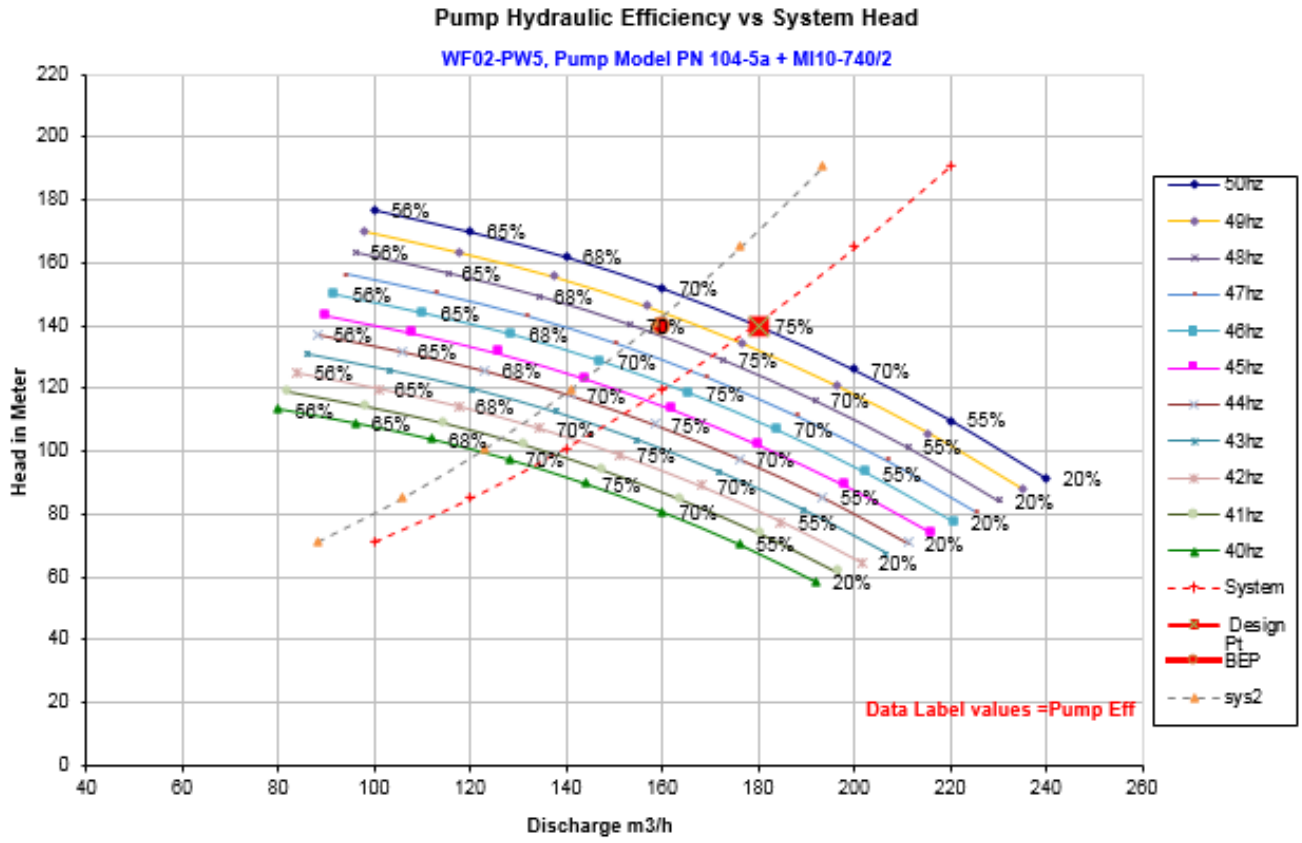

Figure 5.2. Pump hydraulic efficiency versus system head

This particular pump has a hydraulic efficiency of 75 percent at the design point (full flow) and maintains an efficiency of approximately 70 percent at minimum flow. This represents an excellent range of efficiency and will have a large impact on energy savings and the cost of operation. The slope of the efficiency isomer is also important. At 160m^3/hr actual flow of the pump the best efficiency of the 47 hz curve is 74 percent.

Figure 5.3 shows the head produced and power (KW) required at various flow and frequency points. From design point to actual flow point of the pump, the KW ranges from 82 to 92 kilowatts across the range of flow. It also shows a 10 KW reduction at 160m^3/hr versus control valve operation of 180 m^3/hr.

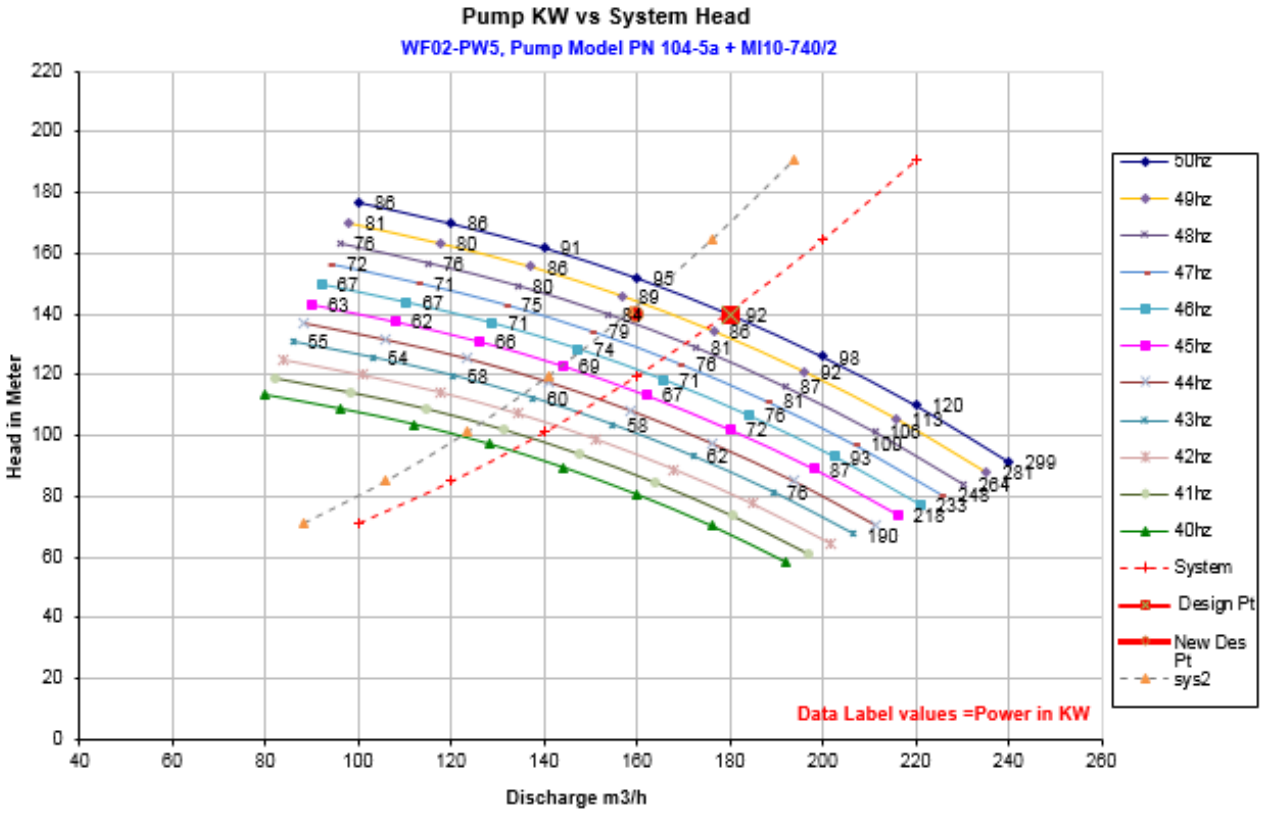

Figure 5.3. Pump KW versus system head

The effectiveness of a pumping task can be evaluated using the specific energy consumption, which describes the energy used per pumped volume. The specific energy consumption is given by

$$E_S = \frac{P_{in}}{Q} \quad \text{..... (Eq. 5.2)}$$

$$P_{in}(\text{KW}) = \frac{P_{Hyd}}{\eta_{pump}} \quad \text{..... (Eq. 5.3)}$$

Where:

E_s = the specific energy consumption,

P_{in} = the input power,

Q_{tot} = the total flow rate.

Comparing energy consumption between the design point and best efficiency point BEP according to current pumping capacity are as follows:

At BEP Pump efficiency of 72%, flow rate 163 m^3/hr the pump power are calculated from the following equation,

$$P_{in}(\text{KW}) = \frac{P_{Hyd}}{\eta_{pump}}$$

$$P_{in}(\text{KW}) = \frac{163 * 140 * 9.81}{3600 * 0.72} = 82.4KW$$

At Design Point Pump efficiency of 75%, flow rate 180 m^3/hr the pump power are calculated from the following equation,

$$P_{in}(\text{KW}) = \frac{P_{Hyd}}{\eta_{pump}}$$

$$P_{in}(\text{KW}) = \frac{180 * 140 * 9.81}{3600 * 0.75} = 91.6KW$$

5.2.2 Variable Speed Pump Analysis for WF02-PW07 well field

Design data of pump model QN 102-8a + VNI12-110/2, discharge Q = 288m^3/hr, total head H=200 m, power P=250kw and maximum pump efficiency η =76%.

This particular pump has a hydraulic efficiency of 76 percent at the design point (full flow) and maintains an efficiency of approximately 60 percent at minimum flow. This represents an excellent range of efficiency and will have a large impact on energy savings and the cost of operation. The slope of the efficiency isomer is also important. At 132m^3/hr actual flow of the pump the best efficiency of the 44hz curve is 62 percent.

The head produced and power (KW) required at various flow and frequency points. From design point to actual flow point of the pump, the KW ranges from 91 horsepower to 210kilowatts across the range of flow. It also shows a 99KW reduction at 132m^3/hr versus control valve operation of 288 m^3/hr.

Comparing energy consumption between the design point and best efficiency point BEP according to current pumping capacity are as follows:

At BEP Pump efficiency of 61%, flow rate 132 m^3/hr the pump power are calculated from the following equation,

$$P_{in}(\text{KW}) = \frac{P_{Hyd}}{\eta_{pump}}$$

$$P_{in}(\text{KW}) = \frac{132 * 200 * 9.81}{3600 * 0.61} = 117.9KW$$

At Design Point Pump efficiency of 76%, flow rate 288m3/hr the pump power are calculated from the following equation,

$$P_{in}(\text{KW}) = \frac{P_{Hyd}}{\eta_{pump}}$$

$$P_{in}(\text{KW}) = \frac{288 * 200 * 9.81}{3600 * 0.76} = 206.5KW$$

Note: Using VFD for this pump may upgrade its efficiency from 47.43% which was valve controlled system calculated at chapter 4 to 61 percent. Due to vast difference between design flow and actual pump working point replacing this pump may be the best option.

5.2.3 Variable Speed Pump Analysis for WF02-PW08 well field

Design data of pump model PN 104-5a + MI10-740/2, discharge Q= 180m^3/hr, total head H=140 m, power P=140 kw and maximum pump efficiency η =74%.

This particular pump has a hydraulic efficiency of 76 percent at the design point (full flow) and maintains an efficiency of approximately 70 percent at minimum flow. This represents an excellent range of efficiency and will have a large impact on energy savings and the cost of operation. The slope of the efficiency isomer is also important. At 105 m^3/hr actual flow of the pump the best efficiency of the 44hz curve is 70 percent.

The head produced and power (KW) required at various flow and frequency points. From design point to actual flow point of the pump, the KW ranges from 53 horsepower to 92kilowatts across the range of flow. It also shows a 39KW reduction at 105 m^3/hr versus control valve operation of 180 m^3/hr.

Comparing energy consumption between the design point and best efficiency point BEP according to current pumping capacity are as follows:

At BEP Pump efficiency of 70%, flow rate 105 m3/hr the pump power are calculated from the following equation,

$$P_{in}(\text{KW}) = \frac{P_{Hyd}}{\eta_{pump}}$$

$$P_{in}(\text{KW}) = \frac{105 * 140 * 9.81}{3600 * 0.7} = 57.2KW$$

At Design Point Pump efficiency of 75%, flow rate 180 m^3/hr the pump power are calculated from the following equation,

$$P_{in}(\text{KW}) = \frac{P_{Hyd}}{\eta_{pump}}$$

$$P_{in}(\text{KW}) = \frac{180 * 140 * 9.81}{3600 * 0.75} = 91.6KW$$

5.2.4 Variable Speed Pump Analysis for WF02-PW09 well field

Design data of pump model QN 102-6a + MI10-960/2, discharge Q = 288m^3/hr, total head H=140 m, power P =190 kw and maximum pump efficiency η =75%.

This particular pump has a hydraulic efficiency of 76 percent at the design point (full flow) and maintains an efficiency of approximately 70 percent at minimum flow. This represents an excellent range of efficiency and will have a large impact on energy savings and the cost of operation. The slope of the efficiency isomer is also important. At 210 m^3/hr actual flow of the pump the best efficiency of the 42hz curve is 75 percent.

The head produced and power (KW) required at various flow and frequency points. From design point to actual flow point of the pump, the KW ranges from 82 horsepower to 140kilowatts across the range of flow. It also shows a 35KW reduction at 210m^3/hr versus control valve operation of 288 m^3/hr.

Comparing energy consumption between the design point and best efficiency point BEP according to current pumping capacity are as follows:

At BEP Pump efficiency of 75%, flow rate 210m3/hr the pump power are calculated from the following equation,

$$P_{in}(\text{KW}) = \frac{P_{Hyd}}{\eta_{pump}}$$

$$P_{in}(\text{KW}) = \frac{210 * 140 * 9.81}{3600 * 0.75} = 106.82KW$$

At Design Point Pump efficiency of 76%, flow rate 288m3/hr the pump power are calculated from the following equation,

$$P_{in}(\text{KW}) = \frac{P_{Hyd}}{\eta_{pump}}$$

$$P_{in}(\text{KW}) = \frac{288 * 140 * 9.81}{3600 * 0.76} = 144.6KW$$

5.2.5 Variable Speed Pump Analysis for WF02-PW11 well field

Design data of pump model QN102-6a + MI10-880/2, discharge Q = 252m^3/hr, total head H=140 m, power P =170kw and maximum pump efficiency η =75%.

This particular pump has a hydraulic efficiency of 75 percent at the design point (full flow) and maintains an efficiency of approximately 62 percent at minimum flow. This represents an excellent range of efficiency and will have a large impact on energy savings and the cost of operation. The slope of the efficiency isomer is also important. At 149m^3/hr actual flow of the pump the best efficiency of the 40hz curve is 62 percent.

The head produced and power (KW) required at various flow and frequency points. From design point to actual flow point of the pump, the KW ranges from 85 to 128kilowatts across the range of flow. It also shows a 48KW reduction at 149m^3/hr versus control valve operation of 252 m^3/hr.

Comparing energy consumption between the design point and best efficiency point BEP according to current pumping capacity are as follows:

At BEP Pump efficiency of 62%, flow rate 149m3/hr the pump power are calculated from the following equation,

$$P_{in}(\text{KW}) = \frac{\text{P}_{Hyd}}{\eta_{pump}}$$

$$P_{in}(\text{KW}) = \frac{149 * 140 * 9.81}{3600 * 0.62} = 91.68KW$$

At Design Point Pump efficiency of 75%, flow rate 252m3/hr the pump power are calculated from the following equation,

$$P_{in}(\text{KW}) = \frac{\text{P}_{Hyd}}{\eta_{pump}}$$

$$P_{in}(\text{KW}) = \frac{252 * 140 * 9.81}{3600 * 0.75} = 128.2KW$$

5.2.6 Variable Speed Pump Analysis for WF02-PW12 well field

Design data of pump model QN101-7a + MI10-880/2, discharge Q = 216m^3/hr, total head H=170 m, power P =170kw and maximum pump efficiency η =73.5%.

This particular pump has a hydraulic efficiency of 73 percent at the design point (full flow) and maintains an efficiency of approximately 64 percent at minimum flow. This represents an excellent range of efficiency and will have a large impact on energy savings and the cost of operation. The slope of the efficiency isomer is also important. At 135m^3/hr actual flow of the pump the best efficiency of the 46hz curve is 62 percent.

The head produced and power (KW) required at various flow and frequency points. From design point to actual flow point of the pump, the KW ranges from 70 to 138 kilowatts across the range of flow. It also shows a 33KW reduction at 135m^3/hr versus control valve operation of 216 m^3/hr.

Comparing energy consumption between the design point and best efficiency point BEP according to current pumping capacity are as follows:

At BEP Pump efficiency of 62%, flow rate 135m3/hr the pump power are calculated from the following equation,

$$P_{in}(\text{KW}) = \frac{\text{P}_{Hyd}}{\eta_{pump}}$$

$$P_{in}(\text{KW}) = \frac{135 * 170 * 9.81}{3600 * 0.62} = 100.87KW$$

At Design Point Pump efficiency of 75%, flow rate 216m3/hr the pump power are calculated from the following equation,

$$P_{in}(\text{KW}) = \frac{\text{P}_{Hyd}}{\eta_{pump}}$$

$$P_{in}(\text{KW}) = \frac{216 * 170 * 9.81}{3600 * 0.75} = 133.4KW$$

5.2.7 Variable Speed Pump Analysis for WF02-PW13 well field

Design data of pump model QN102-6a + MI10-880/2, discharge Q = 252m^3/hr, total head H=140 m, power P =170kw and maximum pump efficiency η =75%.

This particular pump has a hydraulic efficiency of 75 percent at the design point (full flow) and maintains an efficiency of approximately 64 percent at minimum flow. This represents an excellent range of efficiency and will have a large impact on energy savings and the cost of operation. The slope of the efficiency isomer is also important. At 200m3/hr actual flow of the pump the best efficiency of the 48 hz curve is 72 percent.

The head produced and power (KW) required at various flow and frequency points. From design point to actual flow point of the pump, the KW ranges from 100 to 129 kilowatts across the range of flow. It also shows a 28KW reduction at 200m^3/hr versus control valve operation of 252 m^3/hr.

Comparing energy consumption between the design point and best efficiency point BEP according to current pumping capacity are as follows:

At BEP Pump efficiency of 72%, flow rate 200 m^3/hr the pump power are calculated from the following equation,

$$P_{in}(\text{KW}) = \frac{P_{Hyd}}{\eta_{pump}}$$

$$P_{in}(\text{KW}) = \frac{200 * 140 * 9.81}{3600 * 0.72} = 105.97KW$$

At Design Point Pump efficiency of 75%, flow rate 252m3/hr the pump power are calculated from the following equation,

$$P_{in}(\text{KW}) = \frac{P_{Hyd}}{\eta_{pump}}$$

$$P_{in}(\text{KW}) = \frac{252 * 140 * 9.81}{3600 * 0.75} = 128.2KW$$

5.2.8 Variable Speed Pump Analysis for WF02-PW14 well field

Design data of pump model QN102-6a + MI10-880/2, discharge Q = 252m^3/hr, total head H=150 m, power P =170kw and maximum pump efficiency η =75%.

This particular pump has a hydraulic efficiency of 75 percent at the design point (full flow) and maintains an efficiency of approximately 66 percent at minimum flow. This represents an excellent range of efficiency and will have a large impact on energy savings and the cost of operation. The slope of the efficiency isomer is also important. At 198 m^3/hr actual flow of the pump the best efficiency of the 48hz curve is 70 percent.

The head produced and power (KW) required at various flow and frequency points. From design point to actual flow point of the pump, the KW ranges from 114 to 137 kilowatts across the range of flow. It also shows a 23KW reduction at 198 m^3/hr versus control valve operation of 252 m^3/hr.

Comparing energy consumption between the design point and best efficiency point BEP according to current pumping capacity are as follows:

At BEP Pump efficiency of 70%, flow rate 198 m^3/hr the pump power are calculated from the following equation,

$$P_{in}(\text{KW}) = \frac{P_{Hyd}}{\eta_{pump}}$$

$$P_{in}(\text{KW}) = \frac{198 * 150 * 9.81}{3600 * 0.70} = 113.87KW$$

At Design Point Pump efficiency of 75%, flow rate 252m3/hr the pump power are calculated from the following equation,

$$P_{in}(\text{KW}) = \frac{P_{Hyd}}{\eta_{pump}}$$

$$P_{in}(\text{KW}) = \frac{252 * 150 * 9.81}{3600 * 0.75} = 137.3KW$$

5.2.9 Variable Speed Pump Analysis for WF02-PW20 well field

Design data of pump model QN102-7a + MI10-1070/2, discharge Q = 288m^3/hr, total head H=160 m, power P =210kw and maximum pump efficiency η =75%.

This particular pump has a hydraulic efficiency of 76 percent at the design point (full flow) and maintains an efficiency of approximately 66 percent at minimum flow. This represents an excellent range of efficiency and will have a large impact on energy savings and the cost of operation. The slope of the efficiency isomer is also important. At 260 m^3/hr actual flow of the pump the best efficiency of the 48 hz curve is 75 percent.

The head produced and power (KW) required at various flow and frequency points. From design point to actual flow point of the pump, the KW ranges from 142 to 167 kilowatts across the range of flow. It also shows a 25KW reduction at 260m^3/hr versus control valve operation of 288 m^3/hr.

Comparing energy consumption between the design point and best efficiency point BEP according to current pumping capacity are as follows:

At BEP Pump efficiency of 75%, flow rate 260 m^3/hr the pump power are calculated from the following equation,

$$P_{in}(\text{KW}) = \frac{P_{Hyd}}{\eta_{pump}}$$

$$P_{in}(\text{KW}) = \frac{260 * 160 * 9.81}{3600 * 0.75} = 151.15KW$$

At Design Point Pump efficiency of 76%, flow rate 288m3/hr the pump power are calculated from the following equation,

$$P_{in}(\text{KW}) = \frac{P_{Hyd}}{\eta_{pump}}$$

$$P_{in}(\text{KW}) = \frac{288 * 160 * 9.81}{3600 * 0.76} = 165.2KW$$

Table 5.1 Power Consumption Comparison of Pumping Systems:

No.	Well Name	Actual Normal System power (KW)	Re- designed system VFD Power (KW)	Power Ratio (%)
1	WF02-PW05	91.6	82.4	10.04%
2	WF02-PW07	206.5	117.9	42.9%
3	WF02-PW08	91.6	57.2	37.55%
4	WF02-PW09	144.6	106.82	26.13%
5	WF02-PW11	128.2	91.68	28.49%
6	WF02-PW12	133.4	100.87	24.32%
7	WF02-PW13	128.2	105.97	17.39%
8	WF02-PW14	137.3	113.87	17.1%
9	WF02-PW20	165.2	151.15	8.5%

From the above table we can notice using VFD at least from 9 Akaki well field submersible pumps in the system will minimize the electric power consumption of the pumps. The VFD provides low energy consumption depends on the flow capacity as well as pressure of the wells, and the redesigned models minimize the power consumption in KW by an average by **23.45%** from the normal fixed speed pumping system.

In addition, the figures in Appendix-E: pump analysis shows, how pump flow is reduced with RPM reduced which exactly leads to best efficiency point (BEP), pump hydraulic efficiency versus system

head across the range of flow shows the slope of the efficiency isomers as pump speed or frequency is reduced and how they intersect the system curve, and the hydraulic power (KW) required at various flowrate and frequency points from design point to actual flow point of the pump.

The main difference between a variable frequency drive and a throttling discharge valve is that a VFD changes a pump performance curve, while a throttled valve working point is moving to left on the pump performance curve and changes a system curve. A pump operates at the intersection between its pump performance curve and a system curve, and a change in either of the curves moves the operating point to a new intersection.

CHAPTER 6

6. ECONOMIC EVALUATION

6.1 Economic Evaluation Introduction

Economic analysis gives us the tools to perform this evaluation. Often the decision to make is to proceed or not to proceed with a project. In cases involving investment, we want to know if the project is economically viable in order to proceed. In effect, we compare the net benefit of proceeding with the project against the consequences (good or bad) of proceeding the investment [5].

To be able to make the go/no go decision or to compare different projects, systems, or courses of action, we have to find a common measure to reflect all the costs and benefits and their time of occurrence.

Scope of the present study is to make a thorough economic analysis of the Project by means of a Cash Flow Analysis. In particular this analysis compares the costs for the construction and the operation & maintenance of the water pumping system and the revenues obtained from the annual electric cost saving from the new VFD system.

In any economic approach in order to evaluate a certain investment, income and expenditure at different dates are compared by discounting the relevant amount to a certain date in accordance with a normative interest rate called a discount rate. The value so obtained is called Present Value (PV). For a given investment, the discount rate at which the PV of the costs and revenue cash flows are equivalent (or the discount rate that makes the NPV for a project equal to zero) is called Internal Rate of Return (IRR) [34]. A project is convenient when its IRR is higher than the opportunity cost of capital in the country.

When we think of VFD control, the first thing that comes to mind is energy savings. Variable frequency drives (VFDs) is one proven method to better control the amount of energy electric motors use. More and more facilities are paying for the minimum power needed and no more. When management applies this minimum requirements principle to flow control, energy consumption is drastically reduced. Decreased power use, reduced stress on machinery, and better flow control for liquids and gases, such as water and air, are just a few reasons VFDs are growing in popularity [30].

A clear operational advantage must be obtained to justify the use of a large, variable speed motor when compared to the conventional methods of operation and design. The problems of environment and

technical complexity introduced by the variable speed approach will add significantly to the unit capital costs, since the system is bound to be more complicated and will have additional rather sophisticated equipment.

Observing the actual operating system over a period of time allows to view how the actual system is working during a range of operating conditions.

By developing a model of the system, a comparison can be made between the system resistance curve and the pump characteristic curves to determine the operating point of the pump. Regardless of the approach adopted, the objective is to gain a clear picture of how the system operate in the previous chapters.

Comparing energy consumption between the design point and best efficiency point BEP according to current pumping capacity of the pumps from the well field are conducted, and a very important result of this comparison is the fact that a relatively small change in speed can result in a much larger reduction in power [30].

The potential energy savings available through variable speed control is calculated. In this chapter the consumption amount of conventional or actual operating process and the employed VFD system process will be discussed. First the operating cost per KWH and then evaluate the investment cost or (initial cost) of the system with variable speed control operation.

6.2 Operating Cost Analysis

This section shows the economic analysis through comparison between the actual pumping system operating energy consumption and cost and the re-designed pumping system by using VFD control system.

Energy consumption in at least 9 submersible pumps in the field evaluated for each selected pumps in the network at Akaki Phase-3A well-field, make comparison between the manufacturer design points for fixed speed pumping system and the re-designed system made in the previous chapter by implementing VSD control and presented here for both pumping systems.

WF02-PW05 well field

Energy in KWh per 160 m^3/hr can be calculated from:

$$(\text{KWh}) = \frac{P_{in} * Amount\ pumped\ (m3)}{\eta_{Motor} * Q} = \frac{82.4 * 16o\ (m3)}{0.97 * 160(\frac{m3}{hr})} = 85.03\ KWh$$

And electrical power cost for 85.03 KWh are: 85.03 x 0.5691 = 48.39 Birr

Where the average motor efficiency 97% are taken from Simulink analysis made before and power consumption cost of Ethiopia for equivalent flat rate above 50 KWH are 0.5691 birr per KWh [24] used.

Energy in KWh per 180 m^3/hr can be calculated from:

$$(\text{KWh}) = \frac{P_{in} * Amount\ pumped\ (m3)}{\eta_{Motor} * Q} = \frac{91.6 * 180\ (m3)}{0.97 * 180(\frac{m3}{hr})} = 94.39\ KWh$$

And electrical power cost for 94.39 KWh are: 94.39 x 0.5691 = 53.72 Birr

WF02-PW07 well field

Energy in KWh per 165 m^3/hr can be calculated from:

$$(\text{KWh}) = \frac{P_{in} * Amount\ pumped\ (m3)}{\eta_{Motor} * Q} = \frac{117.9 * 132\ (m3)}{0.97 * 132(\frac{m3}{hr})} = 122.85\ KWh$$

And electrical power cost for 122.85 KWh are: 122.85 x 0.5691 = 69.91 Birr

Energy in KWh per 288 m^3/hr can be calculated from:

$$(\text{KWh}) = \frac{P_{in} * Amount\ pumped\ (m3)}{\eta_{Motor} * Q} = \frac{206.5 * 288\ (m3)}{0.97 * 288(\frac{m3}{hr})} = 212.91\ KWh$$

And electrical power cost for 212.91 KWh are: 212.91 x 0.5691 = 121.19 Birr

WF02-PW08 well field

Energy in KWh per 105 m^3/hr can be calculated from:

$$(\text{KWh}) = \frac{P_{in} * Amount\ pumped\ (m3)}{\eta_{Motor} * Q} = \frac{57.2 * 105\ (m3)}{0.97 * 105(\frac{m3}{hr})} = 58.99\ KWh$$

And electrical power cost for 58.99 KWh are: 58.99 x 0.56.91 = 33.57 Birr

Energy in KWh per 180 m^3/hr can be calculated from:

$$(\text{KWh}) = \frac{P_{in} * Amount\ pumped\ (m3)}{\eta_{Motor} * Q} = \frac{91.6 * 180\ (m3)}{0.97 * 180(\frac{m3}{hr})} = 94.39\ KWh$$

And electrical power cost for 94.39 KWh are: 94.39 x 0.5691 = 53.72 Birr

WF02-PW09 well field

Energy in KWh per 210 m^3/hr can be calculated from:

$$(\text{KWh}) = \frac{P_{in} * Amount\ pumped\ (m3)}{\eta_{Motor} * Q} = \frac{106.82 * 210\ (m3)}{0.97 * 210(\frac{m3}{hr})} = 110.12\ KWh$$

And electrical power cost for 110.2 KWh are: 110.12 x 0.56.91 = 62.67 Birr

Energy in KWh per 288 m^3/hr can be calculated from:

$$(\text{KWh}) = \frac{P_{in} * Amount\ pumped\ (m3)}{\eta_{Motor} * Q} = \frac{144.6 * 288\ (m3)}{0.97 * 288(\frac{m3}{hr})} = 149.04\ KWh$$

And electrical power cost for 149.04 KWh are: 149.04 x 0.5691 = 84.81 Birr

WF02-PW11 well field

Energy in KWh per 129 m^3/hr can be calculated from:

$$(\text{KWh}) = \frac{P_{in} * Amount\ pumped\ (m3)}{\eta_{Motor} * Q} = \frac{91.68 * 149\ (m3)}{0.97 * 149(\frac{m3}{hr})} = 94.52\ KWh$$

And electrical power cost for 94.52 KWh are: 94.52 x 0.5691 = 53.8 Birr

Energy in KWh per 252 m^3/hr can be calculated from:

$$(\text{KWh}) = \frac{P_{in} * Amount\ pumped\ (m3)}{\eta_{Motor} * Q} = \frac{128.2 * 252\ (m3)}{0.97 * 252(\frac{m3}{hr})} = 132.15\ KWh$$

And electrical power cost for 132.15 KWh are: 132.15 x 0.5691 = 75.21 Birr

WF02-PW12 well field

Energy in KWh per 135 m^3/hr can be calculated from:

$$(\text{KWh}) = \frac{P_{in} * Amount\ pumped\ (m3)}{\eta_{Motor} * Q} = \frac{100.87 * 135\ (m3)}{0.97 * 135(\frac{m3}{hr})} = 103.99\ KWh$$

And electrical power cost for 103.99 KWh are: 103.99 x 0.5691 = 59.18 Birr

Energy in KWh per 216 m^3/hr can be calculated from:

$$(\text{KWh}) = \frac{P_{in} * Amount\ pumped\ (m3)}{\eta_{Motor} * Q} = \frac{133.4 * 216\ (m3)}{0.97 * 216(\frac{m3}{hr})} = 137.54 KWh$$

And electrical power cost for 137.54 KWh are: 137.54 x 0.5691 = 78.27 Birr

WF02-PW13 well field

Energy in KWh per 200 m^3/hr can be calculated from:

$$(\text{KWh}) = \frac{P_{in} * Amount\ pumped\ (m3)}{\eta_{Motor} * Q} = \frac{105.97 * 200\ (m3)}{0.97 * 200(\frac{m3}{hr})} = 109.25\ KWh$$

And electrical power cost for 109.25 kWh are: 109.25 x 0.5691 = 62.17 Birr

Energy in KWh per 252 m^3/hr can be calculated from:

$$(\text{KWh}) = \frac{P_{in} * Amount\ pumped\ (m3)}{\eta_{Motor} * Q} = \frac{128.2 * 252\ (m3)}{0.97 * 252(\frac{m3}{hr})} = 132.15\ KWh$$

And electrical power cost for 132.15 kWh are: 132.15 x 0.5691 = 75.21 Birr

WF02-PW14 well field

Energy in KWh per 195 m^3/hr can be calculated from:

$$(\text{KWh}) = \frac{P_{in} * Amount\ pumped\ (m3)}{\eta_{Motor} * Q} = \frac{113.87 * 198\ (m3)}{0.97 * 198(\frac{m3}{hr})} = 117.39\ KWh$$

And electrical power cost for 117.39 kWh are: 117.39 x 0.5691 = 66.81 Birr

Energy in KWh per 252 m^3/hr can be calculated from:

$$(\text{KWh}) = \frac{P_{in} * Amount\ pumped\ (m3)}{\eta_{Motor} * Q} = \frac{137.3 * 252\ (m3)}{0.97 * 252(\frac{m3}{hr})} = 141.59\ KWh$$

And electrical power cost for 141.59 kWh are: 141.59 x 0.5691 = 80.58 Birr

WF02-PW20 well field

Energy in KWh per 260 m^3/hr can be calculated from:

$$(\text{KWh}) = \frac{P_{in} * Amount\ pumped\ (m3)}{\eta_{Motor} * Q} = \frac{151.15 * 260\ (m3)}{0.98 * 260(\frac{m3}{hr})} = 154.23\ KWh$$

And electrical power cost for 154.23 kWh are: 154.23 x 0.5691 = 87.77 Birr

Energy in KWh per 288 m^3/hr can be calculated from:

$$(\text{KWh}) = \frac{P_{in} * Amount\ pumped\ (m3)}{\eta_{Motor} * Q} = \frac{165.2 * 288\ (m3)}{0.98 * 288(\frac{m3}{hr})} = 170.33\ KWh$$

And electrical power cost for 170.33 kWh are: 170.33 x 0.5691 = 96.93 Birr

Table 6.1 Power Cost Comparison of Pumping Systems:

No.	Well Name	Actual Normal System			Re- designed system VFD			Cost Ratio (%)
		power (KW)	Energy (KWH)	Cost (Birr)	Power (KW)	Energy (KWH)	Cost (Birr)	
1	WF02-PW05	91.6	94.39	53.72	82.4	85.03	48.39	9.92 %
2	WF02-PW07	206.5	212.9	121.16	117.9	122.85	69.91	42.30 %
3	WF02-PW08	91.6	94.39	53.72	57.2	58.99	33.57	37.50 %
4	WF02-PW09	144.6	149.04	84.82	106.82	110.12	62.67	26.11 %
5	WF02-PW11	128.2	132.15	75.21	91.68	94.52	53.79	28.48 %
6	WF02-PW12	133.4	137.54	78.27	100.87	103.99	59.18	24.39 %
7	WF02-PW13	128.2	132.15	75.21	105.97	109.25	62.17	17.33 %
8	WF02-PW14	137.3	141.59	80.58	113.87	117.39	66.81	17.09 %
9	WF02-PW20	165.2	170.33	96.93	151.15	154.23	87.77	9.45 %

From the above table we notice using VFD in the system will minimize the operation cost of the pumps in birr per KWH. The VFD provides low energy consumption depends on the flow capacity as well as pressure of the wells and minimize the operation cost in average of **23.6%** for the redesigned models.

Let the pumps running for 22 hours a day and 355 days a year by considering reservoir is getting full and taking about 15 days in a year for maintenance and overall system checkup and considering other factors to run the system.

Table 6.2 Annual cost saving Comparison of Pumping Systems

No.	Well Name	Actual Normal System		Re- designed system VFD		Annual Power Cost Saving in Birr
		KWh Cost in Birr	Annual Power Consumption Cost in Birr	KWh Cost in Birr	Annual Power Consumption Cost in Birr	
1	WF02-PW05	53.717349	419,532.50	48.390573	377,930.38	41,602.12
2	WF02-PW07	121.16139	946,270.46	69.913935	546,027.83	400,242.62

3	WF02-PW08	53.717349	419,532.50	33.571209	262,191.14	157,341.35
4	WF02-PW09	84.818664	662,433.77	62.669292	489,447.17	172,986.60
5	WF02-PW11	75.206565	587,363.27	53.791332	420,110.30	167,252.97
6	WF02-PW12	78.274014	611,320.05	59.180709	462,201.34	149,118.71
7	WF02-PW13	75.206565	587,363.27	62.174175	485,580.31	101,782.97
8	WF02-PW14	80.578869	629,320.97	66.806649	521,759.93	107,561.04
9	WF02-PW20	96.934803	757,060.81	87.772293	685,501.61	71,559.20
Total for 9 selected Pumps			**5,620,197.59**		**4,250,750.00**	**1,369,447.58**

The annual cost saving from the energy use from the selected nine pumps are **1,369,447.58 ETB.** Taking average lifespan of pumps and VFD controller 15 years, the total saving can be **20,541,713.73 ETB**.

6.3 Investment or Initial Cost Analysis

The economic study has been carried out on a period of 20 years of operation for pumps and in average 15 years for VFD controller. Since the pumps are in operation for the past five years, using VFD controller with a lifetime of 15 years can be more feasible in this system for economic evaluation.

Initial cost of introducing new component or equipment includes; components cost, construction cost, engineering operations cost and training cost. For project alternatives that use new (for the user) and relatively proven technologies, special care is needed to develop realistic estimates of the initial costs [34].

When designing and installing a new pumping system, the capital cost of a VFD can be offset by eliminating control valves, bypass lines and conventional starters. VFD controller can be two or three times expensive than the conventional controlling system, and requires higher expertise to integrate it to the system.

6.3.1. VFD controller models, specification and price summary

GK3000 series VFD has 2 kinds of voltage levels, 230V and 400V. The range of applicable motor is from 0.4KW to 450KW. Models of GK3000 series for only three phase are shown in the following table 6.3 [35]:

Table 6.3. Models description

Voltage level	Models	Light duty	VFD Capacity (KW)	Capacity (KVA)	Rated current (A)	Applicable motor (KW)
400V Three phase	GK3000-4T0900G	GK3000-4T0900P	90	116	176	90
	GK3000-4T1100G	GK3000-4T1100P	110	138	210	110
	GK3000-4T1320G	GK3000-4T1320P	132	167	253	132
	GK3000-4T1600G	GK3000-4T1600P	160	200	304	160
	GK3000-4T1850G	GK3000-4T1850P	185	234	355	185
	GK3000-4T2000G	GK3000-4T2000P	200	248	377	200
	GK3000-4T2200G	GK3000-4T2200P	220	280	426	220
	GK3000-4T2500G	GK3000-4T2500P	250	318	474	250
	GK3000-4T2800G	GK3000-4T2800P	280	342	520	280
	GK3000-4T3150G	GK3000-4T3150P	315	390	600	315
	GK3000-4T3500G	GK3000-4T3500P	350	435	660	350
	GK3000-4T4000G	GK3000-4T4000P	400	493	750	400
	GK3000-4T4500G	GK3000-4T4500P	450	560	850	450

Three phase GoHz variable frequency drive price list from the manufacturer are as follows:

Table 6.4 Three phase VFD price list in USD [35]:

VFD Model No.	Price (USD)	Power (Kw)	Current (A)	Dimension (mm)	G.W (Kg)
GK3000-4T0900G	3146.6	90	176	618*398*306	50
GK3000-4T1100G	4683.11	110	210	760*485*324	85
GK3000-4T1320G	5960.35	132	253	760*485*324	85
GK3000-4T1600G	6499.23	160	304	1440*600*399	180
GK3000-4T1850G	8689.91	185	355	1440*600*399	180
GK3000-4T2200G	9813.41	220	426	1440*600*399	180
GK3000-4T2500G	10234.45	250	474	1440*600*399	180

The overall investment cost for the equipment including supply, installation, test, commissioning and training at site for 10 selected pumps are summarized as the following table.

Table 6.5 investment cost summary

	COST SUMMARY	
	Costs for supply and installation of the equipment:	
1	VFD Controller DDP to Akaki site cost in ETB	3,286,464.04
2	Installation, Test, Commissioning and Training cost in ETB for 10 Pumping Wells	450,000.00
	Total in Birr	**3,736,464.04**
	Total cost of the plant with 10% profit & 15% vat	
		ETB 4,726,627.01
	Operation and maintenance (O&M) costs for 15 years of operation	
3	10,000 Birr for maintenance in every other 2 years of operation for each pump, and considering the 15 years operation	**675,000.00**

6.3.2. Payback Period and Cash Flow Analysis

The Present Value of each element of the analysis (i.e. Investment Costs, O&M Costs and Benefits) and the total Net Present Value are shown in the below table. The table is completed with the Internal Rate of Return and Repayment Period of the original investment cost.

Table 6.6: Internal Rate of Return and Repayment Period of the original investment cost

	Present Value in ETB
Investment Costs	**4,726,627.01**
O&M Costs	**675,000.00**
Total Expenses (C)	**ETB 5,401,627.01**
Benefits (B)	**ETB 20,541,713.73**
Total NPV (B–C)	**ETB 15,140,086.72**
Benefit on Cost Ratio (B-C)/C	**2.80**
Internal Rate of Return (%)	**24.39%**
Repayment Period (years)	**3.80**

With power consumption cost of Ethiopia for equivalent flat rate above 50 KWh 0.5691 birr per KWh selling price, the NPV would result **15,140,086.72 ETB** and the IRR **24.39 %,** the original investment amount **5,401,627.01 ETB** could be repaid after **3.8** years.

CHAPTER 7

7. CONCLUSION AND RECOMMENDATION

7.1 Conclusion

The motive of this thesis is studying and evaluate the efficiency the actual groundwater pumping system, make energy efficiency/saving analysis and economic analysis for the improved system on ten deep-well submersible pumps at Akaki well-field Phase-3A groundwater pumping system.
The actual water pumps used to withdraw water from ground at this locations are fixed speed high capacity centrifugal submersible pumps, and throttled to the amount of water availability in the ground. The pumps consume maximum energy full time regardless of water availability in the system as I observe during actual pumping system inspection and data collection. Also the well test data shows high draw down of water from static level to the dynamic level of the pumping system, since the recharging capacity of the ground system is decreasing due to factors affecting the groundwater system.

To mitigate this problem throttling and add extra riser pipe is a control mechanism taken in this pumping system. This types of control techniques are characterized by low efficiency and high energy consumption.

As per the analysis in chapter 3, the actual pump efficiency of the pumping system the pumps perform under manufacturer recommended efficiency, thus, the energy conservation measures for the this system is essential to save energy and to run the pumps at its best efficiency point.

Many researchers and pump manufacturers recommend, when large flows must be controlled and motor energy consumption is significant, varying the motor speed is the answer to control the system energy consumption and efficiency as per the availability of the water. Controlling pumps by adjustable speed drive avoid wasting energy and improve the pump efficiency.

There are many advantage for using variable speed drive control in submersible pump applications. Variable speed drives offers a great energy saving where there is a need to vary flow rate, head, or velocity. This is highly significant in this Akaki Phase-3A water pumping system applications since the pumps run for a long hours.

The Matlab/Simulink result for both fixed speed and variable speed system model comparison suggested that, a variable frequency drive control enables the pump motor to maintain at its high

efficiency point. Furthermore, it provides lower power to the system, without having a significant impact on the efficiency of the system. This is accomplished by proper Hz control of the induction motor in PMW generator. In contrast, providing lower output power using fixed speed pumping system by reducing the input voltage, it reduces the efficiency of the system significantly and it becomes dangerous to operate motors at a such low efficiencies, as to much copper loss might overheat and burn the stator windings of the induction motor.

Re-designing this water pumping system by employing VFD control using variable speed pump analysis of nine submersible pumps in Akaki Phase-3A well-field minimizes the power consumption by an average of **23.45%** compared to the normal fixed speed pumping system.

The overall energy saving or the financial benefit in this system is substantial over a prolonged period of time. The main aim of this thesis is to reduce energy consumption of Akaki well-field submersible pumps by the implementation of VFD and the proper control of the water flow rate as per the ground water capacity in the field which affected by seasonal climate variation, drought, treats in the aquifers and increasing demand requirement.

Economic analysis to implement this variable speed controlling system is essential to demonstrate go/no go. The economic analysis of the redesigned system is done by means of a Cash Flow Analysis. This analysis compares the revenues obtained from the annual electric cost saving of the re-designed VFD system and cost of construction, operation & maintenance of the newly implemented system in the field.

With power consumption cost of Ethiopia for equivalent flat rate above 50 KWh 0.5691 birr per KWh selling price, the operation cost of the pump KWh minimized by 8.5% to 42.9% in an average of **23%** compared to current energy usage of fixed speed submersible pumps, and the NPV would result **15,140,086.72 ETB** and the IRR **24.39 %,** the original investment amount **5,401,627.01 ETB** could be repaid after **3.8** years.

When using VFD control in existing submersible pumping system, there are a few complications that user need to be aware of, but these can be overcome with some careful planning on voltage spikes, motor insulation, cable length, and other technical issues before installation.

This thesis results provide a potential energy saving from using VFD in Akaki Phase-3A well-field submersible pumps. Implementing VFD control system minimize the power consumption of the pumps motor in KW and the operation cost of the pumps in birr as KWh consumption of the pumps.

7.2 Recommendations

Instead of using direct grid electricity to pump the ground water, using hybrid system in that area will benefit the country since water pumping system demand high energy. Using solar powered, diesel and electric driven variable speed motor in that area will help the in every aspect, since the Akaki well-field site is near to the capital city Addis Ababa and open site, it is capable to use this technology to pump the ground water at the site.

The initial cost for VFD system and hybrid system is high comparing to the current installed pump cost. But comparing the initial cost (project cost) for the new systems with the running cost and the energy wasted in each pump, the country can save money and build green environment.

In addition assigning technically skilled person and continues upgrade of the knowledge of the technicians will have significant change in equipment management, water management and energy saving in Akaki well-field water pumping system.

8. REFERENCE

[1] - “Flow and Storage in ground water systems”, William M. Alley, Richard W. Healy, National ground water association, vol 296, 2002.

[2] - “Hydrogeological and Hydro-chemical framework of complex volcanic system in the Upper Awash River basin, Central Ethiopia”, Andarge Yitbarek Baye, University of Poitiers, Faculty of Basic and Applied Sciences, 2009.

[3] - “Ethiopia: Strategic Framework for Managed Groundwater Development”, Ministry of Water Resource, 2011.

[4] - “The Centrifugal Pump”, Research and Technology, Grundfos, 2010.

[5] - “Energy audit and Energy Management”, Gaudani v K, Vol. 1, IECC Press, 2009.

[6] - “Pressure Control for Leakage Minimisation in Water Distribution Systems Management”, Araujo, L.S.; Ramos, H.; Coelho, S.T., Water Resources Management, Vol. 20, 2006.

[7] - "Electric Motor and Control System", Frank D Petruzella, Published by McGraw-Hill, a business unit of The McGraw-Hill Companies, Inc., 2010.

[8] - “Practical Variable Speed Drives and Power Electronics”, Malcolm Barnes, 2010.

[9] - “Data-driven behavioral characterization of dry-season groundwater-level variation”, Rahul Gokhale and Milind Sohoni, Indian Institute of Technology Bombay, Mumbai, 2015.

[10] - “Improving energy efficiency of pumping systems through real-time scheduling systems”, L.K Reynolds and S. Bunn, Integrating Water Systems, 2010.

[11] - “Dynamic Modeling of Pump Drive System utilizing Simulink/MATLAB Program”, Hamad Raad Salih, Ali Abdulwahhab Abdulrazzaq, Basarab Dan Guzun, International Research Journal of Engineering and Technology, 2016.

[12] - “Energy Saving Using Variable Speed Drives”, Robin Priestley, Rockwell Automation, U.S Department of energy, 2014.

[13] - “Control Valves Verses Speed Drive for Flow Control”, Muhammed H Al-Khalifah and Gregory K. McMillan, ISA Authomation, 2012.

[14] - “Energy conservation using VFD in pumping application”, Mr. Ankur P. Desai, Mr. Rakesh. J. Motiyani and Dr. Ajitsinh R. Chudasama, S.N Patel Institute of technology and research center India, 2014.

[15] - “Energy efficiency policy opportunities for electric motor driven system”, Paul Waide and Conrad U. Brunner, International energy agency, 2011.

[16] - “Comparison of Conventional Induction Motor-Pump System with One Containing a Variable Frequency Drive”, M. Ishtiaque Rahman and Khosru M. Salim, 2015.

[17] - “Energy saving in submersible system”, ABB Ltd, World Pump, 2011.

[18] - “Pump Hand Book”, Edited by Igor J. Karassik, Joseph P. Messin, Paul Cooper, Charles C. Heald, Third Edition, 1998.

[19] - “Pump Affinity Laws for Centrifugal Pumps”, Steve Wilson, Grundfos White Paper, 2015.

[20] - “Manual for the Design of Pipe Systems and Pumps”, GEA Mechanical Equipment, 2016.

[21] - “Standard hand book of engineering calculations” Tyler G. Hicks, McGraw-Hill, Inc, third edition, 1994.

[22] - “Power electronics (converters application and design)”, Ned Mohan, Tore M. Undaland and William P. Robbins, Third edition, John Wiley and sons INC, 1995.

[23] - “Aspects of Energy Efficiency in Water Supply System”, Mordecai Feldman, IWA water loss reduction specialist conference, 2007.

[24] - “Euro pump and Hydraulic “, Rossmann and Ellis, Carlson, Hovstadius et al., Gülich, 2008.

[25] - “AC Motors-Synchronous and Asynchronous”, Dr. Levent Çetin, EEE Electrics, 2015.

[26] - “AC Induction Motor Fundamentals”, Rakesh Parkh, Microchip Technology Inc, AN887, 2003.

[27] - “Electric Machines (DC machines, AC machines and polyphase circuits) in S.I. units”, R.K. Rajput, Laxmi publications LTD, Third edition, 2002.

[28] - “Power electronics”, P.C. Sen, McGraw- Hill Education Private Limited, Second edition, 2009.

[29] - “Standard hand book of engineering calculations” Tyler G. Hicks, McGraw-Hill, Inc, third edition, 1994.

[30] - “VFDs Drive Energy Efficiency in Motors: How to Save Energy, Cut Costs Using Variable Frequency Drives,” Kerns, Ken., Green Manufacturer, 2012

[31] - “Improving pumping system performance”, Lawrence Berkeley National Laboratory, A sourcebook for Industry second edition, 2006.

[32] - NRCS-Montana Technical Note, 2010.

[33] - “Variable Frequency Drive”, Craig Hartman, Variable Frequency Drives and Accessories, 2014.

[34] - “Industrial Project Management”, concept, tools and techniques, Adedeji Badiru, Abidemi Badiru, Adetokunboh Badiru, CRC Press, 2008.

[35] - “GK3000 User Manual and price list for VFD controller”, GoHz Inc., USA, 2018.

[36] - “Scaling - Up Renewable Energy Program”, Ministry of Water and Energy, 2012.

[37] - “Technical Characteristics and Performance curves of Submersible Borehole Pumps”, Pleuger Pumps, appendix 1, Consortium CGC Overseas Construction ETH. Ltd. 2010.

[38] - “Variable Speed Pump Analysis (VSPAnalysis)”, Joe Evans, Ph.D, 2010.

9. APPENDIX

Appendix A: Manufacturer Pump Performance Curve

Pump model PN 104-5a + MI10-740/2,

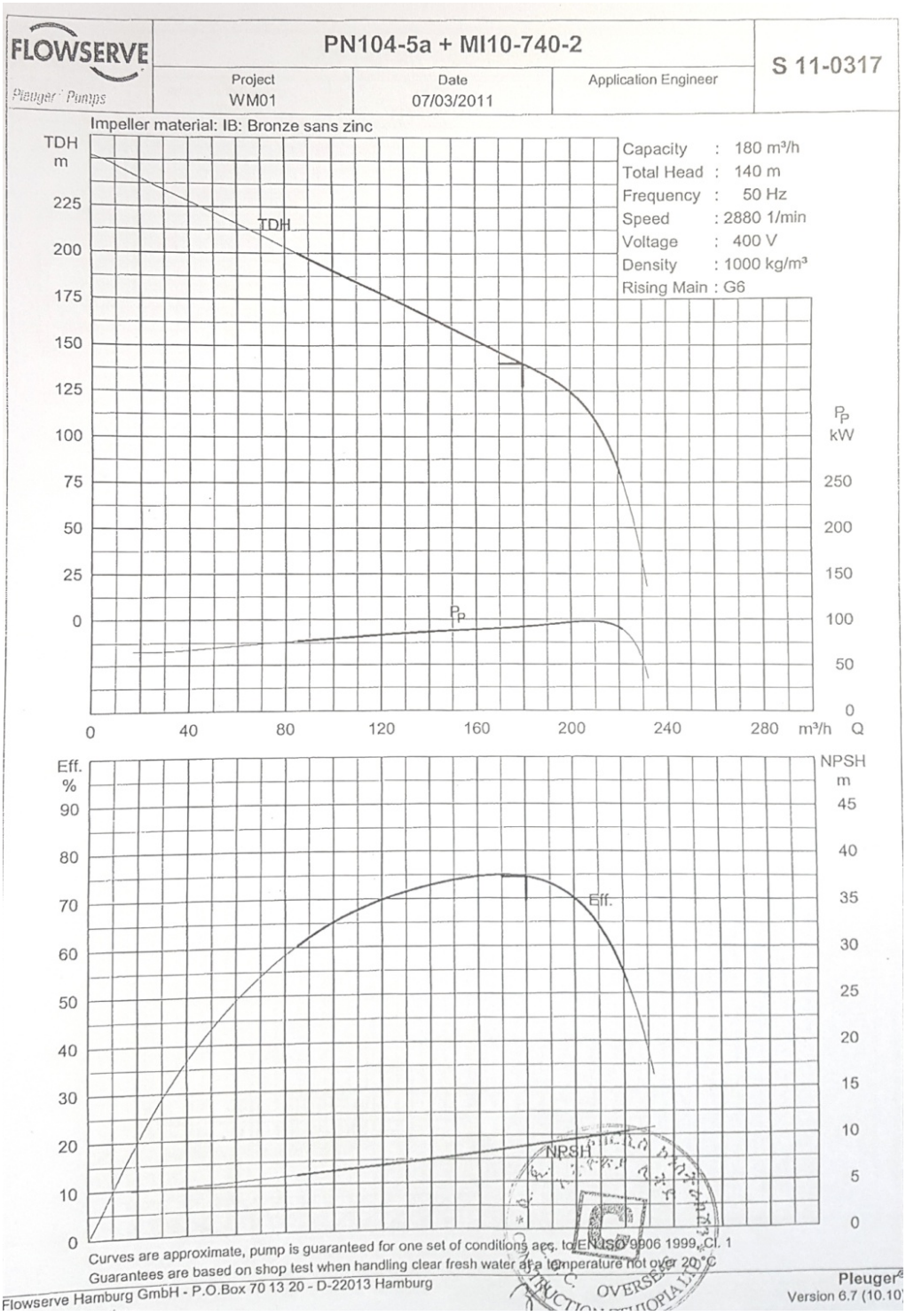

Pump model PN 104-6 + MI10-880-2,

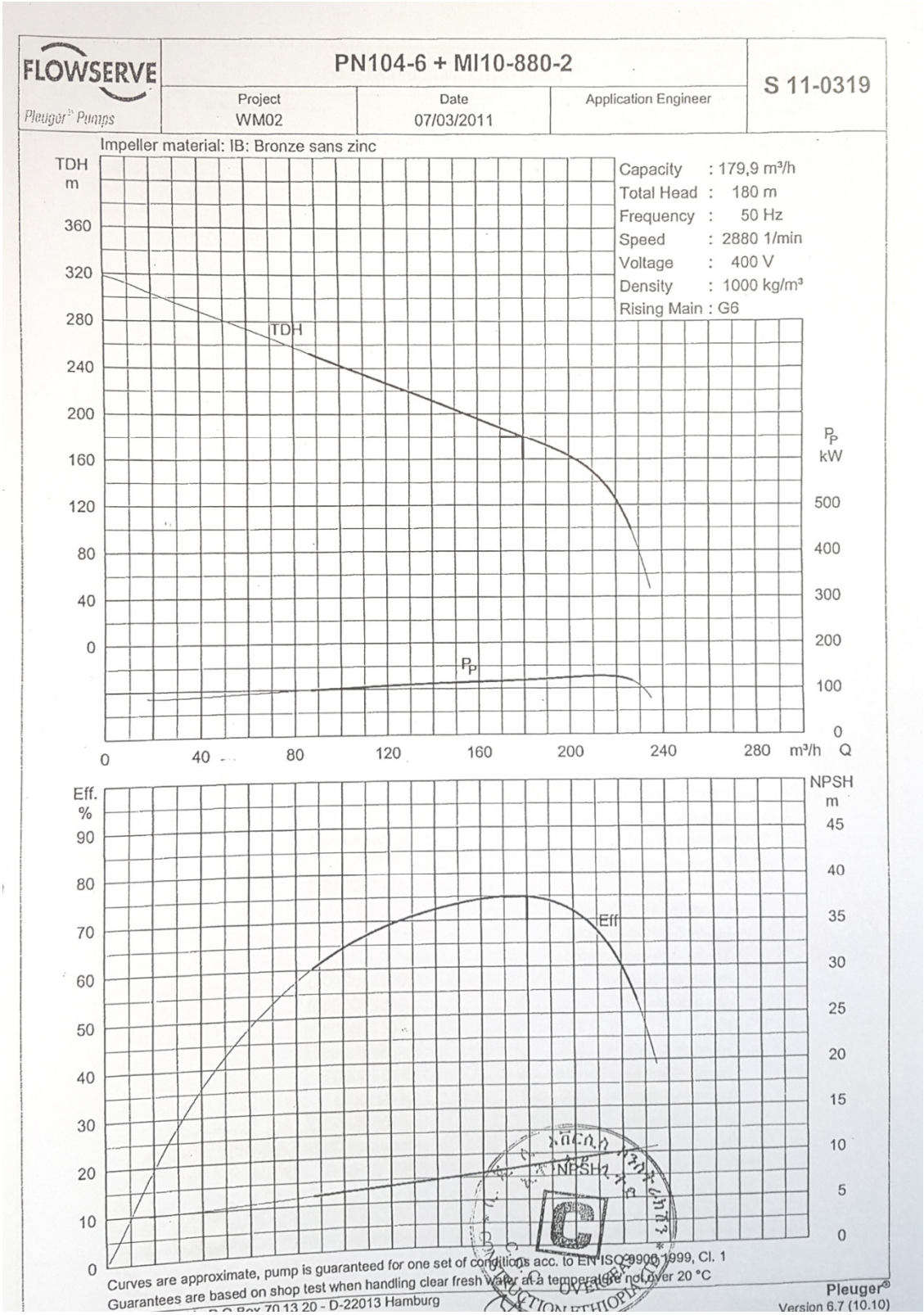

Pump model QN101-7 + MI10-880-2,

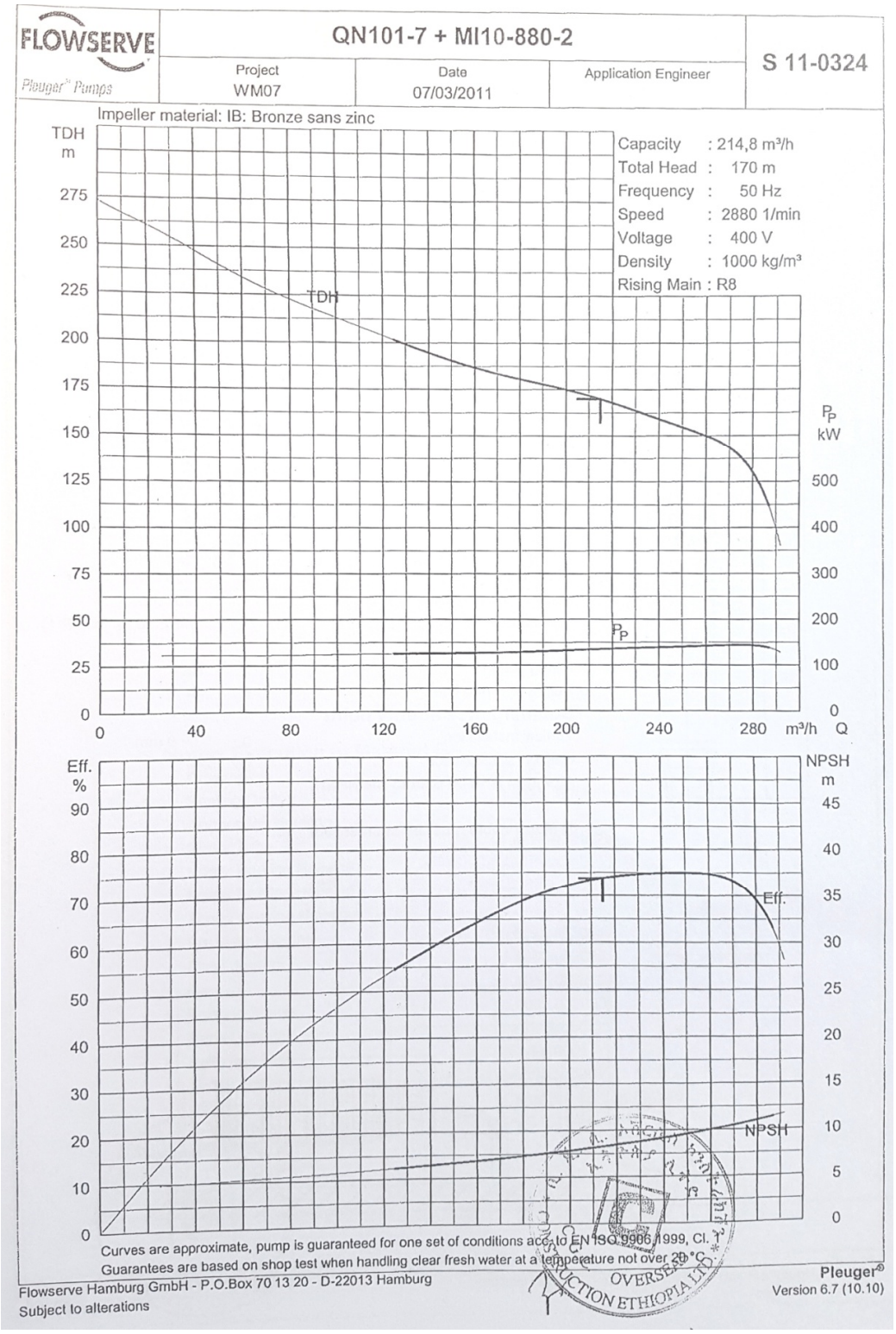

Pump model QN102-6a + MI10-880-2,

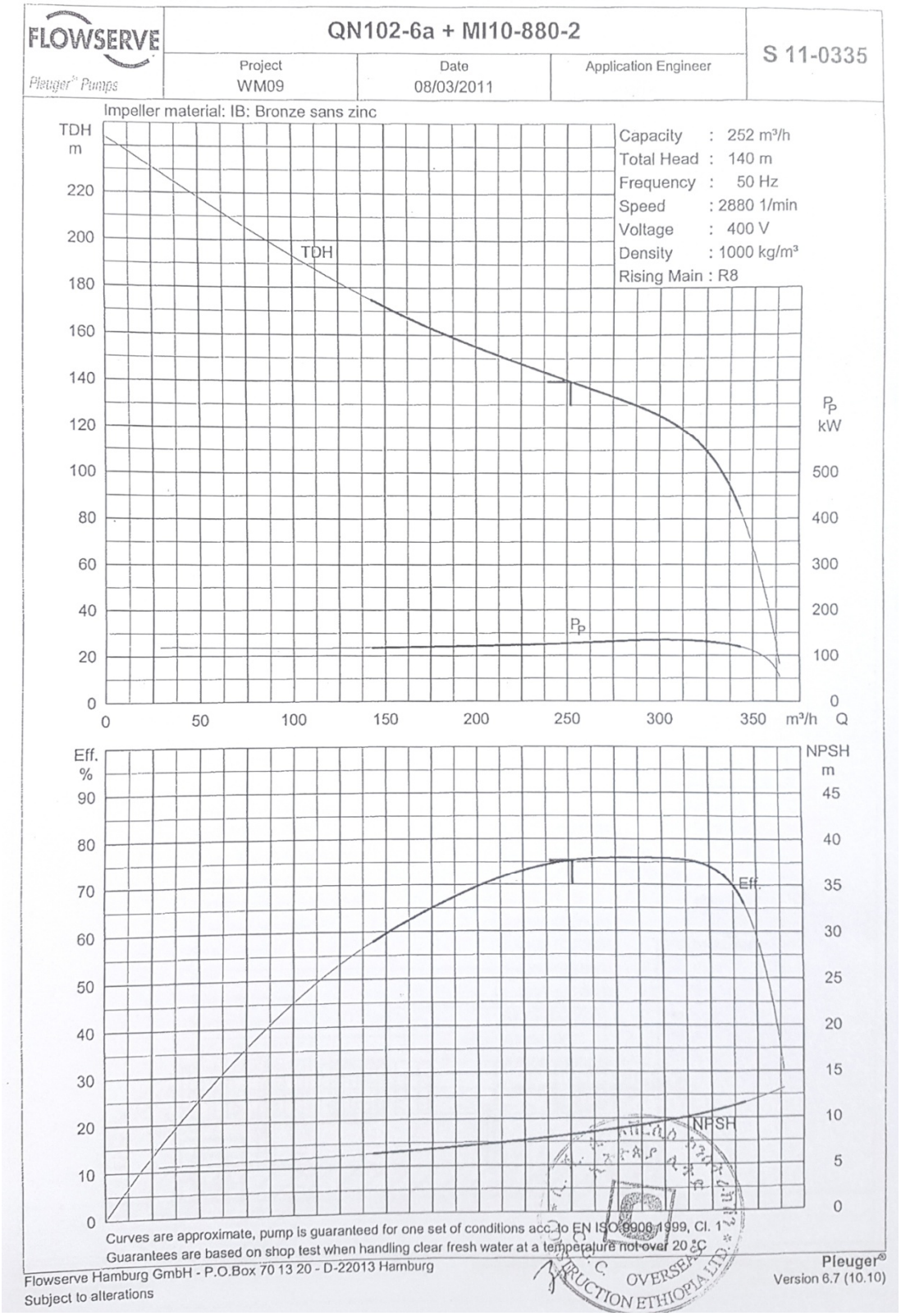

Pump model QN102-6a + MI10-960-2.

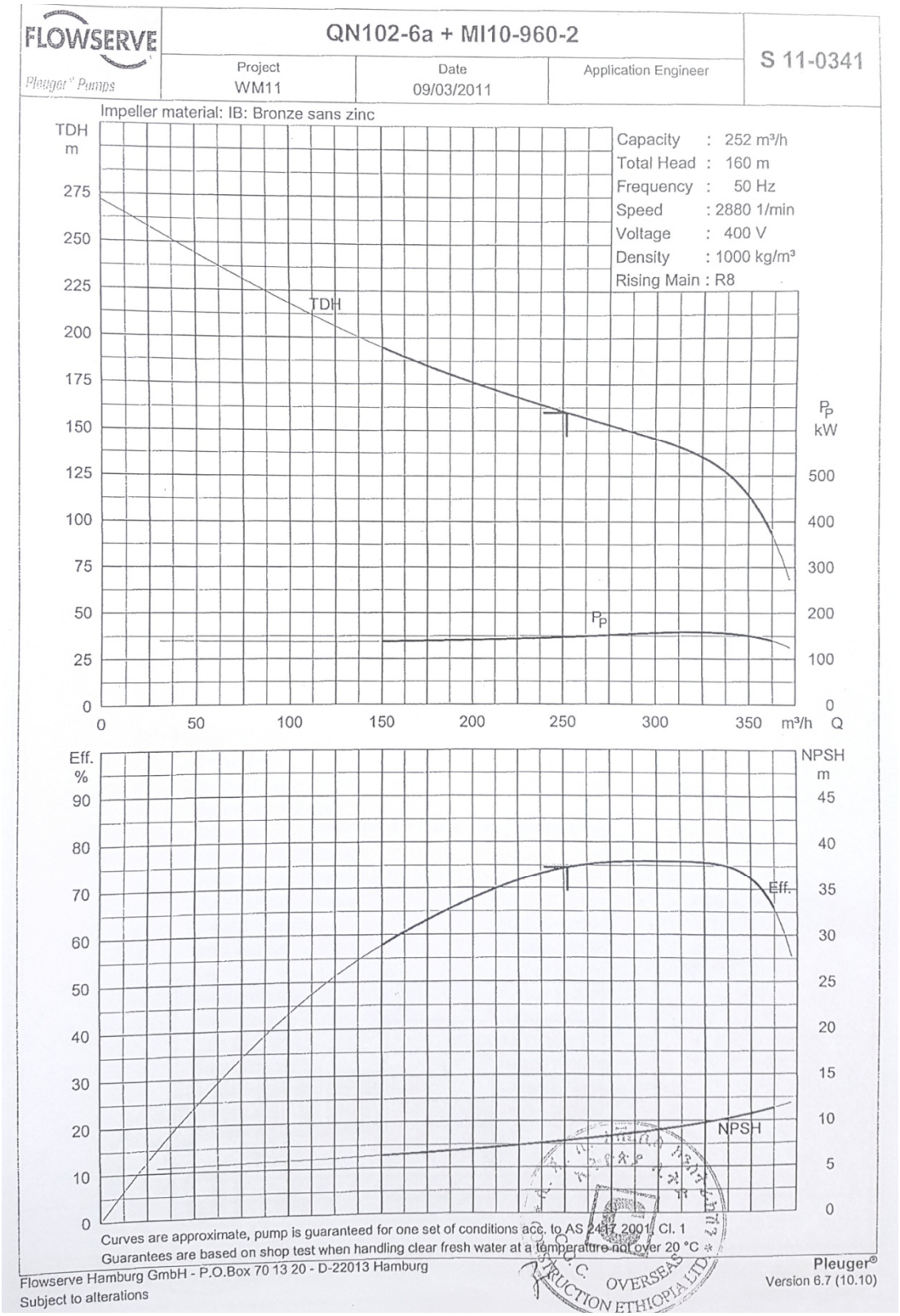

Pump model QN102-6a + MI10-960-2.

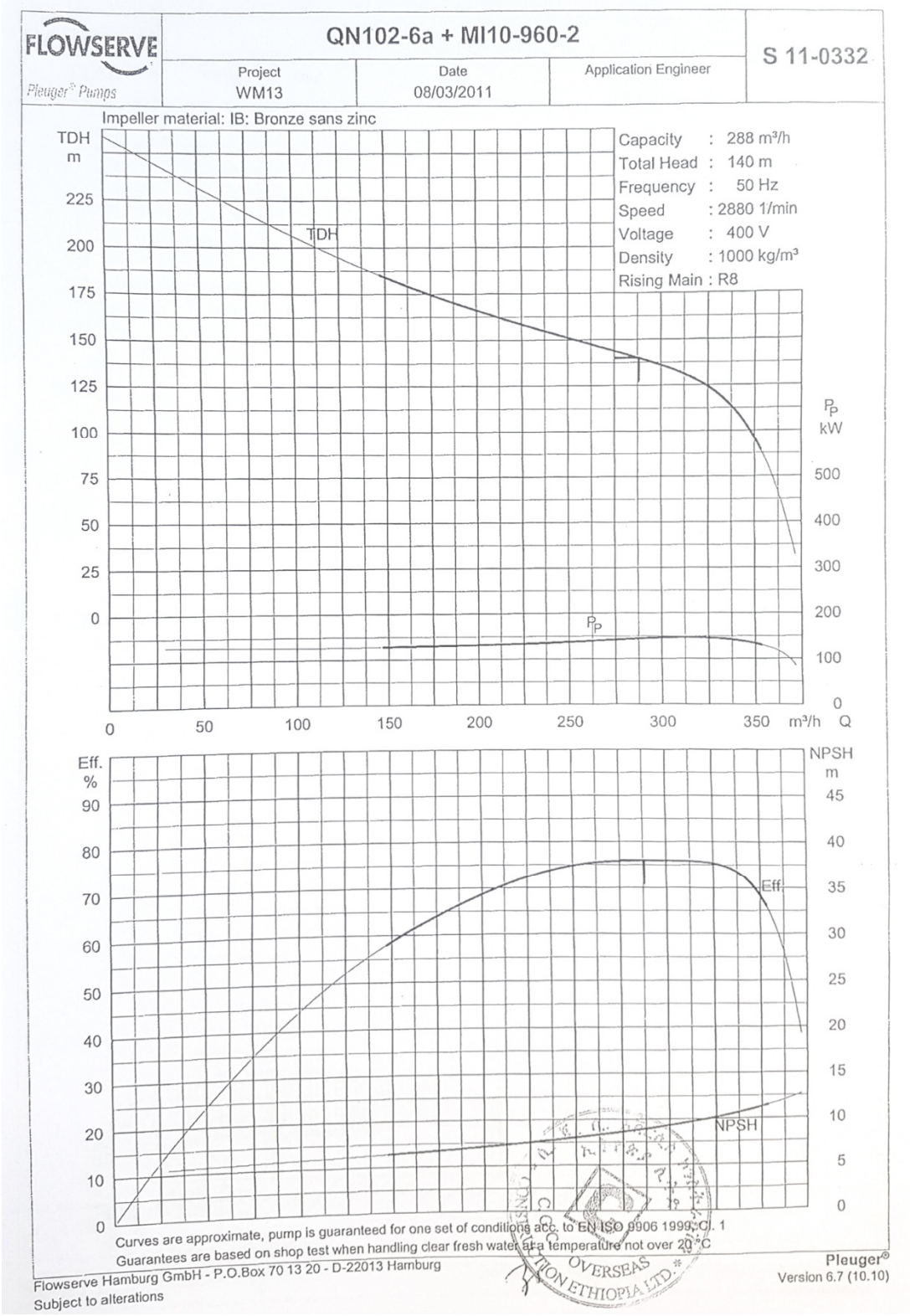

Pump model QN102-7a + MI10-1070-2,

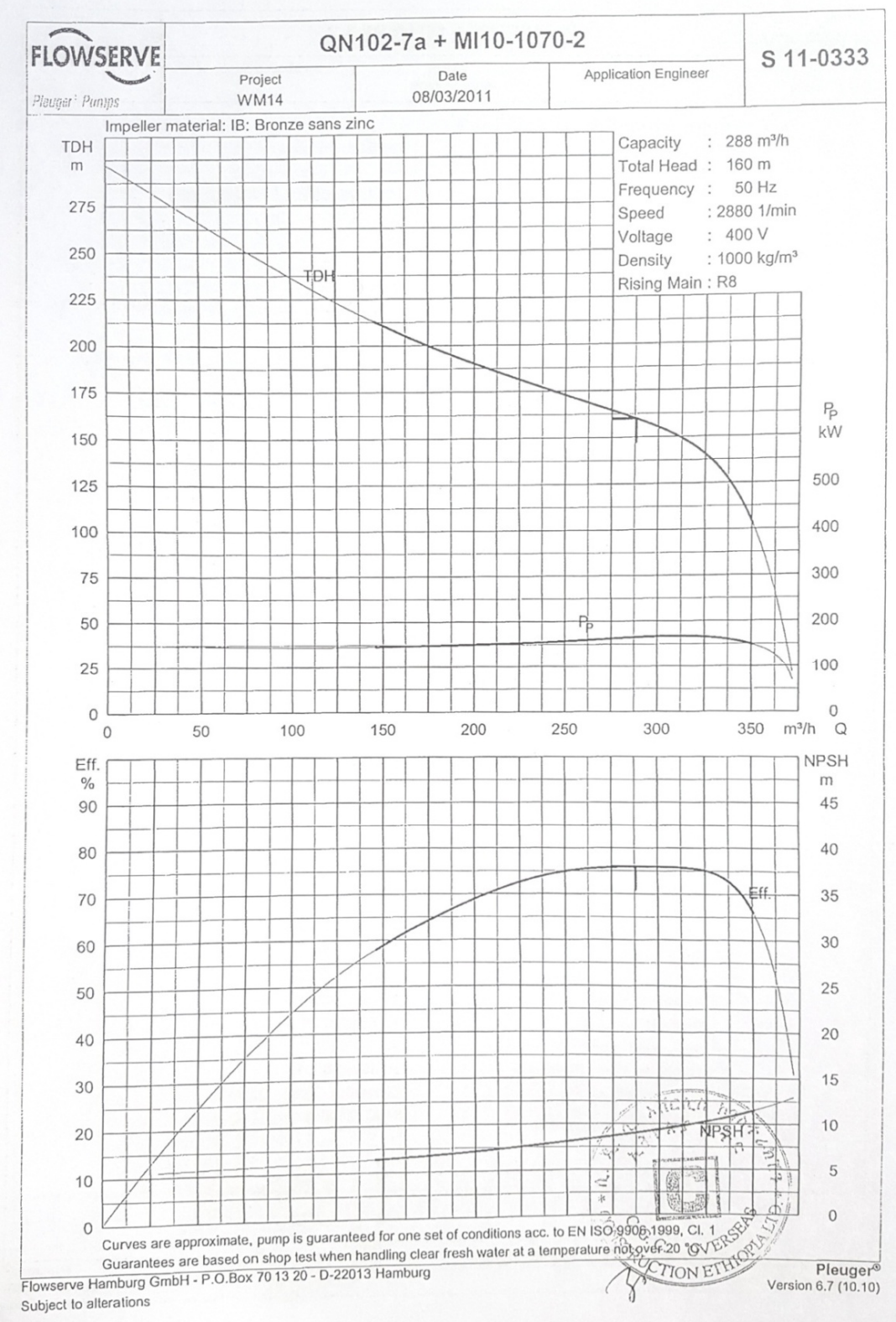

Pump model QN102-8a + VNI12-110-2.

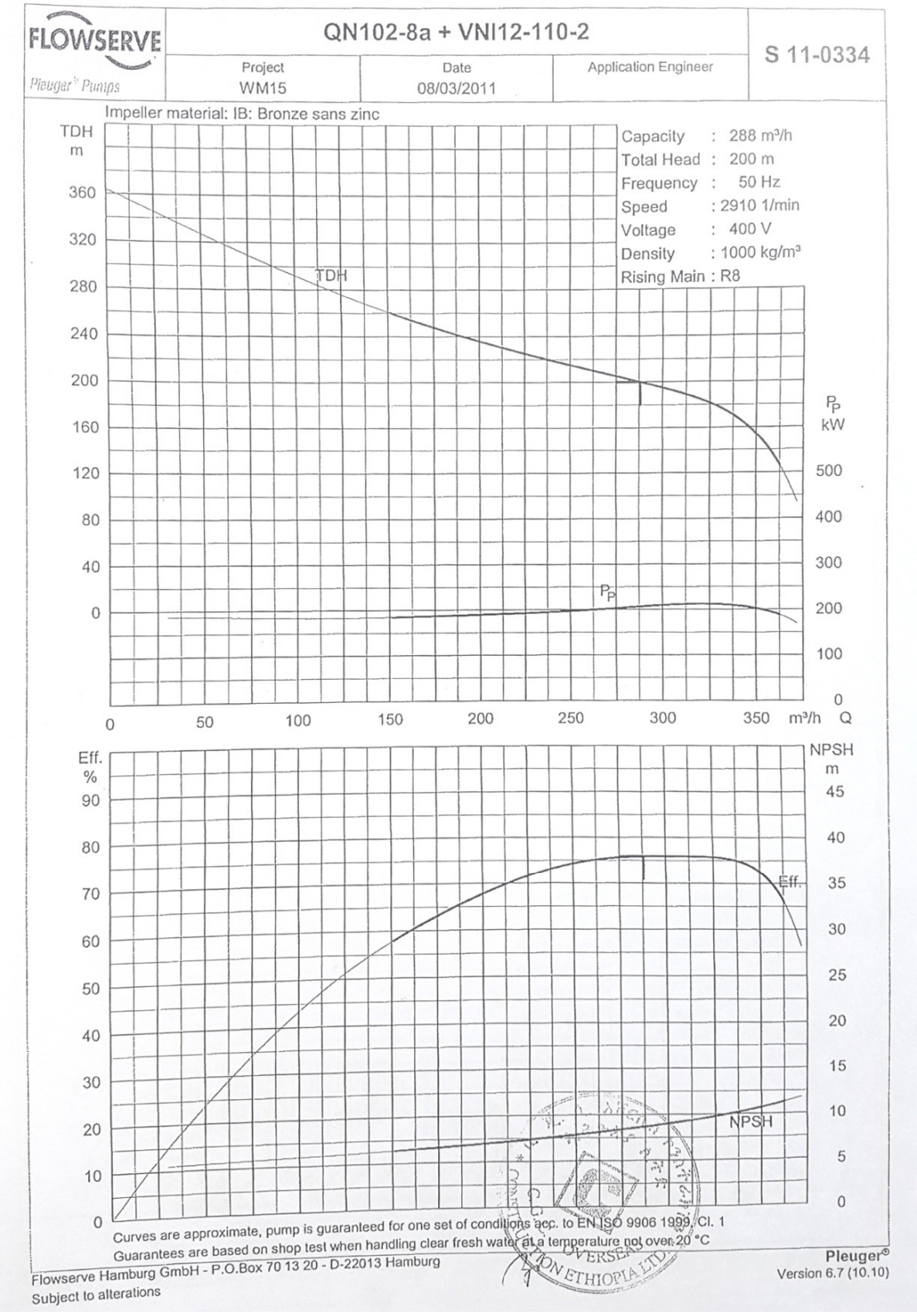

Pump model QN102-6a + MI10-880-2.

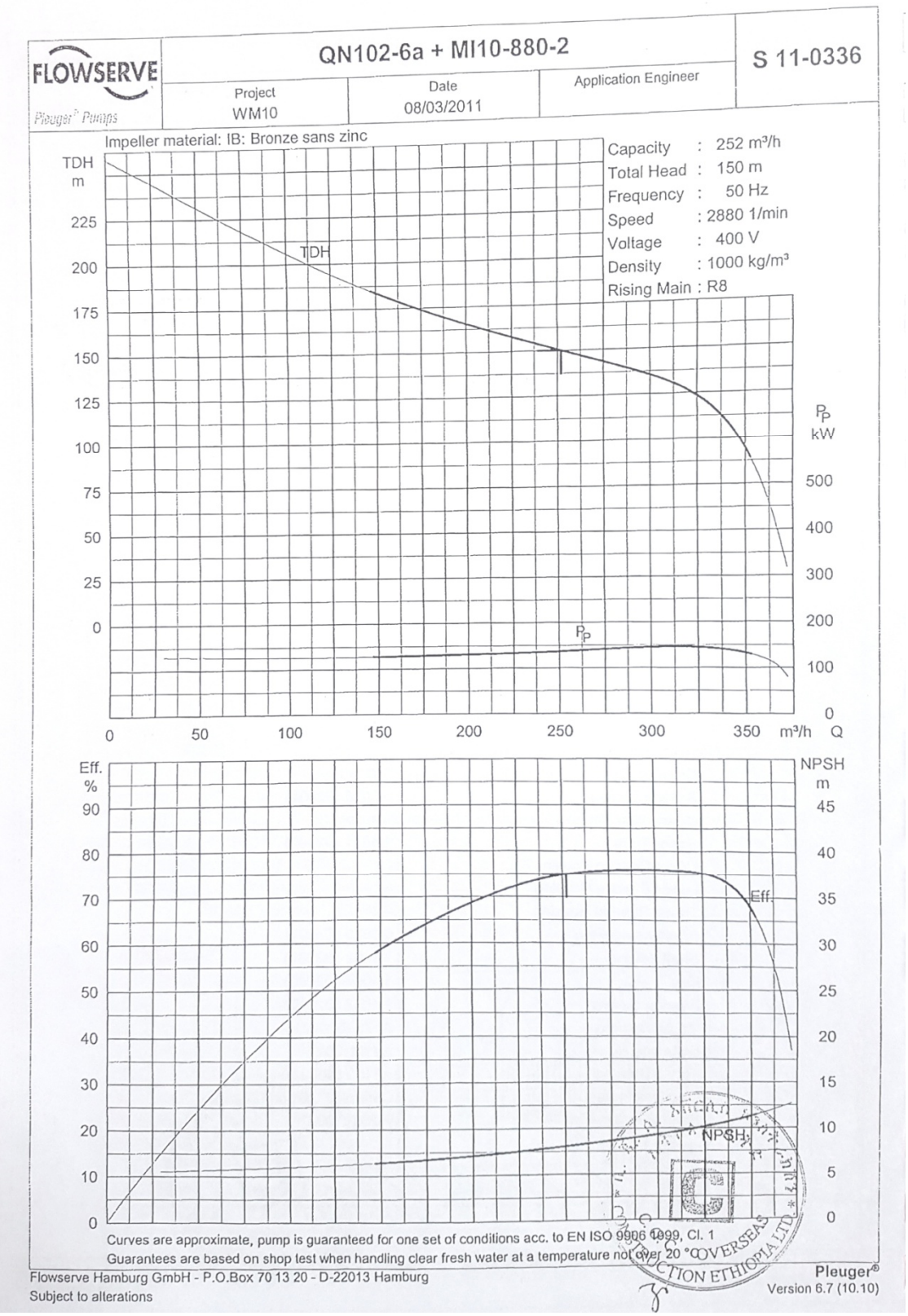

Appendix B: Wells Design Data & Test Result

ADDIS ABABA_ DEEP WELLS WATER SUPPLY PROJECT

PHASE III PART A

Deep Wells Design Data (Phase IIIA project)

N°	Well Index	Pump model	Power (KW)	Discharge (L/S)	Head (M)	Speed (RPM)	Freq (HZ)	Voltage (V)	Density (KG/M3)	Eff (%)	pump test result					Water temperature
											Static Level	Dynamic Level	Discharge (lit/sec)	Pump Position	Draw down	
1	WF02-PW5	PN 104-5a + MI10-740/2	140	50	140	2880	50	400	1000	75	80.10	82.39	50.0	120	2.29	34.30
2	WF02-PW6	PN 101-7a + MI10-490/2	90	30	170	2880	50	400	1000	75	73.83	109.34	30.0	125	35.51	32.50
3	WF02-PW7R	QN 102-8a + VNI12-110/2	250	80	200	2910	50	400	1000	76	53.72	147.71	75.0	230	93.99	33.00
4	WF02-PW8	PN 104-5a + MI10-740/2	140	50	140	2880	50	400	1000	74	45.74	103.33	50.0	128	57.59	36.20
5	WF02-PW9	QN 102-6a + MI10-960/2	190	80	140	2880	50	400	1000	75	50.73	71.56	70.0	90	20.83	36.80
6	WF02-PW10	PN 104-6 + MI10-880/2	75	50	180	2880	50	400	1000	75						
7	WF02-PW11	QN 102-6a + MI10-880/2	170	70	140	2880	50	400	1000	75	83.40	105.82	70.00	130	22.42	30.90
8	WF02-PW12	QN 101-7a + MI10-880/2	170	60	170	2880	50	400	1000	73.5	61.20	94.76	46.0	110	33.56	27.40
9	SL-PW-12	QN 102-6a + MI10-960/2	190	80	140	2880	50	400	1000	75						
10	WF02-PW13	QN 102-6a + MI10-880/2	170	70	140	2880	50	400	1000	75	64.81	71.04	61.0	113.00	6.23	25.40
11	WF02-PW14	QN 102-6a + MI10-960/2	170	70	150	2880	50	400	1000	75	53.40	83.44	60.0	120.0	30.04	32.4
12	WF02-PW15	QN 103-8 + VNI12-120/2	270	100	170	2910	50	400	1000	76	52.73	132.0	142.0	180.0	79.3	34.0
13	WF02-PW16	QN 102-6a + MI10-960/2	190	80	140	2880	50	400	1000	75						
14	WF02-PW17	QN 102-7a + MI10-1070/2	210	80	160	2880	50	400	1000	75						
15	WF02-PW18	QN 102-6a + MI10-880/2	170	70	140	2880	50	400	1000	75						
16	WF02-PW19	PN 101-7a + MI10-490/2	110	30	190	2880	50	400	1000	75	82.1	174.6	26.3	180.0	92.5	28.0
17	WF02-PW20	QN 102-7a + MI10-1070/2	210	80	160	2880	50	400	1000	75	44.0	58.0	90.0	100.0	14.0	25.0

Appendix C : Deep Wells Actual Discharge Data

For 2 continuous days from June 19 and 20 of 2016 Discharge m^3/hr (Phase IIIA project)

Time 24 hr	WF02-PW5	WF02-PW6	WF02-PW7R	WF02-PW8	WF02-PW9	WF02-PW10	WF02-PW11	WF02-PW12	SL-PW-12	WF02-PW13	WF02-PW14	WF02-PW15	WF02-PW16	WF02-PW17	WF02-PW18	WF02-PW19	WF02-PW20
19-Jun-16																	
1	163.3	99.5	133	104.4	194	137.1	129.2	121.5		214.5		285	208.7		189.1	93.4	259.9
2	163.3	98.8	132.8	103.8	194.6	136.7	125.7	121.3		213.6		283.8	210.4		187.9	93.2	260.8
3	163	99.4	134.0	104.2	195.6	137.1	129.2	121.9		215.5		285.9	210.6		188.6	94	262.4
4	163.3	99.2	133.9	103.4	194.5	135.2	128.2	121.1		214.6	177.6	284.1	208.9	222.3	188.8	92.9	261.1
5	163	100.8	132.2	104	195.1	135	128.3	121.7		215.3		285	210		190.1	94	260.4
6	163	99	132.5	103.1	195.1	135.9	129.5	122.9		216.3		286.2	211		189.3	93.8	261.8
7	163.9	100.1	132.7	103.9	195.8	136.9	129.1	122.3		215.3		285.5	209.4		189.1	92.6	260.1
8	163.5	100.2	133.0	105	196.4	136.4	129.4	122.8		217		285.5	210.1		188.9	93.5	262
9	163.1	100.1	133.5	105	195.8	136.3	129.4	122.7		215.3		285.7	210		188.7	94.1	262
10	163.5	99.6	131.0	104	194.7	136.6	129.1	122.2		215.8		286	209		189.1	95.2	262.5
11	168	103.4	132.1	93.2	198.7	135.3	132.9	130.5		212.6		296.5	212.9		191.8	113.9	260.2
12	163	100.1	133.3	105	204.1	136.1	129.7	123.4		216		288	210.1		189.1	94.2	261.7
1	163.1	100.2	130.2	103.9	198.7	136.4	129.4	122.2		215		285.7	209.4		189.7	95.2	262
2	163.5	99		103.1	201	136.9	128.2	121		214.6		285	209		188.7	94.1	260.4
3	163	99.3		104.6	201.1	132.8	126	121.3		214.1		284.7	208.6		186.7	94	261.6
4	163.5	99.1		103.1	201.5	132.2	126.4	122.4		214.1		284.5	208.1		186.1	94.1	216.4
5	163.8	99.6		104.7	202.8	134.1	126.4	122.8		215		285.7	210.3		188	94	262
6	164.9	99.8		105.9	203	134.4	127.7	123		217.1		286.6	210.3		188.3	93.7	263.3
7	164.1	99.5		105.5	197.6	135.8	129.2	121.5		214.3		285	209.2		189.5	95.3	262.7
8	164.1	100.5		106.8	202.5	133.5	128.4	123.4		217.8		286.7	210.3		189.3	94.5	264
9	165.5	100.3		105.6	202.7	132.6	128.5	123.5		216.9		286.4	210.6		187.9	94.1	264.1
10	164.7	101.22		104.7	201.4	135	128.8	121.7		217		285.7	209.7		188.7	95.3	263.2
11	163	99.7		105.7	198.2	137	129.2	122.9		214.7		284.8	210		188.6	94.1	262
12	165.1	101.1		103	201.5	132.6	127.2	123.3		217.1		284.8	209.4		188.2	98.7	262.3

20-Jun-16																	
1	163.5	100.1		104.3	198	132.8	127.5	122.3		216.4		283.9	209.2		187.5	101.9	261.6
2	165.2	100.8		107.9	203.2	135.4	129.4	124.8		219.6		289	214.2		190.8	95.2	261.1
3	164.6	100.9		106.8	201.8	134.6	128.7	123.8		218.1		287.9	212.3		189.4	94.5	261.1
4	164	99.8		106.9	200.9	129.5	128.8	123.6		217.6		285.9	210.7		188.2	94.6	261.1
5	163.8	102.5		108.1	201.9	138	129.5	125.7		219		301.6	211.9		192.4	117.7	261.1
6	165.8	100.5		106.9	203.8	135.2	129.7	125.4		218.1		291.7	212.3		190.2	98	261.1
7	165	100.2		106.2	205.1	135.6	128.9	125.1		218.8		289.4	212.2		190.7	94.9	261.1
8	164.3	100.1		105.4	201.3	138	123.4	124.4		214.2	192.3	290.2	209		186.4	95.3	261.1
9	166	100		105.5	202.6	141.5	127.9	123.7		214.7	191.8	289.8	211.7		186.1	114.6	261.1
10	164.2	100.3		105.4	203	140.7	127.4	123.3		213.2	190.7	289.2	209		185.6	96.9	
11	Reservoir full																
12	Reservoir full																
1	163.8	99.7		105.1	201.8	135.8	128.1	123.4		212	189.7	287.5	207.5		184.7	96.8	260.6
2	163.5	99.2		104.5	200.7	134.1	126.2	123		210	188.1	286.7	205.1		184.2	96.2	260.4
3	162.5	99.3		104	199.5	133.2	125.2	121.6		210.5	185.8	286.9	206.7		183.2	94.1	260.4
4	161.1	99		103.4	197	130.2	123.2	119.2		208.8	184.5	284.9	204.5		181.5	93.7	257.9
5	162.3	99.3		103.4	197.9	132.2	125.1	120.2		210.2	183.7	284.8	205		185.2	94.7	260
6	161.1	99.2		103	199.7	134.1	126.2	120.1		208.9	185.5	286.9	205		181.5	93.9	261
7	176	106.4		129.9	207.9	146.8	138.9	132.1		210	186.1	298.8	71		191.5	117.7	260
8	161.8	99.1		104.4	202.5	142.1	126.8	122.5		211.6	188.8	296.1	71.6		183.8	104.9	261.9
9	163	99.9		103.2	200.6	134.9	127.9	122.5		214.5	198.1	286.6	210.6		187.5	94.7	261.2
10	164	99.1		103.4	202.6	134.8	127.2	122.5		214.6	198.1	286.1	210		187.5	94.9	261
11	164.9	99.2		104	207.6	134.4	123.8	120.1		210.3	195	283.1	210.6		181.1	93.5	258.6
12	163.5	99.9		104.4	202	140.1	123.4	123.4		216.7	195	287.6	210		188.6	94.5	262.1

Appendix D: Parameters used to simulate the models

For different motor power and the corresponding torque and stator current vs speed curve of the motor

For 170 KW, three-phase, 50HZ,2 pole, induction motors from the manufacturer are as follows:

P_N	KW	170	Dir.		Y	
I_N	A	330	M_A/M_N	1.8	M_A/M_N	0.45
M_N	Nm	560	M_K/M_N	2.9	M_K/M_N	0.8
$\cos\varphi_A$		0.43	I_A/I_N	5.9	I_A/I_N	1.6

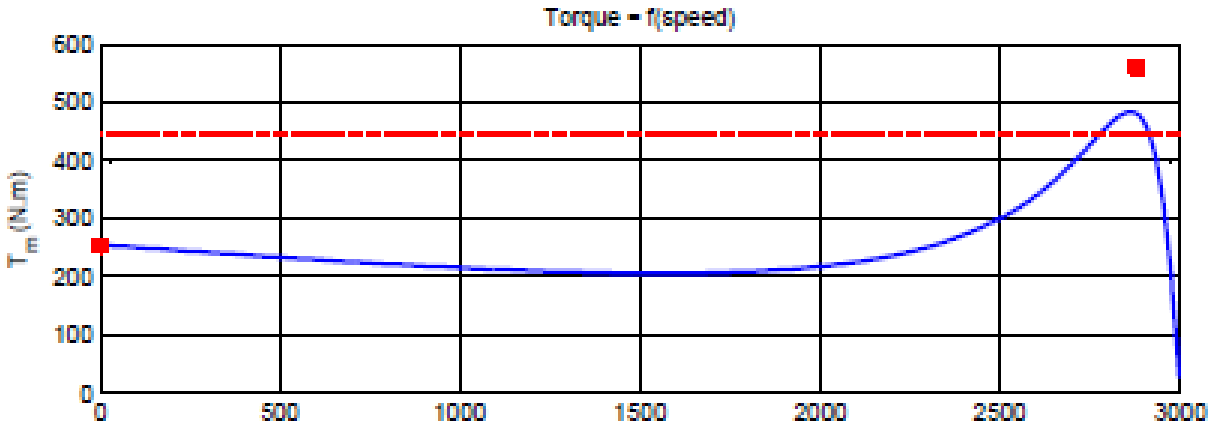

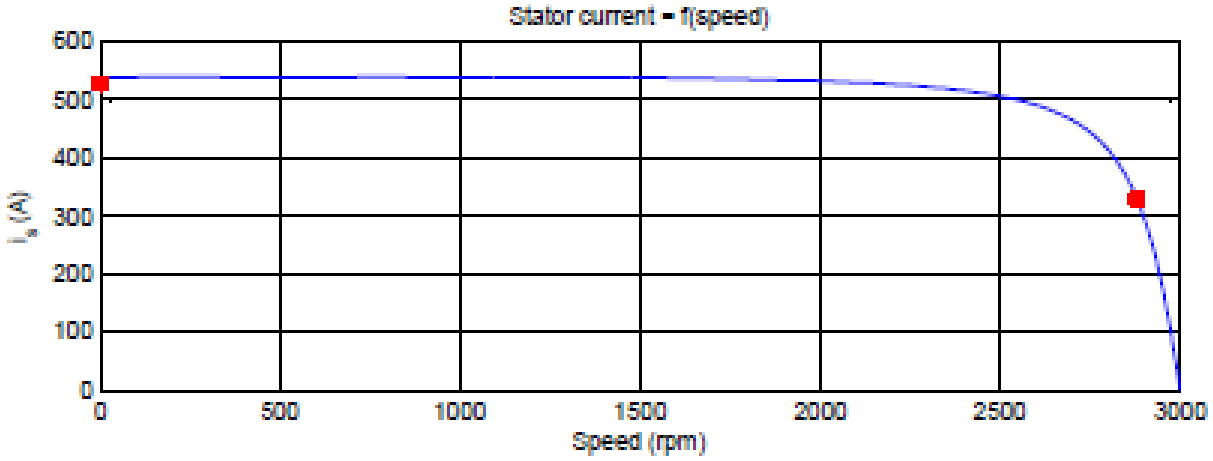

For 190 kw, 2880 rpm, 50HZ, 400v Flowserve submersible motor

P_N	KW	190	Dir.		Y	
I_N	A	370	M_A/M_N	1.9	M_A/M_N	0.45
M_N	Nm	630	M_K/M_N	2.9	M_K/M_N	0.8
$\cos\varphi_A$		0.44	I_A/I_N	5.9	I_A/I_N	1.6

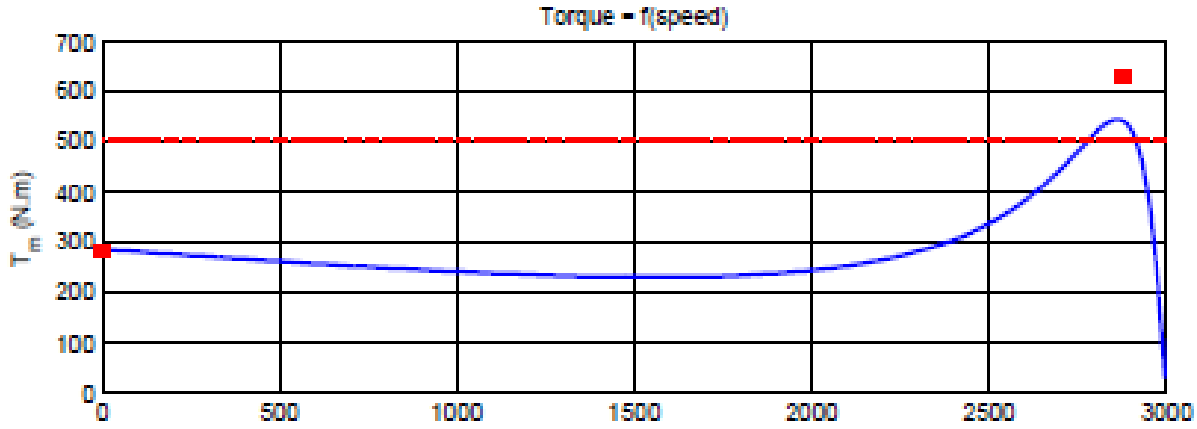

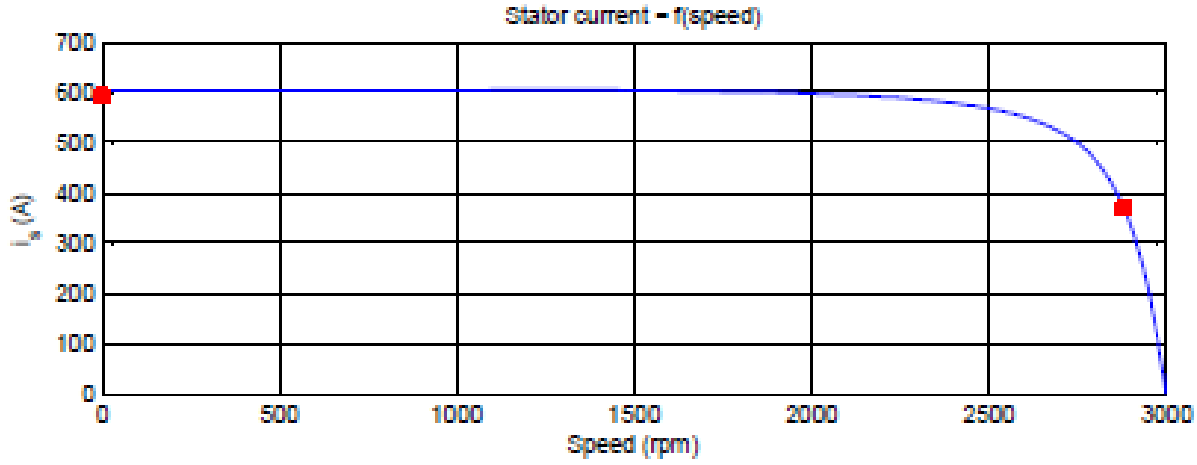

For 210 kw, 2880 rpm, 50HZ, 400v Flowserve submersible motor

P_N	KW	210	Dir.		Y	
I_N	A	410	M_A/M_N	2	M_A/M_N	0.45
M_N	Nm	700	M_K/M_N	3	M_K/M_N	0.8
$\cos\varphi_A$		0.45	I_A/I_N	6	I_A/I_N	1.7

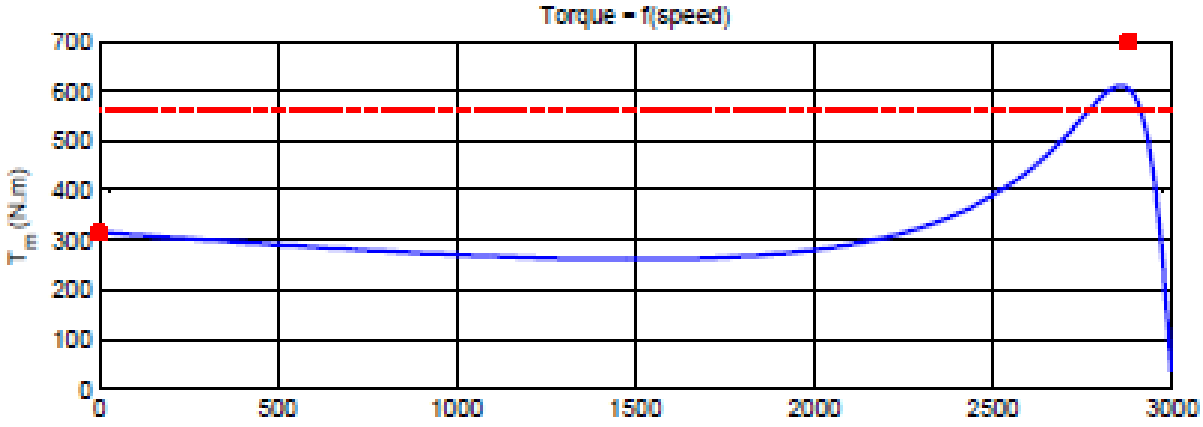

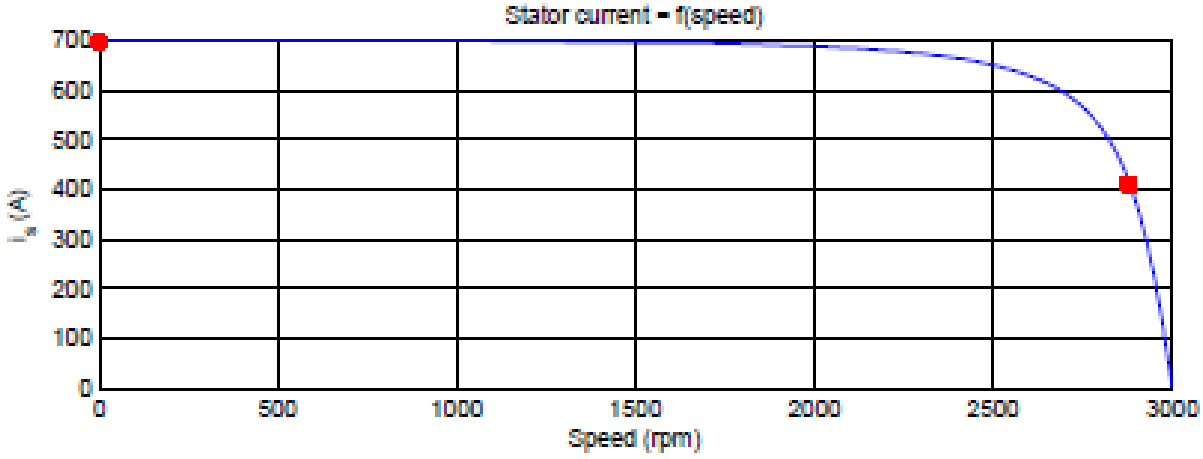

For 250 kw, 2910 rpm, 50HZ, 400v Flowserve submersible motor

P_N	KW	250	Dir.		Y	
I_N	A	460	M_A/M_N	1.6	M_A/M_N	0.45
M_N	Nm	820	M_K/M_N	2.9	M_K/M_N	0.9
$\cos\varphi_A$		0.38	I_A/I_N	6.3	I_A/I_N	1.9

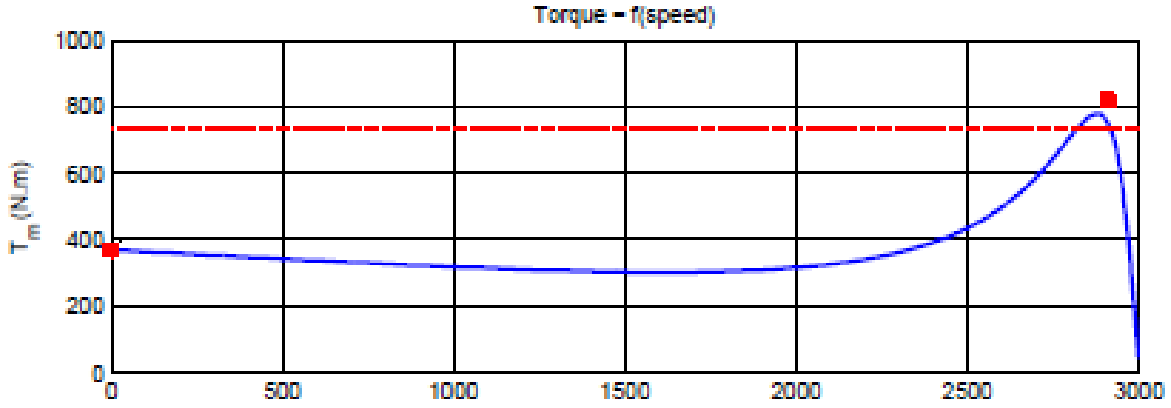

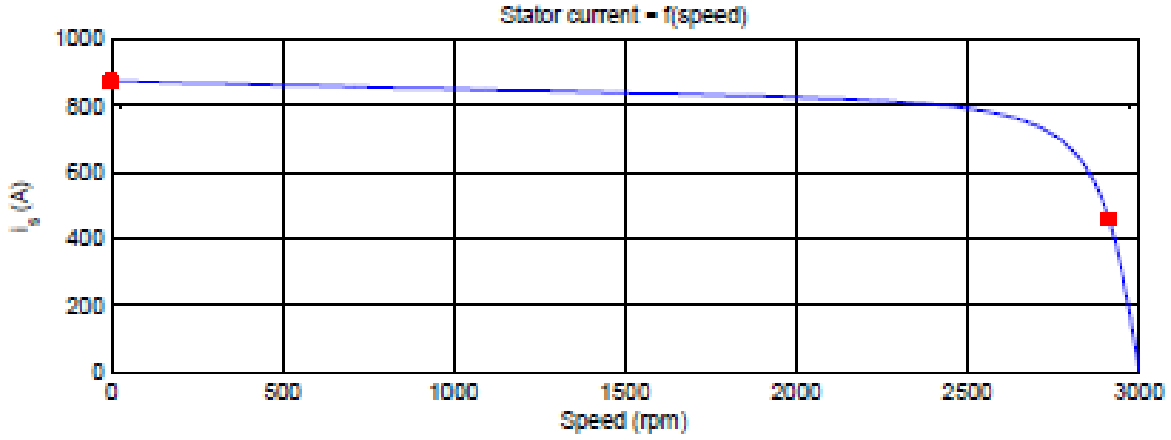

Appendix E: Pump Analysis

Variable Speed Pump Analysis for WF02-PW07 well field

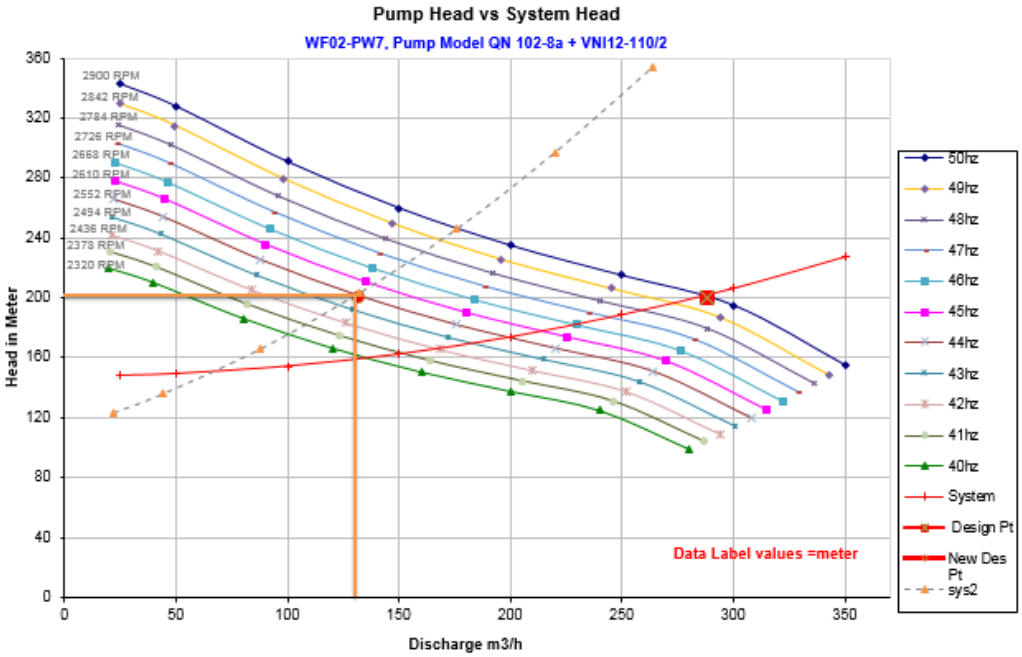

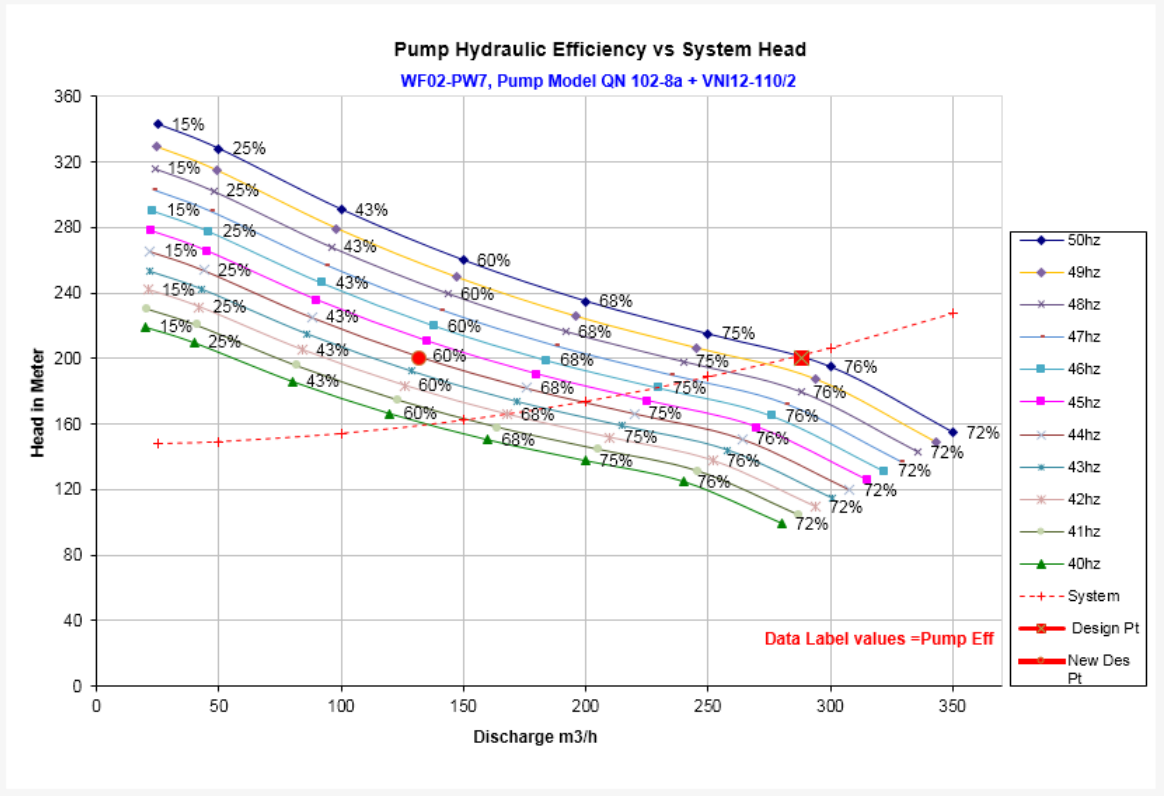

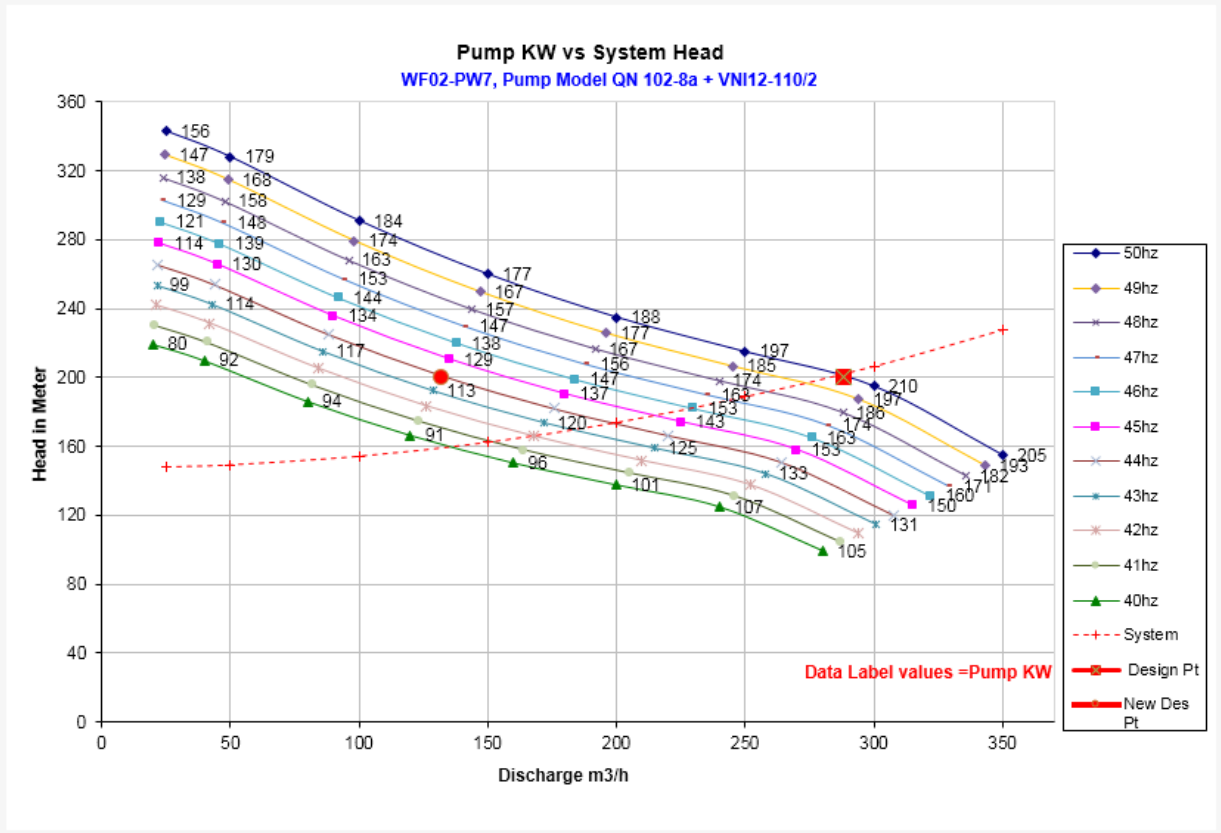

Variable Speed Pump Analysis for WF02-PW08 well field

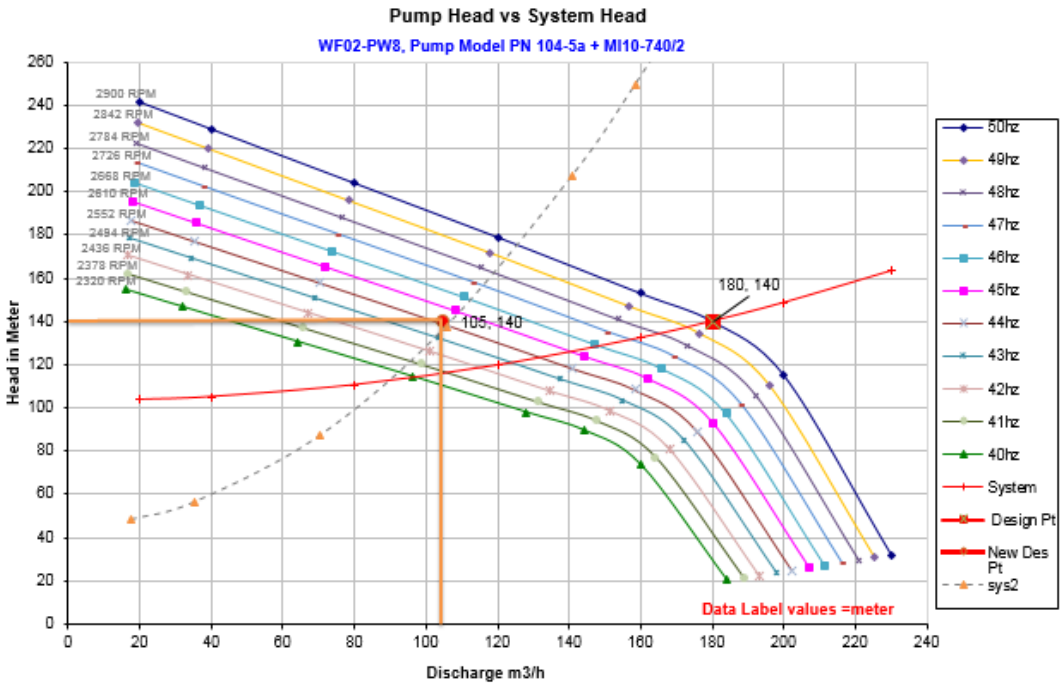

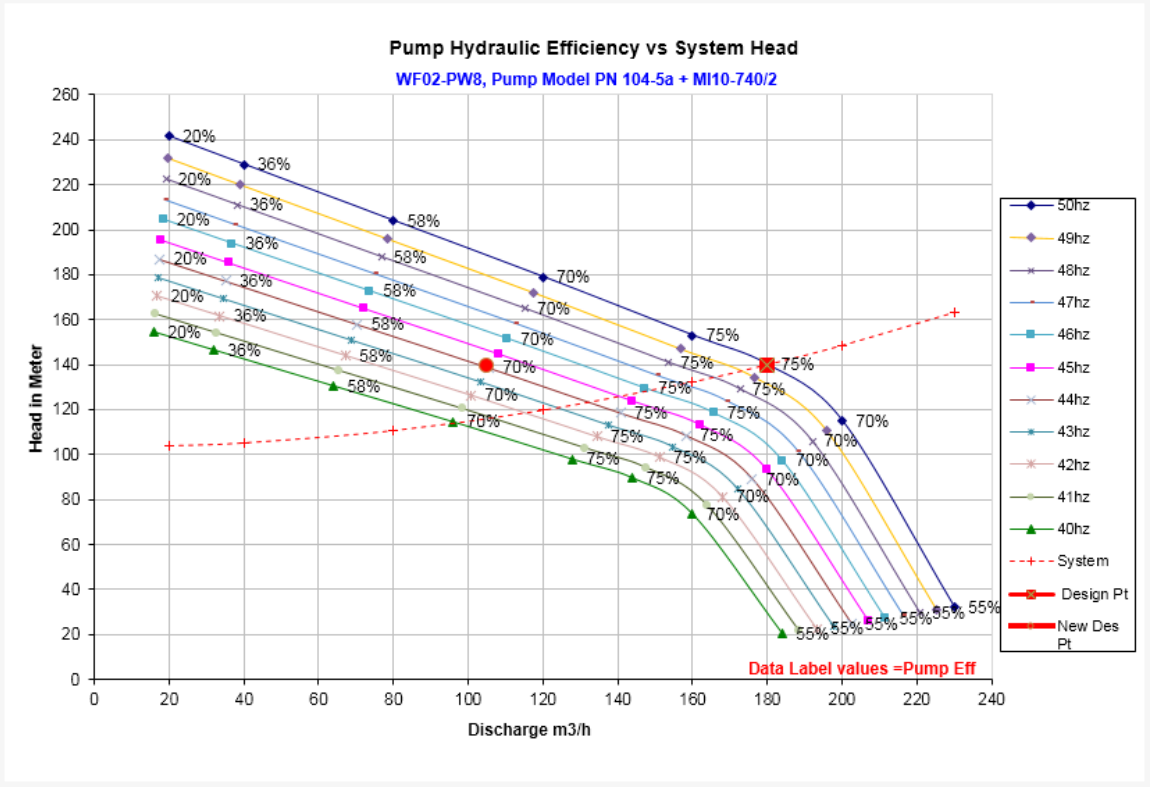
Pump Hydraulic Efficiency vs System Head
WF02-PW8, Pump Model PN 104-5a + MI10-740/2
Head in Meter
Discharge m3/h
Data Label values =Pump Eff
50hz
49hz
48hz
47hz
46hz
45hz
44hz
43hz
42hz
41hz
40hz
System
Design Pt
New Des Pt

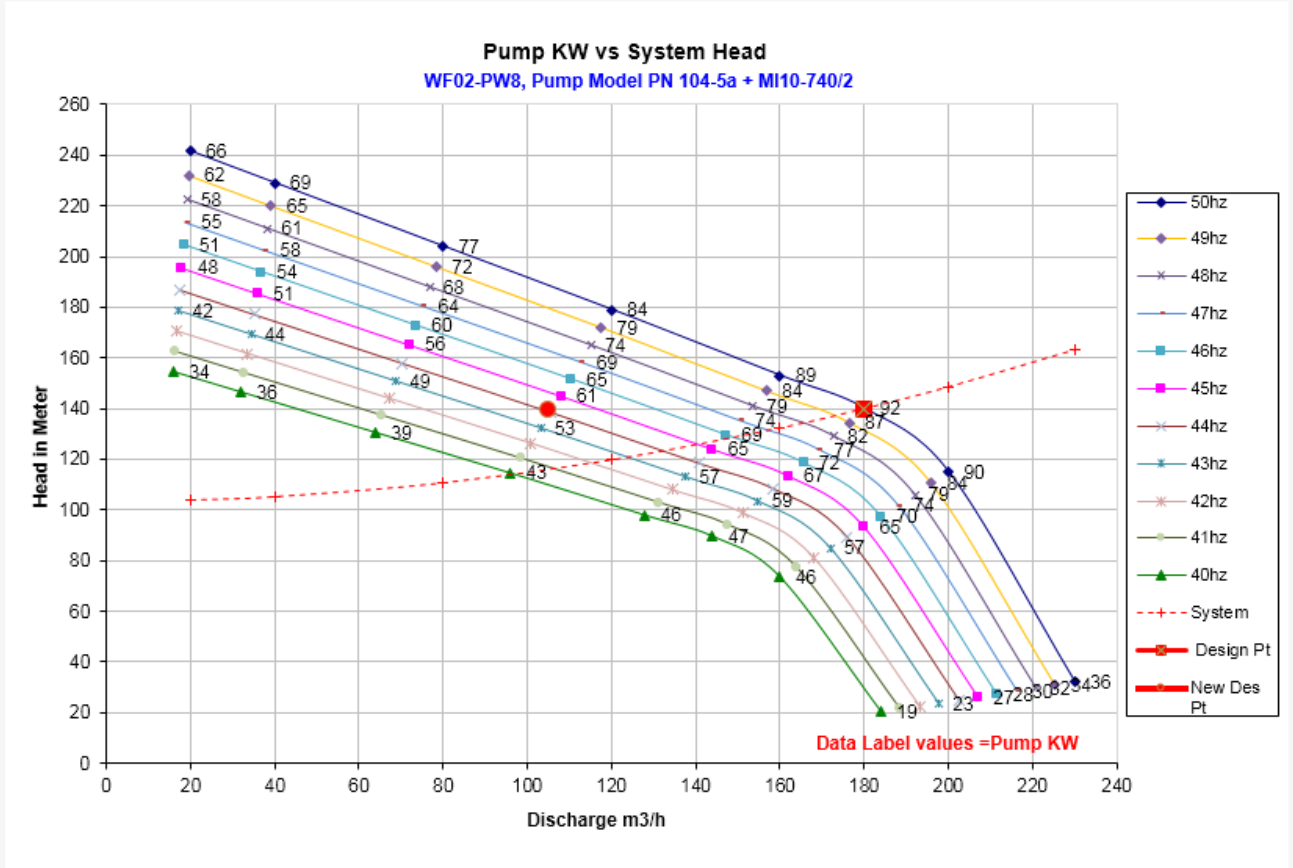
Pump KW vs System Head
WF02-PW8, Pump Model PN 104-5a + MI10-740/2
Head in Meter
Discharge m3/h
Data Label values =Pump KW
50hz
49hz
48hz
47hz
46hz
45hz
44hz
43hz
42hz
41hz
40hz
System
Design Pt
New Des Pt

Variable Speed Pump Analysis for WF02-PW09 well field

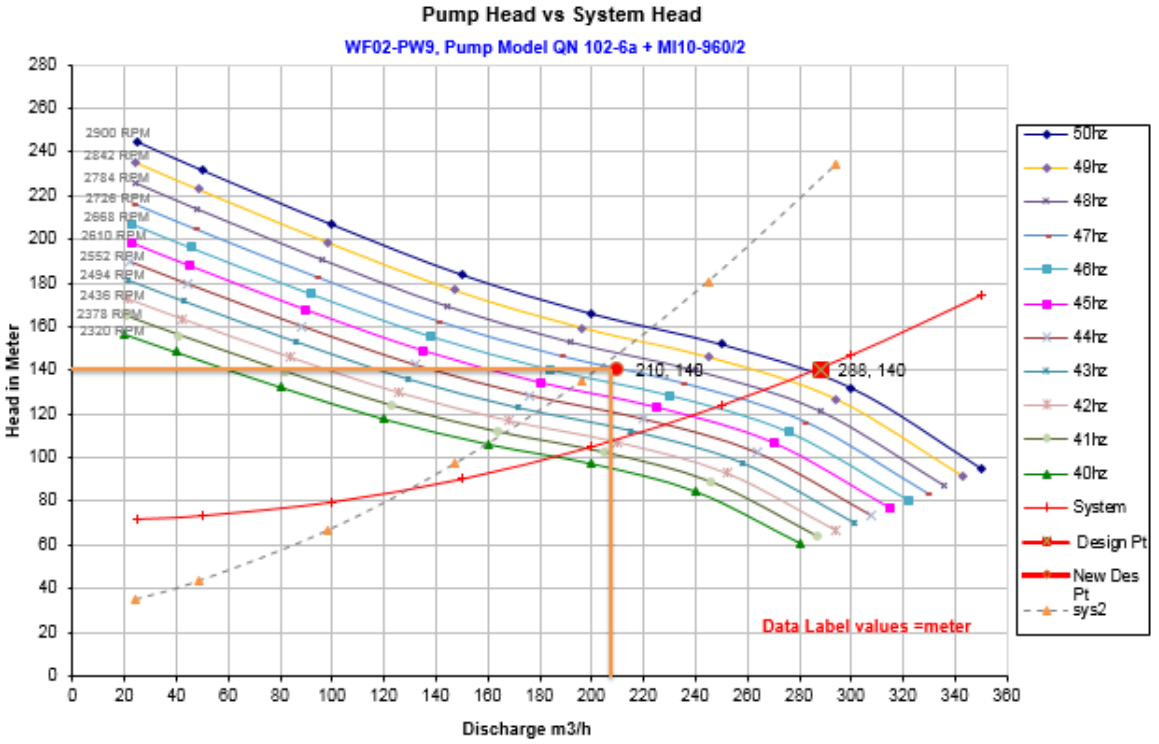

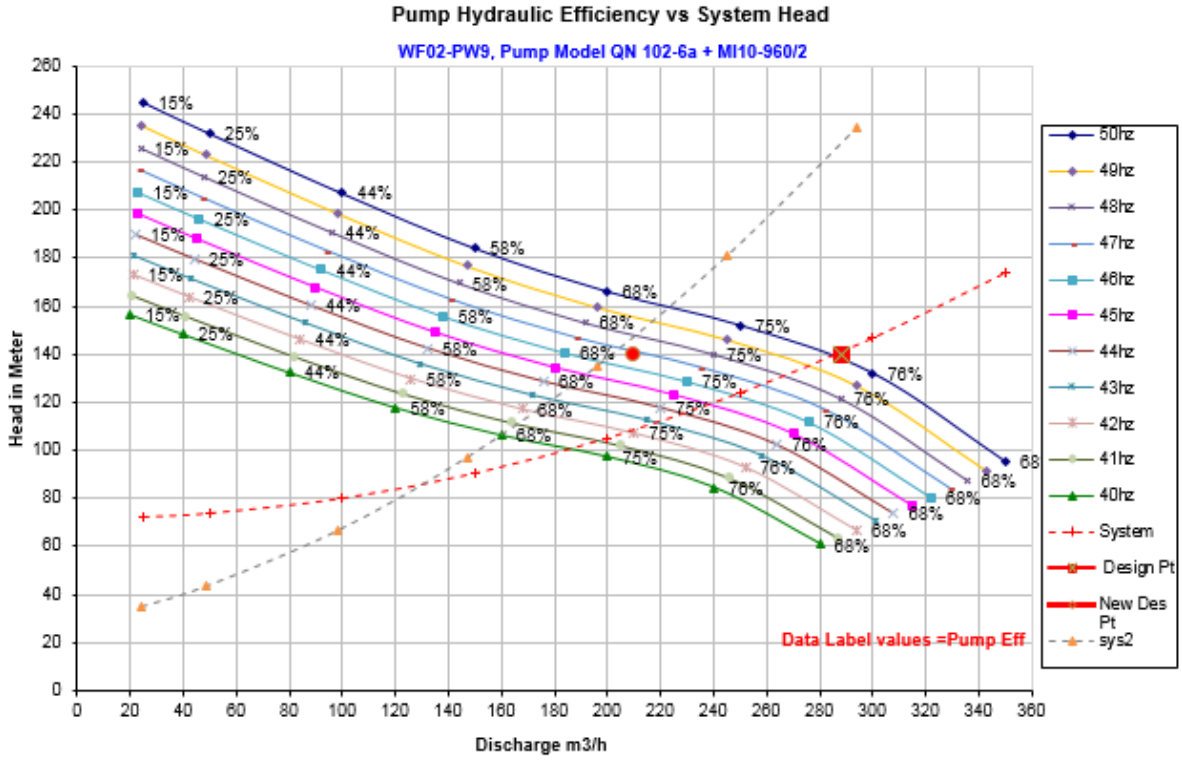

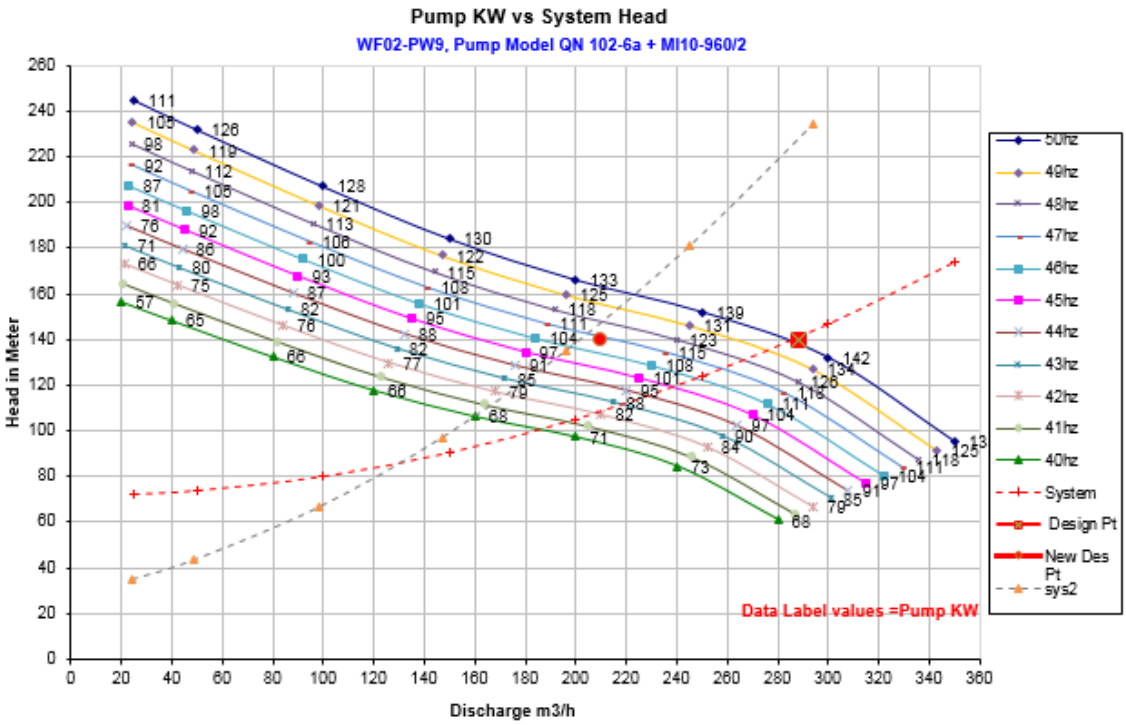

Variable Speed Pump Analysis for WF02-PW11 well field

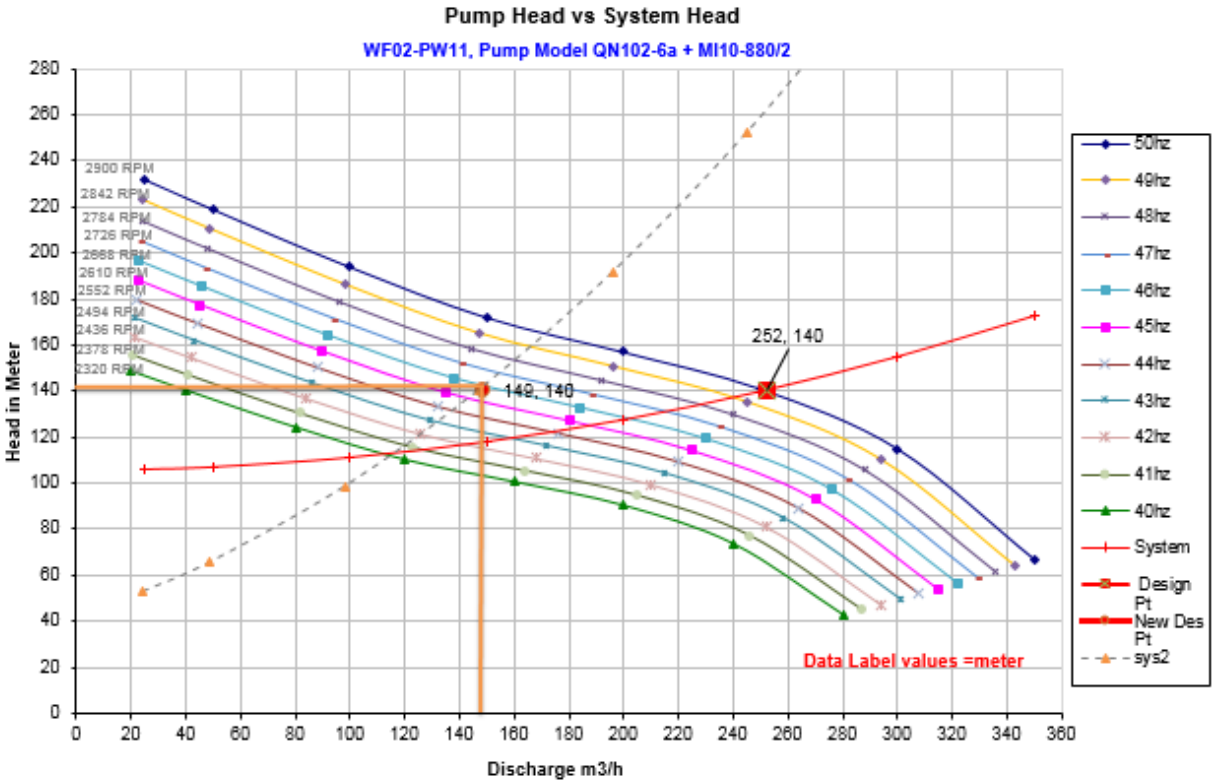

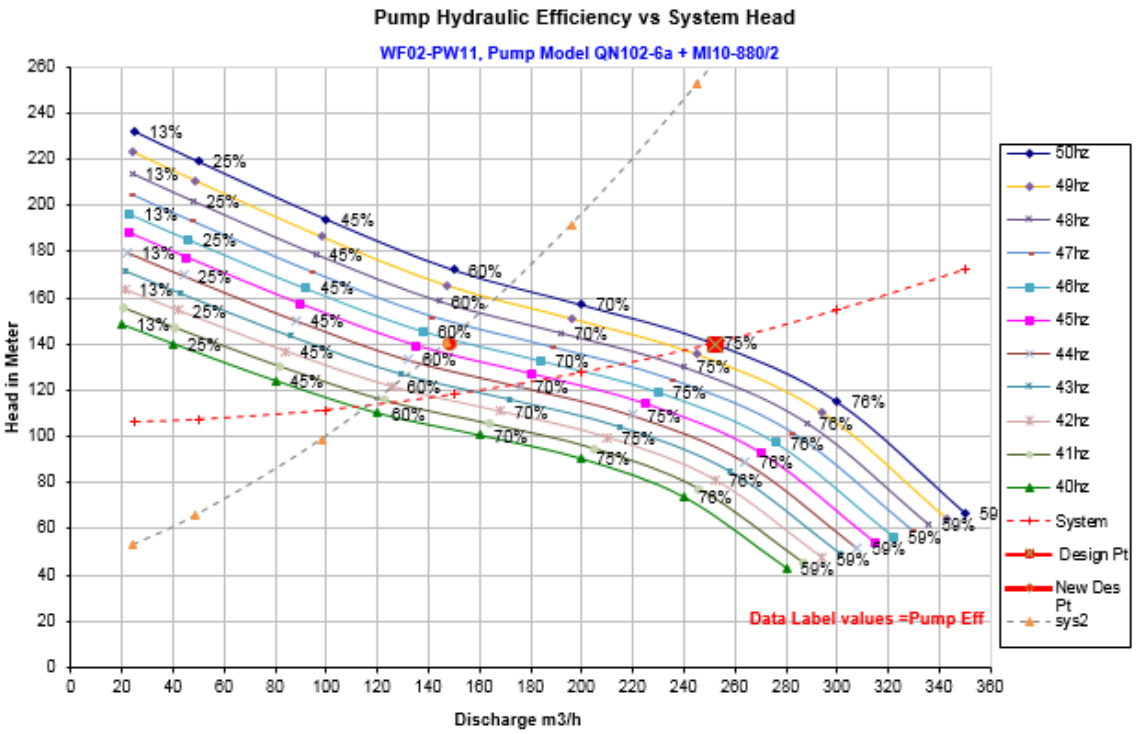
Pump Hydraulic Efficiency vs System Head
WF02-PW11, Pump Model QN102-6a + MI10-880/2
Head in Meter
Discharge m3/h
Data Label values =Pump Eff
50hz
49hz
48hz
47hz
46hz
45hz
44hz
43hz
42hz
41hz
40hz
System
Design Pt
New Des Pt
sys2

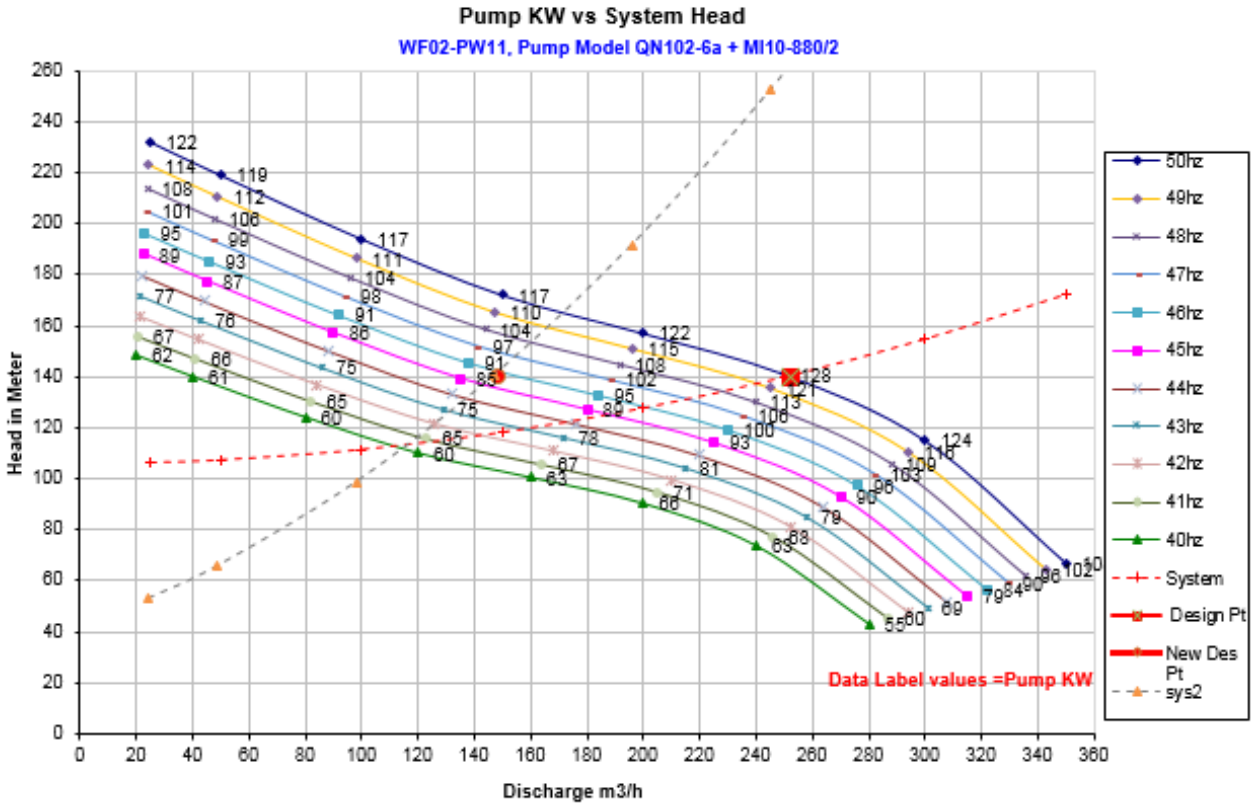
Pump KW vs System Head
WF02-PW11, Pump Model QN102-6a + MI10-880/2
Head in Meter
Discharge m3/h
Data Label values =Pump KW
50hz
49hz
48hz
47hz
46hz
45hz
44hz
43hz
42hz
41hz
40hz
System
Design Pt
New Des Pt
sys2

Variable Speed Pump Analysis for WF02-PW12 well field

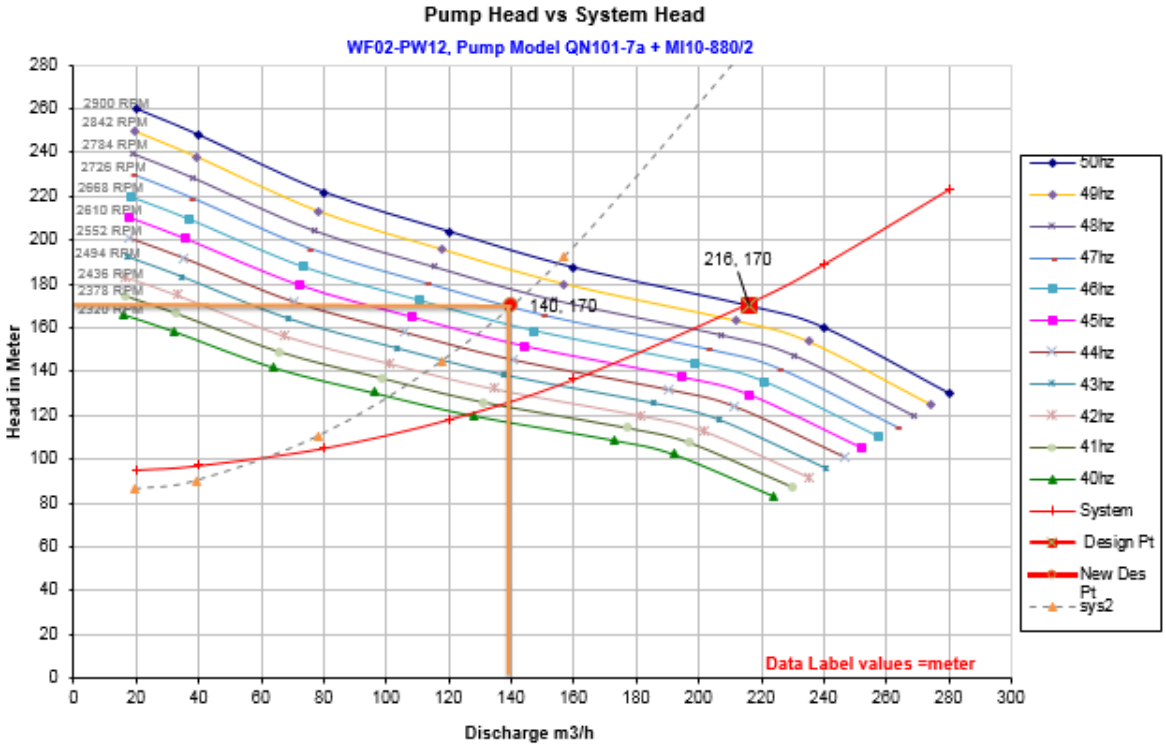

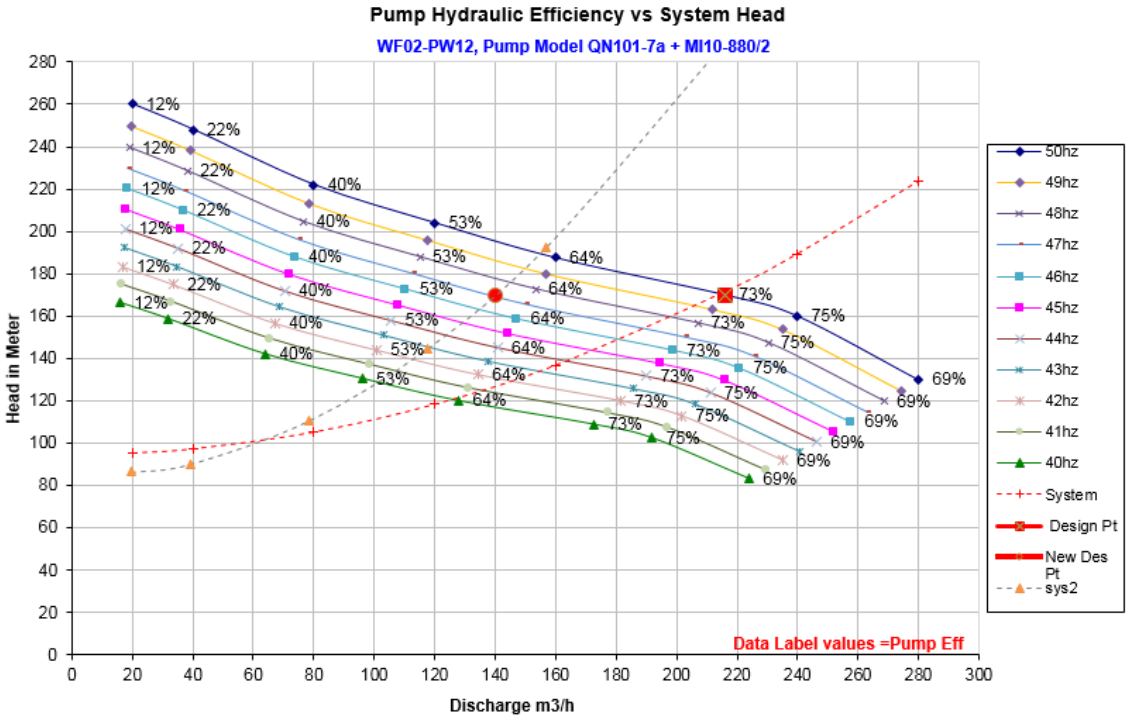

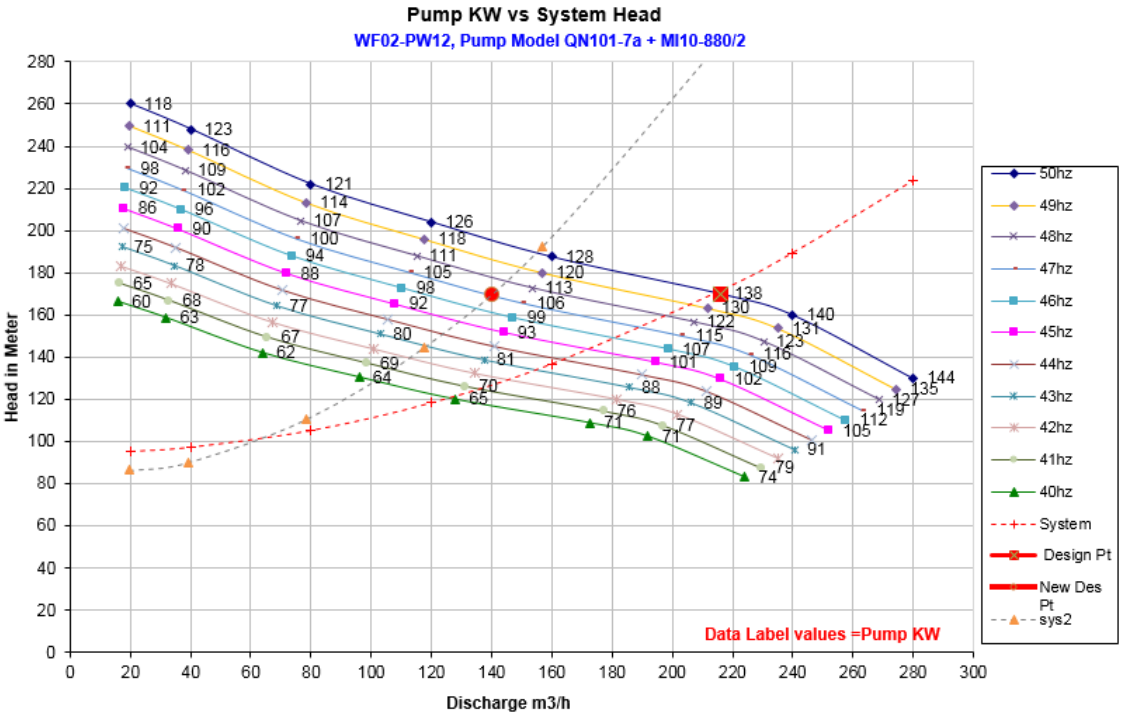

Variable Speed Pump Analysis for WF02-PW13 well field

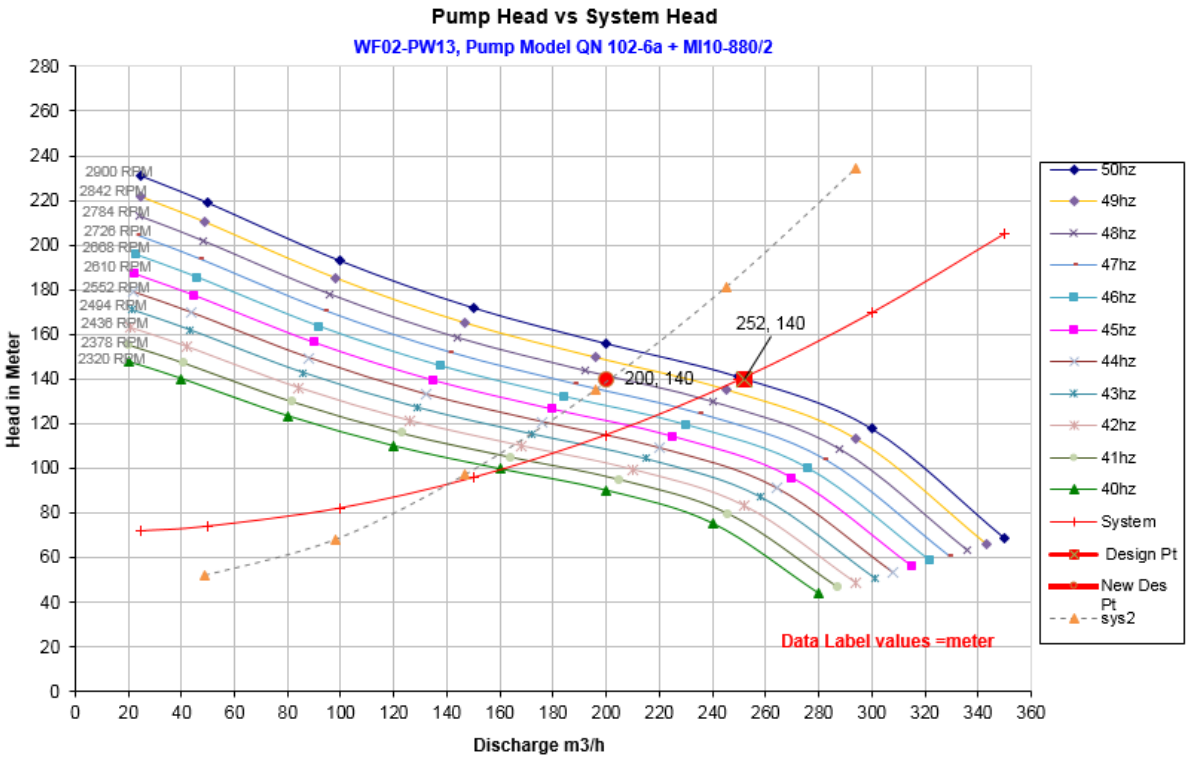

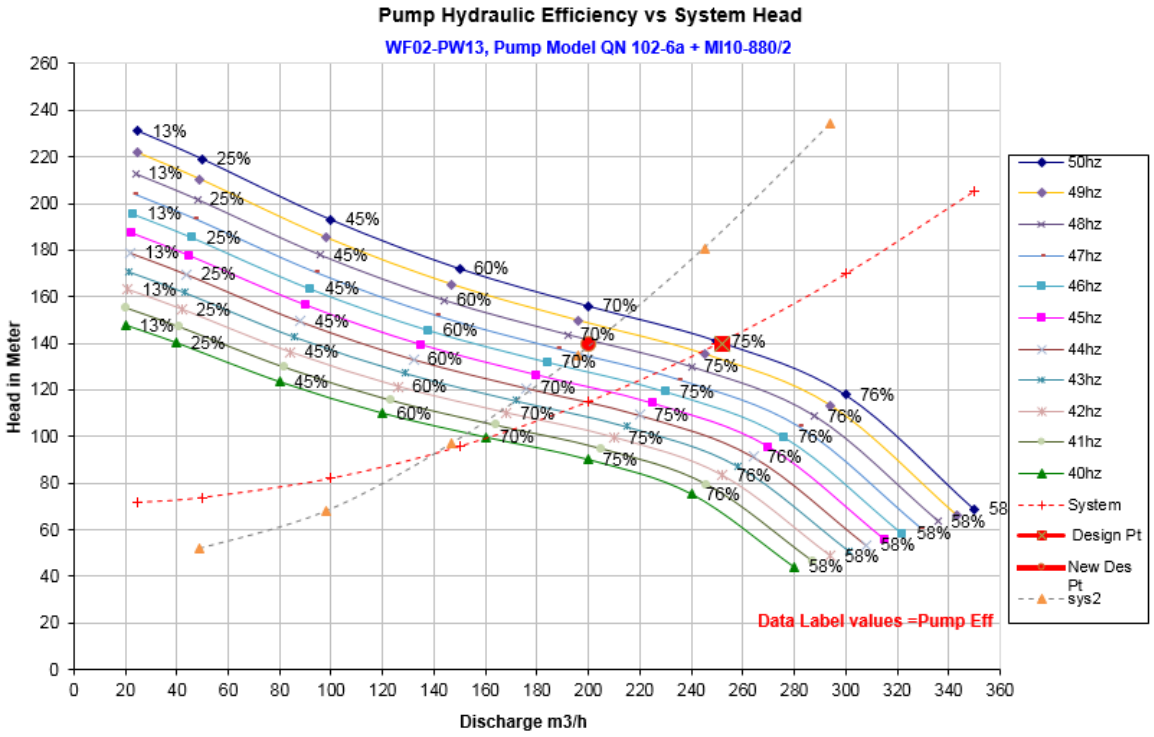
Pump Hydraulic Efficiency vs System Head
WF02-PW13, Pump Model QN 102-6a + MI10-880/2
Head in Meter
Discharge m3/h
Data Label values =Pump Eff
50hz
49hz
48hz
47hz
46hz
45hz
44hz
43hz
42hz
41hz
40hz
System
Design Pt
New Des Pt
sys2

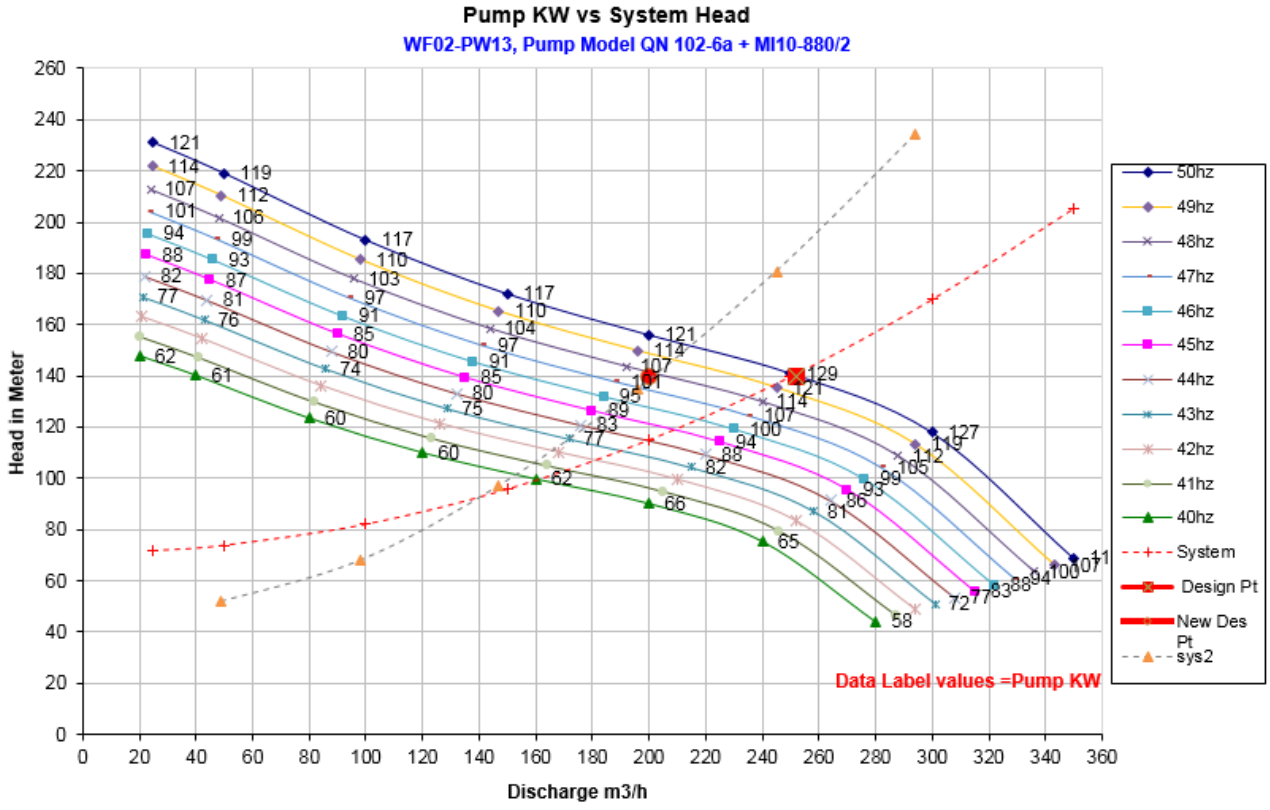
Pump KW vs System Head
WF02-PW13, Pump Model QN 102-6a + MI10-880/2
Head in Meter
Discharge m3/h
Data Label values =Pump KW
50hz
49hz
48hz
47hz
46hz
45hz
44hz
43hz
42hz
41hz
40hz
System
Design Pt
New Des Pt
sys2

Variable Speed Pump Analysis for WF02-PW14 well field

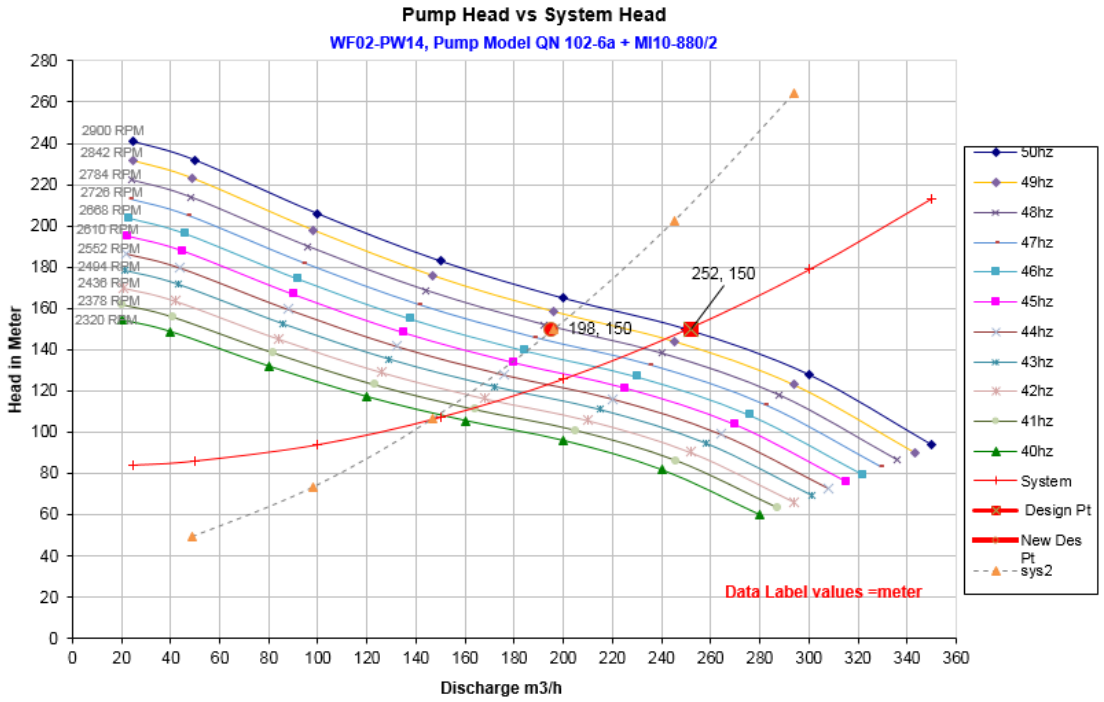

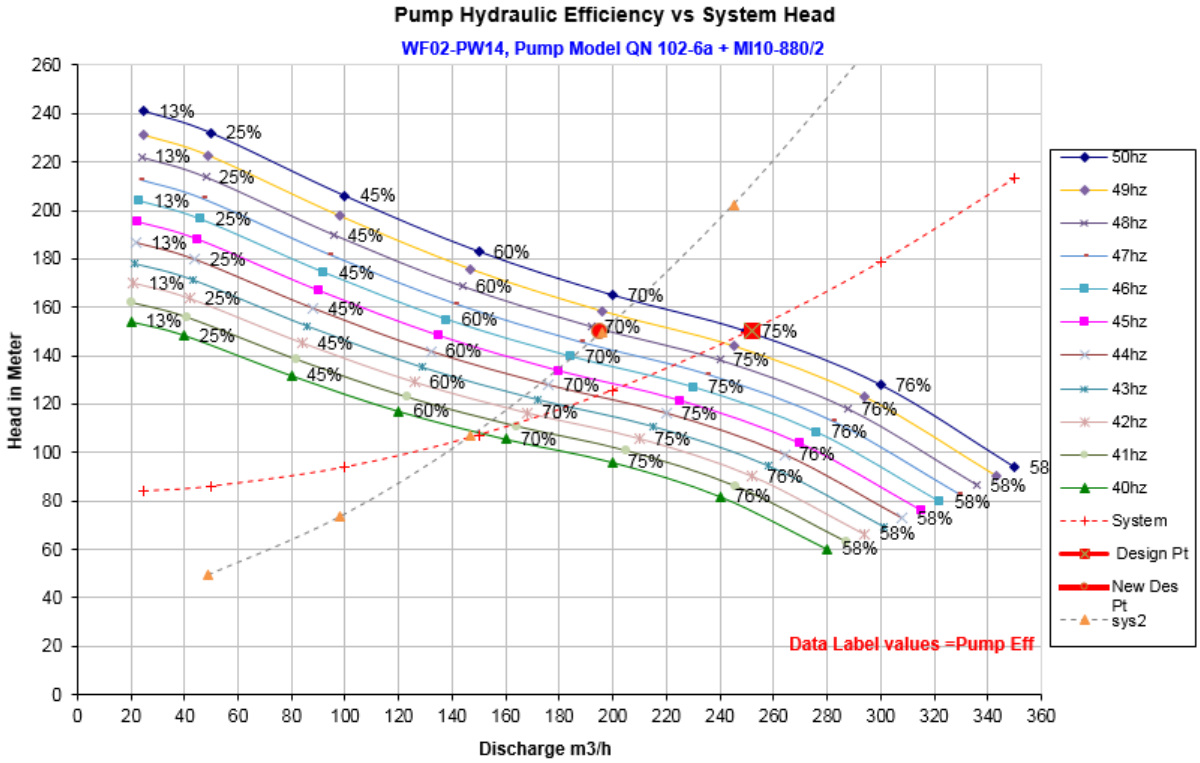

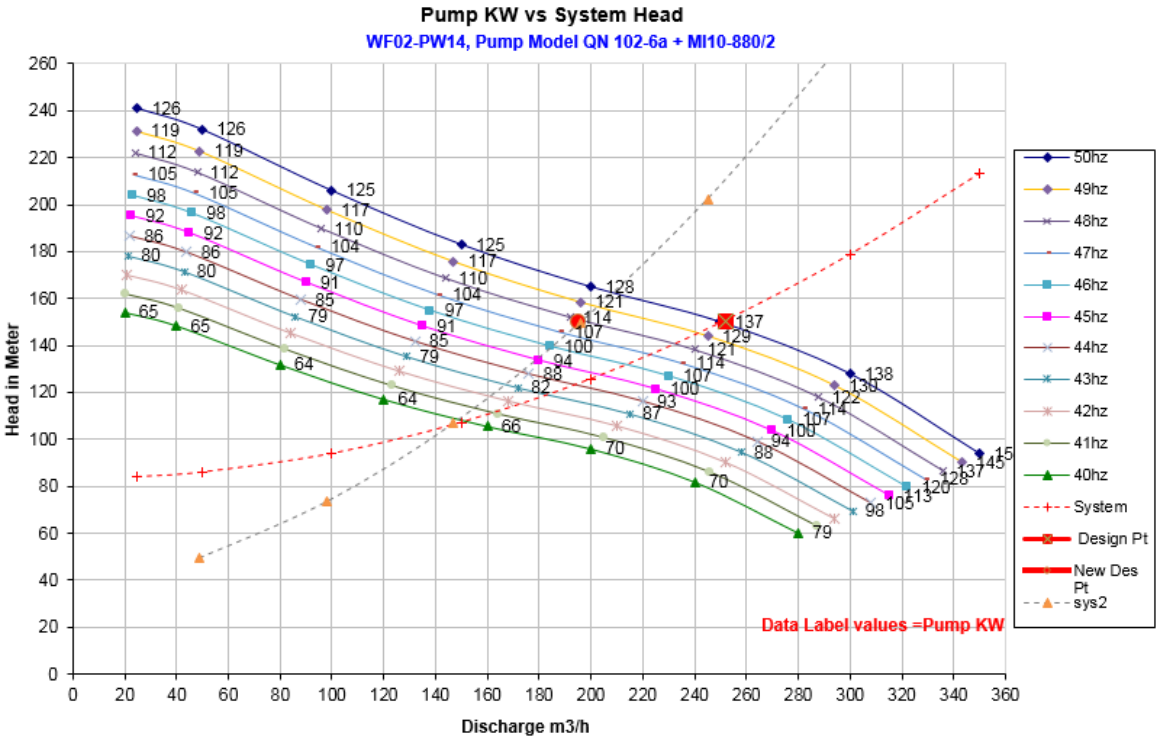

Variable Speed Pump Analysis for WF02-PW20 well field

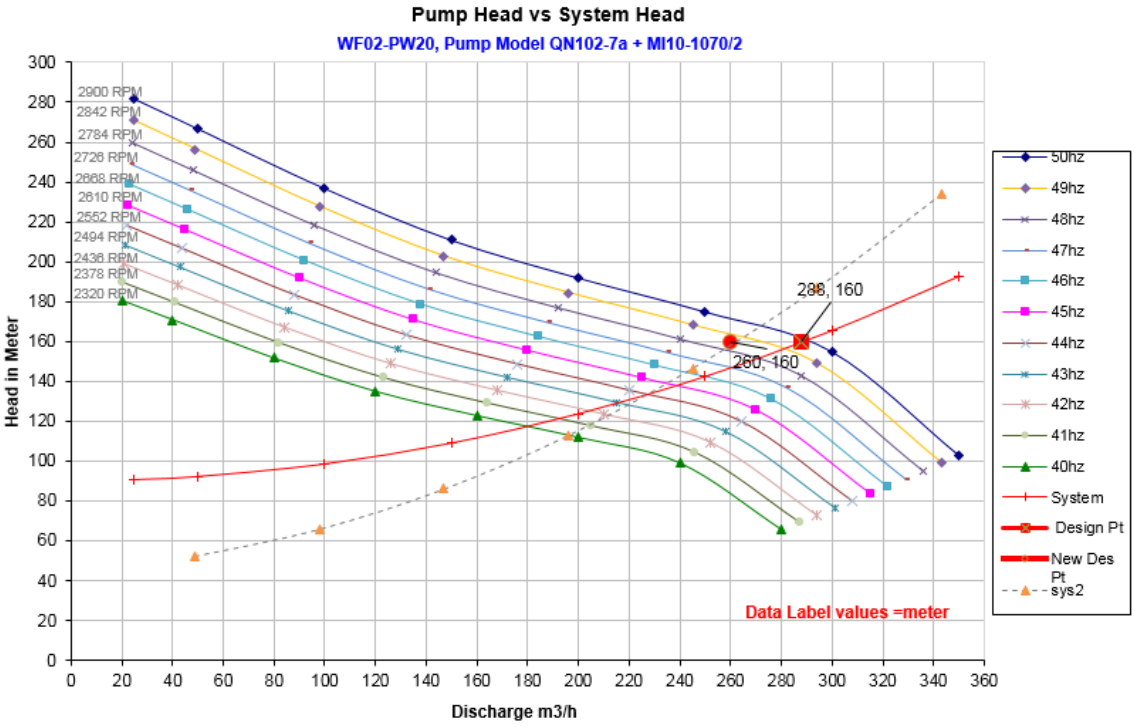

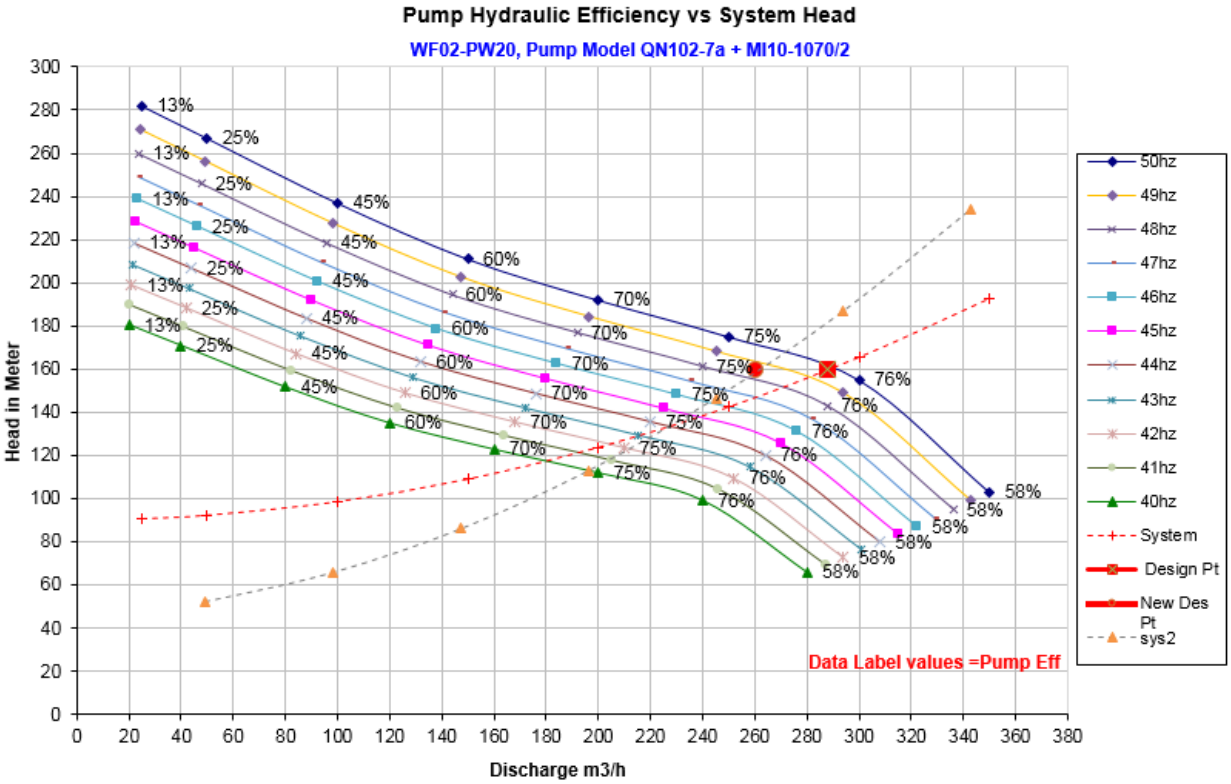
Pump Hydraulic Efficiency vs System Head
WF02-PW20, Pump Model QN102-7a + MI10-1070/2
Head in Meter
Discharge m3/h
Data Label values =Pump Eff
50hz
49hz
48hz
47hz
46hz
45hz
44hz
43hz
42hz
41hz
40hz
System
Design Pt
New Des Pt
sys2

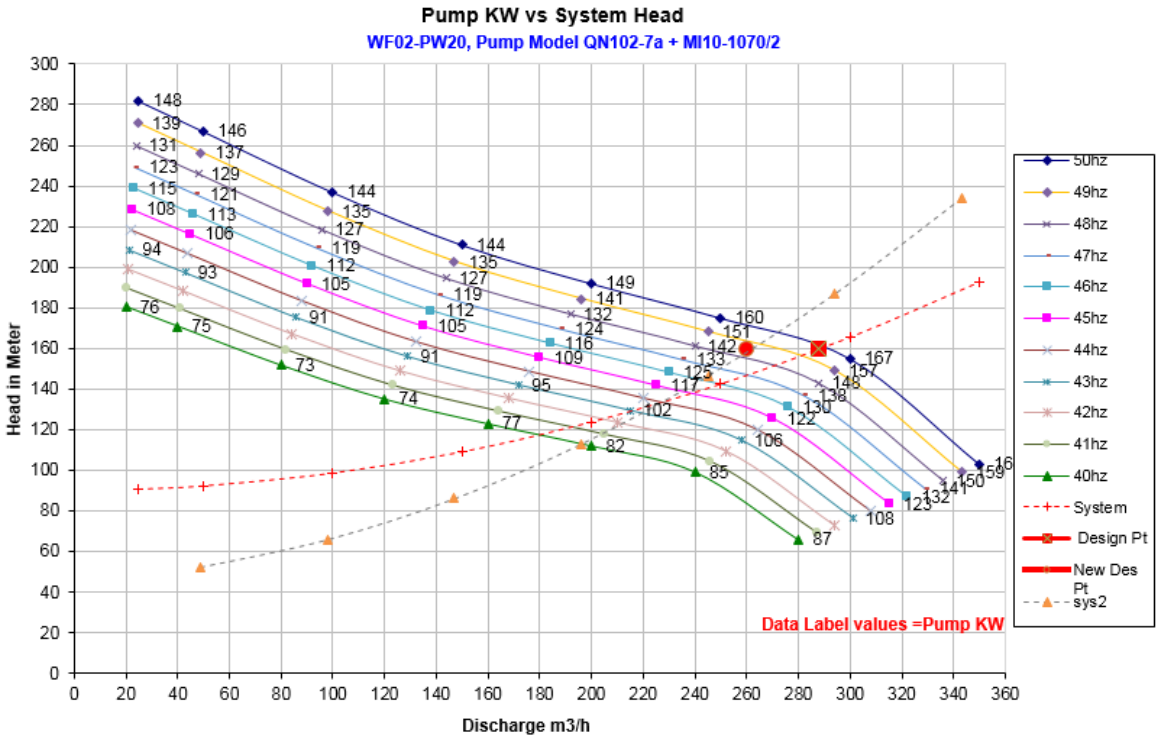
Pump KW vs System Head
WF02-PW20, Pump Model QN102-7a + MI10-1070/2
Head in Meter
Discharge m3/h
Data Label values =Pump KW
50hz
49hz
48hz
47hz
46hz
45hz
44hz
43hz
42hz
41hz
40hz
System
Design Pt
New Des Pt
sys2